

FOUNDED 1925  
INCORPORATED BY  
ROYAL CHARTER 1961

*"To promote the advancement  
of radio, electronics and kindred  
subjects by the exchange of  
information in these branches  
of engineering."*

# THE RADIO AND ELECTRONIC ENGINEER

The Journal of the Institution of Electronic and Radio Engineers

VOLUME 38 No. 5

NOVEMBER 1969

## Supporting Research

**A**PLENTIFUL supply of sealing wax, string and odd lengths of brass tube is, alas! now no longer sufficient for scientific research: for many years research has called for the deployment of resources, equipment and finance to an extent which has led to the use of the term 'big science' to describe the complexes necessary in most fields of nuclear physics, space research, radio astronomy and biophysics.

Much of the scientific research effort in Great Britain today is directed by the Science Research Council, set up in 1965 under the Department of Education and Science. The Council carries out its work through a number of Boards, each of which deals with whole areas of research and thus, under a new organization plan announced in the S.R.C. Report for 1968-69 and which came into effect on 1st October 1969, the Council is now advised by four Boards: the Astronomy, Space and Radio Board; the Engineering Board; the Nuclear Physics Board; and the Science Board.

In view of the growing emphasis on ever-larger research 'tools', the significance of the announcement that two separate Boards, responsible respectively for science and for engineering, will succeed the former 'University Science and Technology Board', will be apparent. The decision to change the organization of the Council has in fact followed its adoption of a policy of selectivity and concentration. The criteria which must be used in selecting areas for special encouragement will be different in pure science from those in technology and engineering, where application to some social, economic or industrial need is a more readily definable objective. In pure science the criteria are the intrinsic merit of the proposed research and the availability of the right techniques and good men to use them. In engineering the same criteria apply, but in addition to timeliness and promise, the relevance of the work to the industrial economy is important. The Engineering Board and the Science Board, each concentrating on a more limited field of responsibility, should find it easier to develop the appropriate criteria for the support of research and training in their respective fields and to devote the great effort necessary to encourage collaboration between the universities and industry.

The Engineering Board will initially be responsible for the support of research and postgraduate training in aeronautical and civil engineering, chemical engineering and technology, electrical and systems engineering, mechanical and production engineering, control engineering, metallurgy and materials, computing science and polymer science. The Science Board will initially be responsible for the support of pure and applied research and postgraduate training in biology, chemistry, enzyme chemistry and technology, mathematics and physics and for the operation of the Atlas Laboratory.

Although there may well seem to be a possible overlap of interests concerned with electronic engineering matters between the Boards, this is something with which electronic engineers themselves are well familiar—we recall Professor Emrys Williams's observation in his Presidential Address three years ago that 'Electronics is the greatest intellectual "nosey-parker" of all time; it has a finger in everybody else's business and is the handmaid of all sciences.' The breadth of the interests of the National Electronics Council is further confirmation of this state of affairs.

Despite these initial reservations, which will undoubtedly be borne in mind and counteracted by the diverse interests of the leading scientists and engineers appointed to the Boards, the reorganization is to be welcomed. We began by referring to the magnitude of effort required in present day scientific research. The gross expenditure of the S.R.C. which totalled over £42M for the year 1968-69 is perhaps not a large proportion of the country's gross national product: it is however, an indication of the backing that is now necessary.

F. W. S.

## INSTITUTION NOTICES

### Subscription Rates for the Journal

The present subscription rate for the Institution's Journal of £6 10s. 0d. per annum was fixed in 1966 and all readers will be aware of the considerable increases in costs of printing, paper, and postage. Further increases in the first two of these items will be made early in 1970.

It has therefore reluctantly been decided that with effect from the January 1970 issue, the annual subscription to *The Radio and Electronic Engineer* will be £8 0s. 0d. (single copies will cost 15s. 0d.).

An increase in the subscription rate for the *Proceedings of the I.E.R.E.* has similarly become necessary and this will now be £2 10s. 0d. per annum (single copies will cost 7s. 6d.). This new rate applies only to non-member subscribers. The *Proceedings of the I.E.R.E.* published in London is sent free of charge to all members in the British Isles and members in other countries may subscribe at a special rate of 25s. 0d.

### Compendium of Courses in Electronic Engineering and Related Disciplines

The Institution has just published a booklet which is intended to help those who wish to obtain qualifications or specialized training in electronic engineering and allied subjects. Entitled 'I.E.R.E. Compendium of Courses in Electronic Engineering and Related Disciplines', the booklet lists courses which are being held at Universities, Polytechnics, Colleges of Technology and Technical Colleges in Great Britain during the current academic year.

It is divided into parts covering respectively degree courses (both University and C.N.A.A.) and non-degree courses (i.e., college associateships and diplomas, national certificates and diplomas, City and Guilds full technological certificate in telecommunications and, of course, C.E.I. Part I and Part II). The third part lists short courses of varying durations on a wide range of subjects for engineers or technicians. Addresses of all the colleges listed are given.

The booklet may be obtained from the Institution, price 7s. 6d., post free.

### Reprints of Journal Papers

Reprints are prepared of all papers published in the *Journal* and copies may be obtained from the Institution, price 5s. 0d. each (post free). Requests for reprints may be made using the form which is included in the end pages of most issues of the *Journal*. It is particularly asked that remittances be sent with orders to avoid book-keeping entries and thus reduce handling costs.

### Reduced Rate Subscriptions for I.E.E. Publications

Under a reciprocal exchange agreement members of the I.E.R.E. are entitled to subscribe to I.E.E. publications at a reduced rate, equivalent to 25% less than the normal non-member customer's rate. These special rates which take into account increases in the normal subscriptions effective from January 1970, are given below. Members are reminded that if they wish to take advantage of these special arrangements they must place their orders through the Publications Department of the I.E.R.E., 9 Bedford Square, London, W.C.1.

<i>Periodical</i>	<i>Reciprocal Rate</i> (Single copy prices in brackets)		
	£	s.	d.
<i>I.E.E. News</i>	1	10	0 (2s. 0d.)
<i>Electronics and Power</i>	6	0	0 (15s. 0d.)
<i>Proceedings I.E.E.</i>	22	10	0 (£2 5s.)
<i>Electronics Record</i>	11	5	0 (£2 5s.)
<i>Power Record</i>	6	15	0 (£2 5s.)
<i>Control and Science Record</i>	6	15	0 (£2 5s.)
<i>Electronics Letters</i>	7	10	0 (7s. 6d.)
<i>Students Quarterly Journal</i>	15	0	0 (5s. 0d.)
<i>Physics Abstracts (PA)</i>	80	0	0 (£4)
<i>Electrical and Electronic Abstracts (EEA)</i>	65	0	0 (£6 10s.)
<i>Computer and Control Abstracts (CCA)</i>	35	0	0 (£3 10s.)
<i>Combined Subscription—EEA and CCA</i>	80	0	0
<i>Current Papers in Physics (CPP)</i>	9	0	0 (9s. 0d.)
<i>Current Papers in Electrical and Electronic Engineering (CPE)</i>	9	0	0 (18s. 0d.)
<i>Current Papers on Computer and Control (CPC)</i>	7	10	0 (15s. 0d.)

### Corrections

In some copies of the October 1969 issue of *The Radio and Electronic Engineer* the paper 'Limitations in Magnetic Disk Storage' contains an error which arose during printing.

Page 231, Section 8, Appendix 2.

The first equation should read

$$f_r \propto \frac{1}{\sqrt{L}}$$

The following correction should be made to the authors' reply to a letter on '1/f Noise' in the October issue:

Page 199, column 2, 3rd paragraph, line 15:

The thickness of the samples should read 2 nm (20Å).

# Transistor Abnormalities as Revealed by Current-Voltage Characteristics

By

P. J. HOLMES,  
M.A., Ph.D.†

**Summary:** The examination of a suspect transistor to determine its mode of degradation or failure always includes, at an early stage, checks on its junction and transistor characteristics, usually with the aid of a visual display on a curve tracer. This paper discusses the diagnostic significance of some of the abnormalities which may be observed on such displays.

## 1. Introduction

The object of this paper is to collect together a number of published explanations of abnormal current-voltage characteristics of transistors as a guide to the interpretation of results obtained from degraded specimens submitted for failure analysis.

The detailed physical causes of the problems will be discussed only very briefly since they have been treated in numerous publications and conferences over the past few years<sup>1</sup> and in some cases there is still doubt about the physical and metallurgical processes involved. We are here primarily concerned with the diagnostic information which can be gleaned from a close study of the current-voltage characteristics, as displayed at d.c. or low frequency on a transistor curve tracer. Some of the conclusions are inevitably ambiguous unless supported by other evidence. Indications of what other factors to look for are provided in a diagnostic table (Table 1).

Over a period of some years, the theory of transistor operation has been developed to the stage where the characteristics of an ideal transistor are understood in detail, and the behaviour of some real configurations is also qualitatively accounted for.<sup>2, 3</sup> It must be recognized that some of the effects described in this paper as abnormalities may be inherent in the design of certain transistor types, and thus not necessarily detrimental to performance within the specified ranges. A defective transistor characteristic can therefore only be defined with reference to the normal behaviour of the type.

## 2. Bulk Junction Effects

The majority of problems arising in the bulk of the junction areas are concerned with the ease of carrier transport through the base region. Whether the transistor is prepared by diffusion or alloying, careful control is necessary to ensure that the two junctions are at exactly the right spacing over the desired area. If the base region is too thick the carrier transport

across it is reduced by recombination during the increased transit time, so that  $h_{FB}$  and  $h_{FE}$  both start to fall off at lower frequencies and the cut-off frequencies are correspondingly reduced.

Since collector-emitter avalanche depends on  $M\gamma\alpha_T$  approaching unity (where  $M$  is the avalanche multiplication factor,  $\gamma$  the emitter efficiency and  $\alpha_T$  the base transport factor), the reduction in  $\alpha_T$  produced by a thick base or low carrier lifetime in the emitter-base junction depletion region means that a higher value of  $M$ , and hence a higher collector voltage, must be attained for avalanche. When the avalanche has started, the rapid increase of emitter current brings about a corresponding increase of emitter efficiency, so that  $M$  no longer needs to be so high. The sustaining voltage is therefore less than the breakdown voltage and a 'snapback' is therefore exhibited by devices with thick bases or high recombination rates in the region of the emitter-base junction.

Obviously, excessive base thickness can result from an abnormally shallow emitter junction and, in planar structures, from an excessively deep collector junction. Apart from inadequate control on the processes of forming the junctions there is the possibility that an undetected impurity abnormality, either extensive or localized, in the starting material can give rise to an incorrect base thickness, or to excessive carrier recombination in the junction region.

An unexpected complication in the planar process was the discovery of the effect variously known as 'emitter dip' or 'push-out'.<sup>4</sup> This is the tendency of the already-formed collector junction to become deeper immediately below the subsequent emitter diffusion. The cause appears to lie in the introduction of lattice defects by the latter diffusion, and the extent of the effect depends on factors such as the actual impurity elements, diffusion temperatures, and cooling rates. The result is to upset the uniformity of thickness of the base region, giving in extreme cases a lateral path from emitter to edge of 'dipped' collector junction which is significantly shorter than the normal path. The effect is more serious in high-frequency transistors with their necessarily thin base layers.

† Radio Department, Royal Aircraft Establishment, Farnborough, Hants.

'Punch-through' (or reach-through) is the phenomenon where the space-charge region of a junction widens under steadily-increasing bias to the point where it meets a discontinuity which can provide additional carriers, such as another junction, a contact, or a boundary with another region of high doping (e.g. that between an n-type epitaxial layer and its n+ substrate). A number of situations can be envisaged for planar transistors, in addition to the simple punch-through between emitter and collector junctions which is liable to take place in any type of transistor. Two significant modes are the linking-up of the collector junction with the epitaxial interface beneath it and the spread of the collector junction space-charge layer at the surface towards the base contact. Punch-through effects due to reverse voltage applied to the emitter junctions of planar transistors are unlikely, in view of the much higher doping levels and the consequently thinner space-charge layer of this junction.

The most common form of punch-through, between collector and emitter, is less likely in diffused transistors, with their fairly high base doping level, than in alloy devices, where the base material is the most pure. Consequently, most planar transistors subjected to collector-emitter voltage attain the avalanche breakdown voltage before the punch-through level is reached.

However, if there is a very small patch of abnormally thin base region, because of some local impurity anomaly, such as a cluster of impurity atoms in the starting material, or a diffusion 'pipe' due to a structural defect, local punch-through can take place. The series resistance of such a small patch may be high enough for the effect on the current-voltage characteristic to be no more than formation of a 'knee' at the local punch-through voltage, followed by a resistive region up to the collector-emitter breakdown voltage of the normal parts of the device.

When we consider the effect of applying collector-base voltage to a transistor (with open emitter) which is liable to punch-through, it can be seen that as soon as the collector junction space-charge region extends beyond the emitter junction into the floating emitter, the latter begins to rise above its normal floating potential and remains at a constant level (the punch-through voltage  $V_{PT}$ ) with respect to the collector. This results in a reverse bias appearing between emitter and base. When this junction breaks down, a collector-base path is established via the emitter junction and the space-charge region. Thus the effective collector-base breakdown voltage is  $V_{(BR)CBO} = V_{PT} + V_{(BR)EBO} = V_{(BR)CEO} + V_{(BR)EBO}$ . In these circumstances, short-circuiting emitter to base makes  $V_{(BR)CES}$  equal to  $V_{PT}$ , which is thus less than

$V_{(BR)CBO}$ , as contrasted with the normal transistor in which these two breakdown voltages are equal.

The other important bulk mechanism in planar devices is reach-through from the collector junction, through the lightly-doped epitaxial collector layer, to the more heavily-doped substrate, again causing an artificially low breakdown voltage, since the expansion of the space-charge layer with voltage is interrupted and the field increases rapidly. There is a corresponding abrupt change in the rate of increase of collector-junction capacitance.

The avalanche process is accompanied by the emission of light from the immediate regions where the generation-recombination processes occur. Observations of the uniformity of this radiation give an effective guide to the distribution of the avalanching regions. The light is emitted from silicon devices in the visible and near infra-red ranges, and can be viewed with an ordinary microscope in a darkroom, or more easily with an image convertor which accepts the infra-red radiation as well. The intensities are such that photography may require several minutes' exposure. Absorption and scattering of the light within the semiconductor result in the deeper parts of the junctions being less amenable to observation than edges and shallow regions, so that emitter junctions of planar silicon transistors are the most rewarding for study by this technique.

### 3. Surface Effects

Punch-through from the collector junction to the base contact can occur in planar transistors with lightly-doped bases or with base contacts too close to the collector junction (either the true metallurgical junction or the effective position as modified by surface effects to be described below). The result is to reduce the peak collector-base voltage below the theoretical avalanche breakdown voltage.

Since both junctions in a transistor necessarily come to the surface, their uniformity is liable to be affected in this region by the presence of surface impurities, passivating layers, and often by the geometrical configuration. The field across the junctions gives rise to fringing effects at the edges, which can result in migration of ionized impurities on the surface of the semiconductor or thin passivating layer, and also within the latter layers if any mobile ions exist. Grown junctions which are cut from uniform slices of epitaxial material, and mesa devices with vertical edges, have no geometrical factors, but planar devices are characterized by the cylindrical nature of their junction edges, coupled with the fact that the edges of the second and subsequent diffusions reach the surface through a region of rapidly changing impurity content. Built-in surface effects also appear in mesa-type devices with edges oblique to the junctions, this being a design feature of many thyristors and similar devices.

3.1. Accumulation, Depletion and Inversion layers

The most important surface factor affecting an active semiconductor device is the departure of the surface conductivity from the bulk value (or the extrapolated value, in the case of a device with graded impurity content). Even a clean, undamaged slab of semiconductor has surface states which cause the band structure to be distorted close to the surface: any charges due to surface impurities will induce equal and opposite charges within the semiconductor and accentuate the effect. We can define three states of the surface:

- (a) Accumulated—the surface is unchanged from the bulk conductivity type but behaves as if more heavily doped.
- (b) Depleted—the surface is nearer intrinsic conductivity than the bulk, or completely intrinsic.
- (c) Inverted—the surface is of opposite conductivity type to the bulk.

The configuration and thickness of most p-n junction space-charge regions will be modified by one of these effects at the surface, altering both junction breakdown voltage and internal leakage current. External leakage currents through the charged layers are a separate problem which may or may not arise.

The possible changes can be illustrated by exploring the results of applying increasing p- or n-type character to the surface of a p<sup>+</sup>-n junction (Fig. 1). In the idealized situation of this figure, the breakdown voltage is determined mainly by the extent of the space-charge layer on the high resistivity n side of the junction, and the leakage current consists of a diffusion component,

controlled by carriers from beyond the space-charge region, and a recombination component, involving carriers generated and recombining within the space-charge region. Both the absolute and relative magnitudes of these components alter with the volume of the space charge.

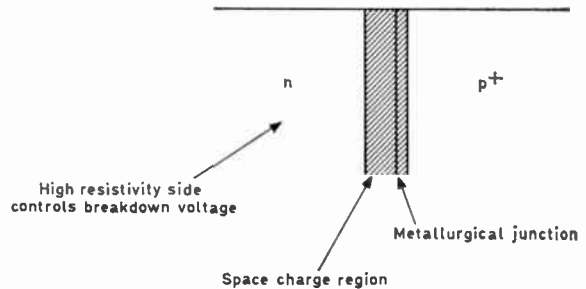
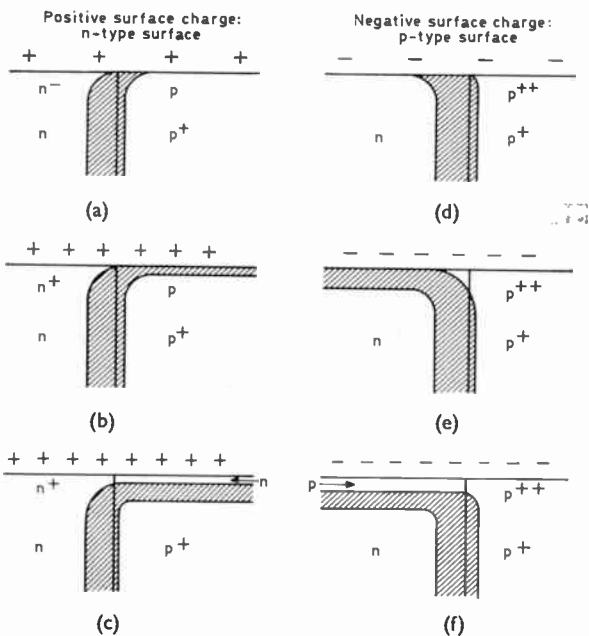


Fig. 1. p<sup>+</sup>-n junction with no surface abnormalities.

In simple structures with no impurity gradation, the former component is independent of the width of the space-charge layer, while the latter component is directly proportional to the width, so their ratio is readily calculated. However, when bulk impurities are graded, and surface space-charges are also involved, both the absolute and relative magnitudes of these components alter with the volume of the space-charge.

Figure 2 shows, in the left-hand column, the effect of an increasing positive surface charge inducing an n-type tendency in the surface. This has initially more effect on the lightly-doped n-side than on the p<sup>+</sup> side,



- (a) Space-charge layer narrowed at surface. Breakdown voltage reduced.
- (b) Surface recombination component in space charge layer added to junction leakage current.
- (c) Permanent channel across p<sup>+</sup> region, increasing effective junction area, but now only involving bulk recombination. Channel breakdown may occur at low voltage.
- (d) Space-charge layer widened at surface. Breakdown voltage increased if previously controlled by surface.
- (e) Space-charge layer narrowed at surface, reducing breakdown voltage. Leakage current increased by surface recombination.
- (f) Permanent channel across n<sup>+</sup> region, increasing effective junction area, but now only involving bulk recombination. Channel breakdown may occur at low voltage.

Fig. 2. Effect of increasing surface charge on p<sup>+</sup>-n junction (charge increasing from top to bottom).

so that the space-charge region is narrowed and breakdown voltage reduced. As the  $p^+$  surface depletes, it links up with the junction depletion (space-charge) layer, increasing the latter's area and volume, giving rise to increased leakage currents, especially since the (often high) surface recombination is now added to the bulk recombination. Further increase in charge converts the  $p^+$  surface completely to an n-type inversion layer or surface channel, so that there is now a field-induced junction, no longer following the original 'metallurgical' junction close to the surface. The depletion region of this field-induced junction no longer contains the surface, with its recombination centres, so the recombination component of leakage current drops to the level determined by bulk recombination alone.<sup>5</sup>

The right-hand column gives the corresponding diagrams for a p-type surface swing. Here, in the early stages, the depletion layer is thickened at the surface, so that if the original junction voltage has previously been surface-limited, it will increase towards the true bulk level, until depletion of the n-type surface alters the geometry and thins the depletion region at the 'corner', again reducing the breakdown voltage. The depletion depth below the surface is greater, for a given surface charge, because of the lower doping level of the n-type side.

The increased volume and area of depletion does not, in fact, fully account for experimental observations of leakage current or channelled p-n junctions. Fitzgerald and Grove<sup>6</sup> performed some calculations with reasonable surface recombination velocities for silicon planar device surfaces and found that this simple view often gave leakage currents orders of magnitude less than those actually observed. Two suggestions were put forward to explain the discrepancy, with experimental evidence in support of both. First was that larger channel currents are generated when the inversion layers extend to regions of abnormally high recombination rate—e.g. scribe lines, dielectric defects or even device edges. Secondly, if the field-induced junction defining a channel has a much lower breakdown voltage than the bulk junction (e.g. if it lies in a heavily-doped surface region), its contribution to the total junction current will appear at low voltages but will thereafter be limited by current saturation in the channel.

Two mechanisms which can produce a current-saturating form of characteristic have been recognized.<sup>7</sup> If the surface mobility is high, and the recombination-generation centre is small, carriers will be swept out as soon as they are generated, and further increase in bias will have no effect. Alternatively, if the centre is large and gives a substantial current flow along the thin channel, an appreciable voltage drop will appear along its length. There will thus be a point

where the field induced junction has zero bias, and this will move away from the parent junction with increasing bias. At some stage, the depletion region of the field induced junction will reach the silicon surface and 'pinch off' the channel, after which no further increase in current or channel length with voltage occurs.<sup>8</sup>

The two mechanisms are distinguished by their temperature sensitivity—the carrier exhaustion process has a high coefficient, since it depends on the carrier generation rate, while the pinch-off mechanism is controlled by the low sensitivity of channel conductance. The former, being dominated by the generation centre, is also less sensitive to surface changes.

An important diagnostic feature for channels connected to junctions is the slope of the forward current-voltage characteristic at low voltages. The forward current of a good junction is given by the sum of two components, diffusion and recombination, with exponential dependences on  $qV/kT$  and  $qV/2kT$  respectively. Channels appear to introduce a third component with a dependence between  $qV/3kT$  and  $qV/4kT$ . If the coefficient of this term is large, it dominates the low-voltage forward current, so that a logarithmic current-voltage plot will indicate whether a significant channel exists (Fig. 3).

### 3.2. Unpassivated Devices

The effect of surface impurities on unprotected devices was of considerable importance in early semiconductor studies. The term 'surface impurities' should be extended to include ambient gases, since exposure to different gases and washing treatments can leave the surface in a variety of different states, from strongly p-type to strongly n-type, thus permitting the whole gamut of accumulation, depletion, and inversion effects to occur on any semiconductor surface. Any ionic impurities which become mobile in the

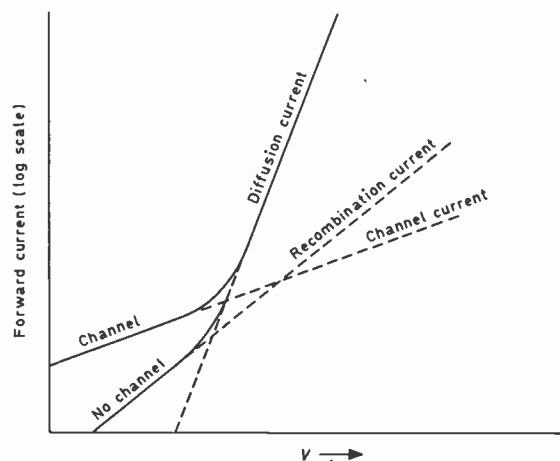


Fig. 3. Forward characteristics of p-n junctions.

presence of moisture or other chemical agents constitute a potential source of leakage currents along the surface of the semiconductor. This was the main reason for the development of passivation treatments for surfaces of transistors, which ultimately showed the way to the planar process.

A further effect of surface condition of a bare semiconductor is the difference in surface recombination velocity produced by various treatments. Since this factor is involved in the equations for current flow near the surface, it can easily dominate the behaviour of unpassivated transistors. A reasonable simplification is to say that strongly p- or n-type surfaces have low recombination velocities, and that a variety of treatments are known to achieve these aims.<sup>9</sup>

The processes of manufacture often result in the exposure of bare semiconductor at the surfaces of devices which are mainly passivated. This may happen by design—e.g. where the oxide of planar devices is removed along lines which are to be scribed for dice separation—or by accident—e.g. where an oversized contact window or an undersized metal contact leaves a gap. The effects of such exposed areas have not been adequately explored, but some possibilities will be put forward here. It is obvious that surface impurities will often provide recombination centres in their own right, in addition to the effect on lifetime through changes in carrier concentration which may be observed even when an insulating layer separates the impurities from the semiconductor. The important point here is that surface impurities can produce channel effects in both cases, so that, for example, two channels under separate areas of planar oxide can be linked by an area of bare silicon. If, at the same time, the impurities introduce a high surface recombination rate, the situation can be far worse than if no bare semiconductor surface was present.

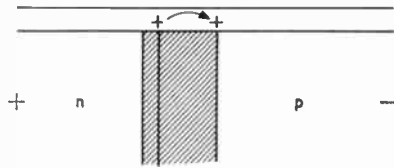
### 3.3. *Passivated Devices*

On passivated surfaces, and in particular on the oxide-covered surfaces of planar silicon devices, surface impurities can still produce induced accumulation depletion, and inversion layers, even though they may no longer be able to generate leakage paths across surfaces. The most important mechanism involving surface-mobile impurities is the charge separation which can occur in the fringing field of the junction, acting through the thin dielectric layer.<sup>8</sup> Positive ions accumulate over the negative (p-type) side of a junction and negative ions over the positive (n-type) side under reverse bias. Since each induces a charge of opposite sign in the underlying semiconductor, a tendency towards depletion appears on both sides, to the obvious detriment of junction behaviour. Since one side of the junction is normally more heavily doped than the other, the usual effect is to move

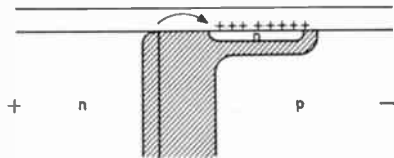
towards inversion of the lightly-doped side, and the production of a channel. Channels formed by this mechanism can usually be removed by the simple process of baking the device and thus eliminating the charge separation by randomizing the mobile ions.

A more complicated situation arises when mobile charges exist within the passivating layer. This is a problem which particularly concerns planar devices with thermally-grown oxide, since the normal result of this process is to produce a positive charge in the oxide and consequently an n-type swing on the underlying silicon. The mechanisms by which this can occur have been the subject of extensive debate and experiment, and it seems probable that several different factors contribute to varying degrees, according to the details of the oxidation process. For our purposes, however, it is sufficient to discuss the effects of two factors regardless of their physical origin: fixed charges (including fixed centres whose charge can be varied) and mobile ions. Their behaviour may be quite different according to whether the fields in which they lie are entirely lateral fringing fields or a component normal to the oxide-silicon interface is introduced by the presence of a metal on the top surface of the oxide, such as an expanded contact or an integrated circuit interconnection. If there is a field normal to the interface, charge redistribution takes place at elevated temperatures but not symmetrically with respect to field direction. With metal positive and semiconductor negative, the positive charge builds up close to the latter, producing an n-type tendency. The reverse effect is much harder to achieve. Lateral fields produce charge separation within the oxide, and reversed fields and elevated temperatures are needed to eliminate the resulting channel effects. When channels are formed by lateral migration in connection with strongly reverse-biased junctions, they may become isolated when the space-charge region contracts on removal of the voltage (Fig. 4), and only become reconnected when the voltage is raised to a threshold level.<sup>6, 10</sup> Thus junction leakage currents may be negligible up to this level and then increase by orders of magnitude when the channels start to conduct.

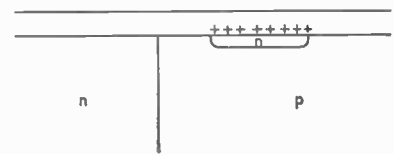
The effects of surfaces on transistor behaviour are best illustrated in terms of the usual n-type tendencies on the surfaces of planar p-n-p and n-p-n transistors, remembering that the collectors are of low, fairly uniform impurity content, and bases have higher, graded content. The effects of emitter depletion and inversion layers are not so obvious because the doping levels are usually such that the normal levels of surface charge in silicon devices are insufficient to produce the full sequence of events shown in Fig. 2. However, when the surface concentration is greater than about  $4 \times 10^{18} \text{ cm}^{-3}$ , the inversion layer becomes so thin that there is an appreciable probability of tunnelling



(a) Reverse voltage applied.



(b) Channel formed by positive ion migration in oxide to far side of space-charge region.

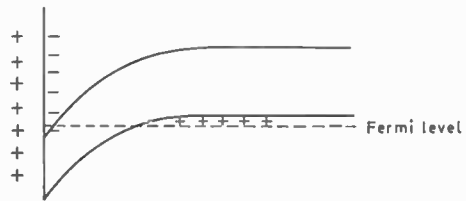


(c) Voltage removed, isolated channel remains.

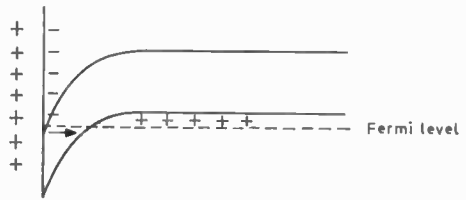
Fig. 4. Formation of an isolated channel by ion migration in the fringing field of a junction.

between valence and conduction bands (or intermediate impurity levels)<sup>11</sup> as shown in Fig. 5. This gives an excess leakage current in what would otherwise behave as a normal one-sided step junction. Although most devices have emitter surface concentrations so high that this effect cannot occur over the majority of the emitter surface (i.e. greater than about  $8 \times 10^{18} \text{ cm}^{-3}$ ), there will always be a region near the junction where the net impurity concentration goes through the critical range for tunnelling, so that there will always be a critical degree of inversion which will produce excess leakage from the emitter side of the junction. The significance of the effect is least in junctions where steep impurity gradients minimize the width of the critical surface region. It should be noted that tunnelling can also occur on the base side of the junction when the appropriate degree of inversion is attained on specimens with heavily-doped bases.

Recalling that the breakdown voltage of a p-n junction depends primarily on the impurity concentration on the lightly-doped side, it is easy to see that with the doping system of the planar transistor, the state of the collector surface normally determines the tendency to surface breakdown of collector junctions and the base surface usually controls emitter junction breakdown. In an n-p-n planar transistor, the  $n^+$



(a) Moderate doping, inversion layer too thick for tunnelling.



(b) Heavy doping, tunnelling across thin inversion layer.

Fig. 5. Surface band structures, illustrating tunnelling in inversion of heavily-doped surfaces.

shift of the collector surface reduces the collector junction breakdown voltage (Fig. 2), while in a p-n-p device, with only a light depletion layer over its collector, the collector breakdown voltage is increased, although heavy depletion or inversion reverses the effect.

The well-known 'walk-out' effect, often seen on curve-tracer displays, in which the breakdown voltage increases rapidly after reverse bias is applied, can usually be attributed to surface impurity or charge changes resulting from the application of the electric field or (less frequently) to rise in surface temperature due to the power input. If the surface is close to the inversion point, the depletion layer configuration of the junction is very susceptible to such changes, so that the diminished breakdown voltage and high leakage current resulting from a thin channel are progressively removed.

In a p-n-p device, base surface accumulation and reduction of the emitter breakdown voltage are produced by swings towards n-type which are insufficient to produce inversion and channelling over the p-type regions. Similarly, n-p-n planar transistors can sometimes have increased emitter breakdown voltages when the p-type surface is depleted. Thus the change of breakdown voltage at the surface of a deteriorating transistor often sets in before any increase in leakage current due to depletion or inversion, and the diagnosis of a leakage current as due to a channel should always be considered in relation to abnormalities in breakdown voltage. Conversely, considerable changes in gain and leakage *without* breakdown voltage changes point to bulk, rather than surface phenomena.

The most common problems of planar devices can now be summarized:

- (a) p-n-p devices with collector channels. High collector-base and collector-emitter leakage currents, either saturating or non-saturating and (like collector junction capacitance) greatly increased when the active area of the channel reaches the exposed edge of the device. Collector breakdown voltages are usually reduced, (though in some cases slight depletion can cause an increase) and the gain is lessened by the contribution of the leakage effects to the base current.
- (b) n-p-n devices with base channels. These may have channels right across the base (or, in annular geometries, in the oxide-covered parts adjacent to emitter and collector, connected by the metallized base ring), or only on the more lightly-doped collector side of the base. The former can produce either a saturating collector-emitter leakage current, with very thin layers, or an ohmic leakage path, with strong channels, or anything between these extremes. A phenomenon which has been seen at low current levels in some n-p-n planar devices, in which the geometry permits the formation of base channels from emitter to collector without reaching the base contact, has been termed 'ultra-high gain'. Rosenbaum and Loro<sup>12</sup> explained this as due to the base channel functioning at low levels as a field-effect transistor, with the bulk of the base acting as the gate. The collector-base currents are normal, and  $\ln I_c$  versus  $V_{BE}$  has less than the ideal slope of  $q/kT$  ( $40V^{-1}$ ), in devices of this sort.  $h_{FE}$  falls to normal levels when the collector current is raised well above the channel pinch-off level.

The effect of a base channel on the collector-base characteristic depends on whether the base metallization is in contact with the channel (or acts as a bridge between two channelled regions) or not. In the former configuration, there may once again be anything between a small saturated leakage and an ohmic shunt path across the junction, while in the latter, the effect is similar to that of an external collector-emitter shunt path, namely that the linked collector-emitter junction will breakdown at about  $V_{(BR)EBO}$  into either a saturated leakage or an ohmic resistance. In this situation, shorting base to emitter will give  $I_{CBS} > I_{CBO} > I_D$  (the base current in the shorted  $I_{CBS}$  condition), whereas in an unchannelled device these three currents are nearly equal.<sup>13</sup> Channels on the collector side of the base do not affect the emitter junction, but their effect on collector-base leakages and breakdown voltages results in their influence on  $I_{CBO}$  being still considerable. The other likely pos-

sibility is inversion of the base surface close to the emitter, where it is *heavily doped*, which may produce tunnelling, giving reduced  $V_{(BR)EBO}$  and increased  $I_{EBO}$ . Since the latter shunts some of the base input, the result is once again a loss of gain. Reddi<sup>11</sup> has shown, experimentally, that inversion of *lightly uniformly-doped* bases can have the opposite effect, since they acquire field-induced junctions which, because of the lower doping, are highly efficient extensions of the emitter area, despite the greater base thickness under them. Thus, although  $I_{EBO}$  is increased, giving a higher  $I_B$ , the increased injection gives a more than proportionate effect on collector current. The result is an *increase* in  $h_{FE}$ .

- (c) p-n-p devices with base accumulation layers. The emitter reverse breakdown voltage is reduced, as described above, so that the detrimental effects of exceeding it (such as drift of  $h_{FE}$ ) may be initiated by the tests of the sharpness of this breakdown which are sometimes used as screening process for transistors.
- (d) n-p-n devices with collector accumulation layers. As already described, collector breakdown voltage is reduced, though except in bad cases the effect will be indistinguishable from other junction edge breakdown phenomena.
- (e) p-n-p devices with emitter inversion. Tunnelling can increase  $I_{EBO}$ , with consequent reduction of gain, and reduce  $V_{(BR)EBO}$  if the surface charge is enough to invert the surface in the critically doped region. Otherwise, the area of inversion is very small, and the excess current, containing no tunnelling component, is likewise small.

In the unlikely event of a p-type surface swing on a planar device, or the more likely event of such a swing on a transistor made in some other way, the above remarks can be applied by reversing the p- and n-type references, and at the same time remembering that transistors other than planar do not necessarily have the same relative impurity levels in their three regions.

The accepted way of limiting the effect of channels is to surround the appropriate side of the junction with an annular guard ring or 'channel-stopper'<sup>8</sup> consisting of a heavily-doped surface layer diffused into the surface at a distance from the junction just beyond the normal extent of the bulk depletion layer at maximum designed reverse voltage. This prevents any inversion of the surface near to the junction. Another expedient, which also helps to avoid stability problems due to migration of ions within the oxide of planar devices, is the 'field relief electrode'. Here a metal layer, connected to an annular guard ring, is extended across the surface of the passivating layer as far as the junction,

thus removing fields in the oxide and ensuring constancy of surface potential.<sup>14</sup> The normal n-type tendency is thus counteracted by expanding the base contacts of n-p-n devices and the collector guard rings of p-n-p devices across the oxide to the collector junction (i.e. the negative contact is expanded in each case).

3.4. *Effects of Moisture and Other Conducting Surface Contaminants*

The presence of condensed moisture often assists in the redistribution of the surface contaminants which cause channels, as well as contributing actual (often ohmic) conducting paths across junctions. Freezing and evaporation cause fairly abrupt changes in the surface leakages due to moisture, so that moisture-induced effects can be distinguished from other leakages by temperature cycling. Leakage currents which are only significant from a little below 0°C to somewhere in the region of 100°C are easily recognizable.  $I_{CBO}$  is the parameter most obviously affected by condensed moisture, since it is ideally very small. It is possible for large droplets of moisture to give rise to intermittent high leakage as random shocks move them from point to point. Removal of the transistor does not necessarily remove moisture-induced leakage instantly and vacuum baking may be required to ensure that all moisture is removed from the surface. Unlike some leakages due to ionic separation, these moisture-induced leakages are not re-established by subsequent operation of the device under dry conditions.

Other conducting surface contaminants may not be removed even by vacuum baking, and must be suspected in cases where ohmic junction leakage current persists.

3.5. *The Effects of External Leakage Currents on Transistor Behaviour*

The inherent bulk leakage currents, which are functions of carrier diffusion and recombination in the junction region, must be distinguished from external leakages whose effects are introduced at the contacts, sufficiently remote from the active regions to have little influence on the inherent leakage currents. Thus we can consider a transistor as a 'black box' with currents  $I_C$ ,  $I_B$  and  $I_E$ , measured at the terminals, made up of the internal currents  $I'_C$ ,  $I'_B$  and  $I'_E$  through the transistor proper, plus currents through shunting resistors representing possible sources of external leakage, such as surface contamination and header faults (Fig. 6). Calling these resistors  $R_{CE}$ ,  $R_{CB}$  and  $R_{BE}$ , we can write the measured currents in terms of the internal currents:

$$\begin{aligned} I_C &= I'_C + V_{CE}/R_{CE} + V_{CB}/R_{CB} \\ I_B &= I'_B - V_{CB}/R_{CB} + V_{BE}/R_{BE} \\ I_E &= I'_E + V_{CE}/R_{CE} + V_{BE}/R_{BE} \end{aligned}$$

In many practical cases only one or two of these leakages may exist. For example, with collector-emitter leakage alone, the effective small-signal gain  $h_{fc} = (\Delta I_C/\Delta I_B)_{V_{CE} = \text{const}}$  is essentially the same as the 'internal' gain in the absence of leakage (Fig. 7(b)), though the parallel shunt path makes measurements of the d.c. gain,  $h_{FE} = I_C/I_B$ , meaningless, and may pass an intolerable standing current.

Emitter-base leakage (Fig. 7(c)) upsets performance at all levels. At  $I_B = 0$ , the internal  $I'_B$  is negative, so  $I_{CEO}$  is reduced, and a certain amount of base drive must be applied to overcome this reverse emitter bias and lift the device above cut-off. Reverse emitter bias also causes the collector breakdown voltage to exceed  $V_{(BR)CEO}$ , so there is a snap-back to normal levels

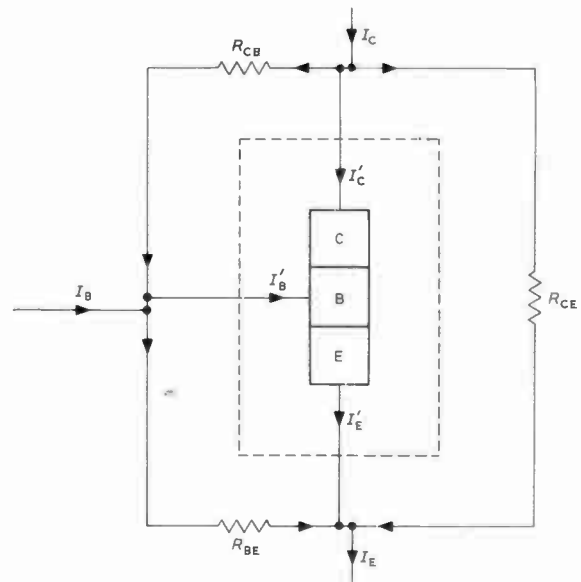


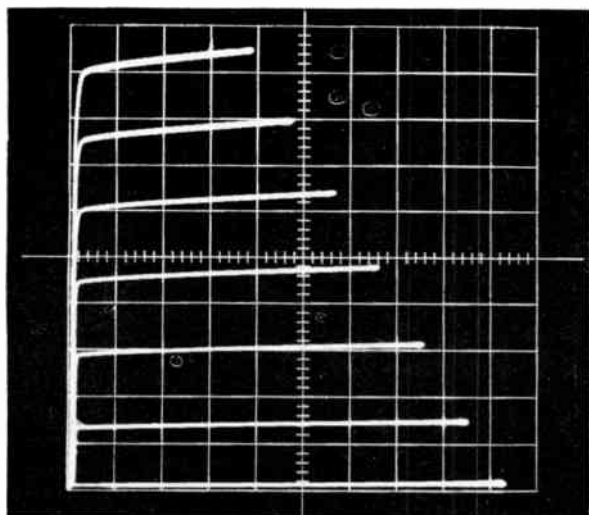
Fig. 6. External leakage paths related to the observed currents in a transistor.

when the bias changes to normal polarity and the collector current rises. Above cut-off the leakage reduces  $h_{fc}$  by shunting part of the base current  $I_B$  direct to the emitter contact, the effect being most marked when the base input is low, and the incremental forward resistance of the emitter-base junction is high.

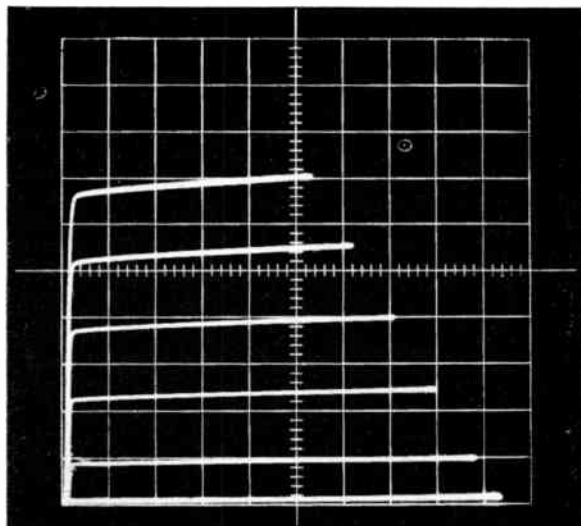
Collector-base leakage means that with no external base current, the transistor still receives an input determined by the collector voltage (Fig. 7(d)). Current gain takes effect and the excess collector-emitter current for a given leakage resistance is much greater than when the same resistance acts as  $R_{CE}$ . When an external base-emitter voltage is applied with  $V_{CE}$  kept constant there is a corresponding reduction in the collector-base voltage, so the leakage current

contribution to the base input is reduced. As the driving voltage is increased, the leakage provides an ever-decreasing proportion of the base input, so that  $h_{FE}$  is not so seriously affected by collector-base leakage at higher input levels. However, the standing current may be intolerable for many applications.

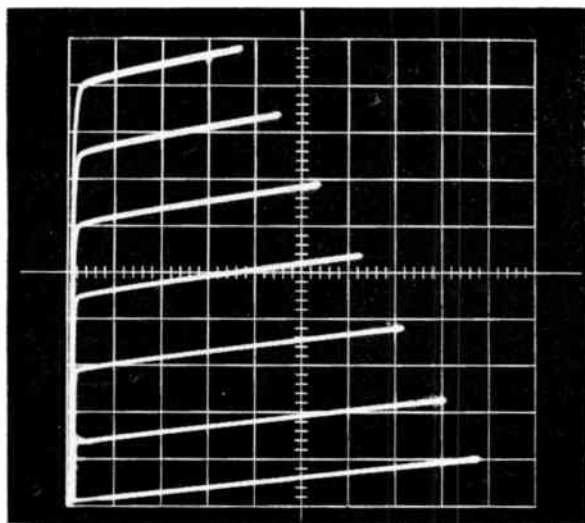
A combination of collector-base and emitter-base leakages of comparable resistance acts as a potential divider (Fig. 7(f)), partially shielding the transistor from the effects of base drive, so that the current gain is reduced and the collector-emitter current at  $I_B = 0$  consists of both direct leakage through the resistances



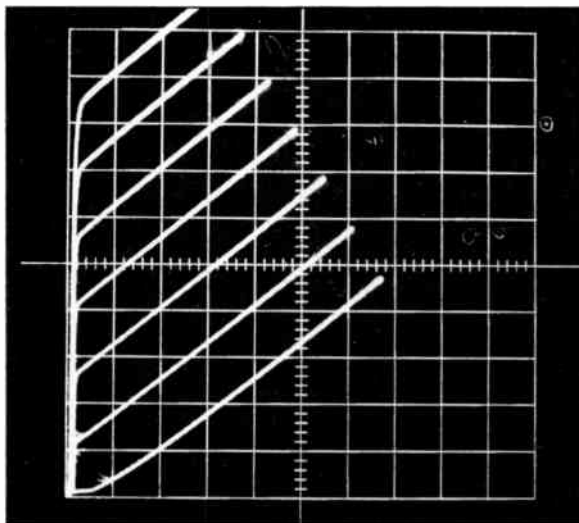
(a) Normal collector characteristics.  
horizontal  $V_{CE}$  2 V/div,  
vertical  $I_C$  2 mA/div,  
base steps  $I_B$  50  $\mu$ A/step,  $h_{FE}$  54-68



(b) 10 k $\Omega$  collector to emitter  
 $h_{FE}$  54-68

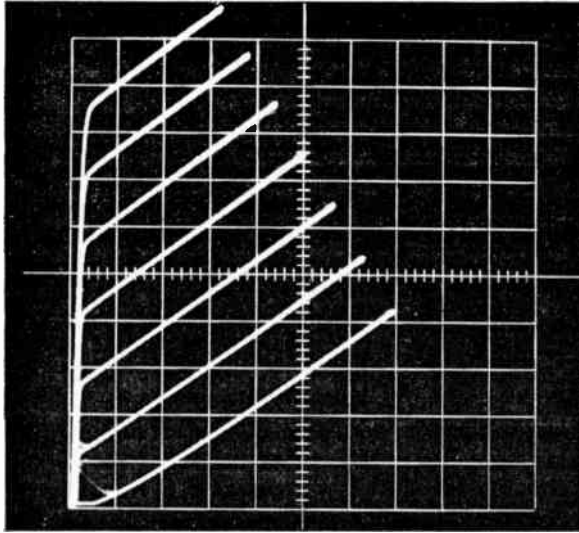


(c) 10 k $\Omega$  base to emitter  
 $I_B = 0$  and  $I_B = 50 \mu$ A  
steps coincide  
 $h_{FE}$  52-64  
(except where cut-off at low levels).

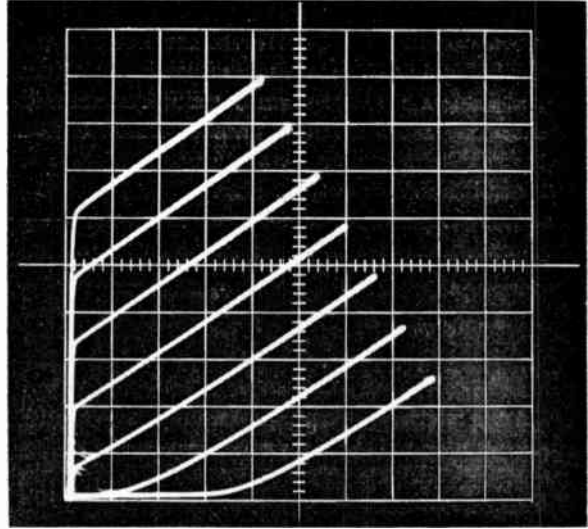


(d) 100 k $\Omega$  collector to base  
Collector slope 1.4 k $\Omega$   
 $h_{FE}$  52-64

Fig. 7. Collector characteristics.



(e) 100 kΩ collector to base  
10 kΩ collector to emitter  
Collector slope 1.3 kΩ  
 $h_{FE}$  52-64



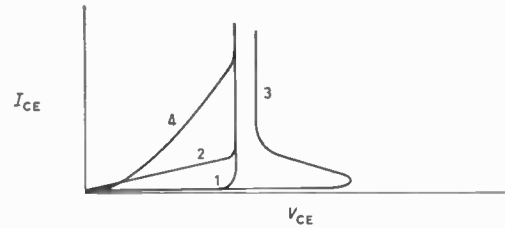
(f) 100 kΩ collector to base  
10 kΩ base to emitter  
 $I_B = 0$  curve 'turns on' at 6 V, where  $V_{BE}$  0.64 V  
Collector slope 1.4 kΩ  
 $h_{FE}$  52-60

Fig. 7 (contd.) Collector characteristics.

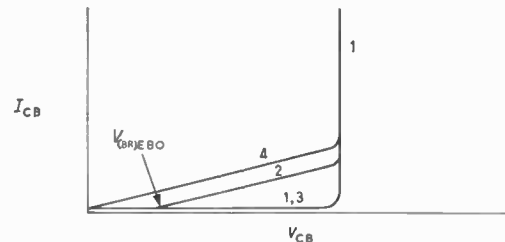
and a larger contribution which comes into play at a threshold  $V_{CE}$  where the voltage applied by the potential divider starts to forward-bias the emitter and thereby produces an input which is amplified by the current gain. At higher levels of base input, this excess current sets in at progressively lower collector voltages until the threshold vanishes. Combinations of comparable collector-base and collector-emitter leakage resistances (Fig. 7(e)) are dominated by the former, for reasons already explained.

These remarks on the form of the characteristics can be taken to apply also to those internal (i.e. channel) leakages which act over a wide voltage range as if they were independent paths parallel to the junctions themselves. Reservations apply, of course in cases where the internal resistances are comparable with the external ones, and also where the breakdown characteristics of the channels are intimately involved in the low-level current-voltage relationships of the transistor junctions. The lines of current flow in the bulk of the device are then altered by the presence of the leakage paths, to the extent that they can no longer be considered as independent parallel paths.

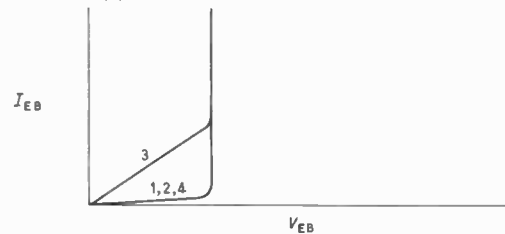
The effects of external leakage paths on breakdown voltages (and also the effects of channels in the rare cases where the channel breakdowns do not complicate the issue) are easily derived (Fig. 8). Collector-emitter leakage does not affect the actual voltage levels significantly, though a subsidiary break-point is seen in the collector-base characteristic at  $V_{(BR)EBO}$ , beyond which  $R_{CE}$  and the emitter junction provide a



(a) Collector-emitter characteristics.



(b) Collector-base characteristics.



(c) Base-emitter characteristics.

Fig. 8. Breakdown characteristics.

- Key: 1. Normal  
2. With external collector-emitter leakage  
3. With external emitter-base leakage  
4. With external collector-base leakage.

shunt path. Emitter-base leakage produces its greatest effect on  $V_{(BR)CEO}$ , by producing a  $V_{(BR)CER}$  condition, with snapback. Collector-base leakage, as already explained, produces a large increase in collector-emitter current, so that overheating and softening of the characteristic may occur before the avalanche voltage, which is still determined by the criterion  $\gamma\alpha_T M \rightarrow 1$ , is attained.

### 3.6. Externally-induced Surface Effects

Two important factors which can affect transistors, especially when operated unencapsulated, in the laboratory, are the effects of illumination and of external capacitances. Illumination increases the generation-recombination rate, and can add to leakage currents, while external means of altering surface potentials can have the same effects as surface charges. An illustration of the latter point was given by Card,<sup>15</sup> who studied the effects of setting up fields between transistors and insulated cans. He showed that with a collector-emitter channel present, +1000V on the can had the same effect on collector leakage current as +0.04V applied to the base, and increased  $h_{FE}$ . The converse effect was found with negative voltages. It was concluded that if the can potential affected only the emitter or collector junction characteristic, and not the collector-emitter leakage, a local channel at the relevant junction was indicated. Sensitivity of exposed devices to the presence of nearby objects thus indicates the presence of channels.

Photo-effects may be photo-voltaic or photo-conductive in nature, and while general illumination will somewhat enhance the leakage of a good transistor, the leakage of a channelled device is much more seriously affected, because of the greater area of sensitive surface. Mathews *et al.*,<sup>10</sup> using a scanning light spot, showed how various channel configurations affected local photo-response most where the space-charge region met the surface, and much less where the channel extended deep enough for the space-charge layer not to extend upwards to the surface. Scanning light spots are now widely used for plotting the locations and extent of channels in faulty devices.

## 4. Thermal Effects

### 4.1. Second Breakdown

Undoubtedly the most important thermal effect in transistors is the 'second breakdown' phenomenon. This has been the subject of extensive study in a number of centres, and although some of the details of the mechanism are still hotly debated, the general pattern of events in the more common designs of transistor is quite well established. An up-to-date review has been given by Schafft.<sup>16</sup>

When a transistor operates under power conditions, it inevitably warms up. It has already been seen that

the lines of current flow can become concentrated in certain parts of the device from purely geometrical considerations, and if we allow for additional factors such as junction inhomogeneities, it is readily understandable that some patches of the active region will become hotter than others. Their carrier concentration thus increases, and the current for a given input voltage rises, giving a 'thermal runaway' effect. It has been suggested that the critical temperature for runaway can be equated to that where the highest resistivity semiconductor layer becomes intrinsically conducting, but this would not be easy to prove. Whether or not the runaway immediately destroys the transistor depends mainly on the associated circuit limitations, and on the contact metal used, since the actual mode of failure is usually the alloying-in of the metals at points where the appropriate temperature is reached.<sup>17</sup> Even if the current is restricted, prolonged operation may ultimately result in degradation (especially of  $h_{FE}$  and  $V_{(BR)CEO}$ ) to the point of failure. The repetitive voltage sweep of the transistor tester is ideally suited to producing such gradual failures, since the current is externally limited and immediate catastrophe is avoided.

Since it is basically a thermal effect, involving excess carrier generation, second breakdown is a slow phenomenon compared with many of the switching applications of transistors. Delay times in the range from microseconds to milliseconds and transition times of microseconds are typical, so that in switching and class C amplification applications, where the current is turned off in less than these times, second breakdown is less likely to occur than in d.c. circuits and class A amplification, where the heating effects build up rapidly.

A form of second breakdown effect can be observed in some individual p-n junction diodes, but in transistors there is an additional complication of the presence of the base and its input, if any. Not much heating is necessary to produce enough current generation in the base to make the transistor largely independent of any external source. Schafft points out that if the collector current is held constant in the second breakdown region, reverse base drive tends to increase current crowding into the 'pinch' region, thus decreasing  $V_{CE}$ , while forward base drive conversely increases  $V_{CE}$  (Fig. 9). (This is the opposite effect to that found in thermal runaway involving overheating of the whole active area.) In fact, the current constriction may sometimes be reduced, by increasing the forward base drive, to the extent that the device moves out of second breakdown while maintaining a high collector current.

The shape of a second breakdown transistor characteristic is similar to that of the normal open base characteristic up to a level which may be well

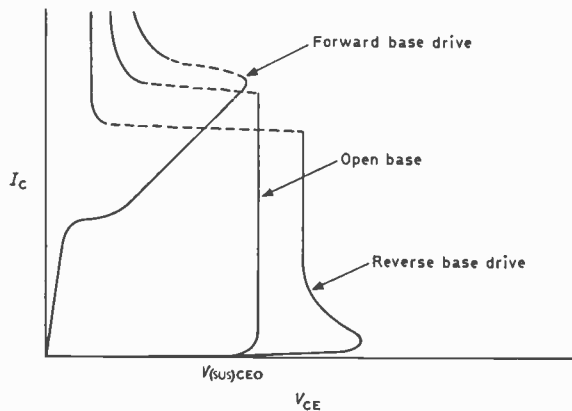


Fig. 9. Effect of base drive on collector-emitter second breakdown characteristics.

into the avalanche breakdown region. At the critical current level (which is not necessarily the same at d.c. or high frequencies as that shown by a low-frequency curve tracer display) a negative resistance region leads sharply to a lower voltage in the stable state of second breakdown, which, according to the transistor design and thermal conditions, may lie between  $V_{CE} = \text{constant}$  (for good heat sinking) and  $V_{CE}I_C = \text{constant}$ . To this must be added the effect of any series resistance due to the test gear.

There have been a number of reports of symptoms associated with a tendency to second breakdown. Switchback on the  $I_{CEO}$  characteristic is one such feature, while a 'ballooning' of the collector characteristics on the curve tracer with open or forward base bias shows that thermal trouble is imminent. The onset of current crowding causes a distortion of the collector family due to decrease in gain, and it has been noticed that triple-diffused and epitaxial transistors sometimes show a sharp increase in  $V_{CE}$  before second breakdown. In the common base configuration, the thermally generated current causes a drop in  $V_{CB}$  after an emitter pulse, by partially discharging the collector-base capacitance. Yet another report suggests that reach-through from the collector junction to the collector contact (or substrate in epitaxial devices) induces second breakdown.

All these apparently disconnected features indicate the complexity of the second breakdown and its dependence on details of transistor design. The methods of avoiding second breakdown appear to have much in common with the means of ensuring linearity of current gain, since both involve minimizing natural tendencies to current crowding by maximizing emitter periphery, and minimizing base resistivity and width.

#### 4.2. Overheating and Thermal Runaway

The incidence of general, rather than localized, thermal runaway is now rare in silicon transistors, though it

can still happen with junctions capable of supporting more than their specified current inputs without breakdown. Obviously, high ambient temperatures or inadequate heat sinking encourage runaway, and in the latter context it must be remembered that the bonding of the transistor to its support is the first link in the thermal resistance chain. If inadequate dice bonding is the cause of thermal runaway, it will introduce other recognizable symptoms, which are described in Section 5 below.

The higher intrinsic carrier concentration of germanium, giving a lower temperature for onset of intrinsic conduction, makes germanium transistors more susceptible to runaway.

### 5. Mechanical and Header Effects

In this Section we will consider types of misbehaviour which can be attributed to factors outside the semiconductor: the contacts, leads, and header, as well as factors related to mechanical stresses or damage to the transistor chip.

#### 5.1. Contact Defects

A high-resistance contact decreases the slope of the forward characteristic of the junction to which it leads, and it often adds a finite resistance beyond avalanche breakdown. In the common-emitter mode, collector resistance, which usually results from a poor die-to-header bond, is recognizable in the abnormal saturation characteristic:  $V_{CE(\text{sat})}$  is high but still linear with respect to current while the corresponding  $V_{BE}$  is normal. The effect of base or emitter resistance is also seen in  $V_{BE}$  and in the  $I_{CES}$  characteristic, which shows something of the 'switchback' normally associated with the  $I_{CER}$  mode.

In addition to these obvious resistive effects, substandard bonds to contact areas are liable to produce hot-spots immediately underneath, which can ultimately lead to failure. Young and Elkins<sup>18</sup> have shown that gold ball bonds to planar devices may melt locally, so that gold alloy penetrates the junctions. The onset of this type of fault at the emitter is often marked by a softening of the reverse characteristic of the junction, as well as by excessive noise from the device in operation and a loss of gain due to decreased emitter efficiency.

Faults in the mounting of devices—base contact tabs of alloy transistors, and collector substrate to header bonds of planar devices—introduce thermal resistance as well as the electrical resistance already noted. A device with such problems will suffer from overheating effects, which increase leakage currents and sometimes soften the avalanche characteristics, as well as making second breakdown and thermal runaway more likely to occur.

### 5.2. Cracks

A fault which occasionally results from bonding pressure errors, or may originate from the cutting or cracking stage of separating the semiconductor chips, is a crack across the active region (including of course, any channels which may exist). By introducing a discontinuity in the field distribution, a crack usually reduces the breakdown voltage for the junction in much the same way as the intersection with a surface. Reliable experimental reports of the effects of such faults, uncluttered by associated defects, are rare, but a 2-volt step-back of an otherwise linear collector-base avalanche characteristic has been associated in one report with a crack under the gold ball bond to the base.

The ingress of impurities into cracks, either during processing or subsequently, causes drift of junction leakage currents, as well as noisy instabilities both in the leakage currents and the breakdown characteristics of junctions affected. If the collector-base junction alone is cracked,  $h_{FE}$  will hardly be affected, and  $I_{CES}$  and floating emitter potential will be normal, so that only the collector-base and collector-emitter characteristics will be upset. On the other hand a crack affecting the emitter junction produces a high floating potential and  $I_{CES}$  much greater than  $I_{CBO}$ , while the high emitter junction leakage degrades the low current  $h_{FE}$ . If both junctions are cracked, the effect is as if a base channel were present in addition to the combined effects on the separate junctions.

### 5.3. Header Leakage Currents

One important external factor which can affect the electrical characteristics is leakage currents across the header, usually attributable to surface contamination or occasionally to insufficient insulation around the leads. If it is on the outside surface some form of washing will usually remove the offending material, but identification of other header leakages are more of a problem. Baking may help, but in the last resort, opening the can and severing the leads inside is the only answer. Leakages of this type can thus be simulated by external resistances on a good transistor, as described above.

## 6. Diagnosis of Faults from Abnormal Electrical Characteristics

The diagnosis of faults from the current-voltage characteristics of transistors is always a qualitative process: it is usually necessary to look for additional evidence to determine where the fault is located and what it consists of. For example, a short-circuit is readily diagnosed, but its identification as due to an internal effect, a surface effect, or an extraneous metallic object may often be a matter of painstaking study. A further difficulty is that because the measure-

ments which show unusual characteristics may be made under different conditions, some faults may show up much better on some tests than on others. An example of this is emitter junction problems, which may show up in  $h_{FE}$  or in  $I_{EBO}$  tests, but very often not both, because the former is a forward-bias test and the latter is done at reverse bias, so that the significant part of the junction is not the same in the two cases.

Table I approaches the diagnosis problem by taking each abnormality in turn, recording as many interpretations as possible, and then, for each of these, indicating other electrical or other tests which might confirm the verdict. It will be assumed that where not otherwise stated, remarks about 'excessive leakage current' imply 'for a given voltage, as compared with a perfect sample', and so on. The lists can obviously not be exhaustive: circumstances may sometimes give unexpected combinations or cancellations of effects, which can only be interpreted if additional evidence becomes available from visual or other observations.

The interpretations given in this Table must not be applied mechanically to the results given by many automatic testing methods, in which current levels at fixed voltages or, more commonly, voltage levels at fixed currents are recorded. For example, an automatic test for junction breakdown voltage might be to measure the voltage which produces 1mA avalanche current. However, if a shunt path existed, this amount of current might be recorded well below the true breakdown voltage, so that the record would show high leakage *and* low breakdown, where the true verdict should be high leakage alone. Similarly a collector-emitter shunt path will upset the d.c. ratio  $I_C/I_B$  used to measure gain at low collector currents, even though the high current and small-signal gains are normal.

A visual display of the characteristics on a curve tracer is essential.

## 7. Progressive Changes in Properties

The majority of devices presented to a failure analyst have little or no record of previous history attached, so that the levels of leakage currents and breakdown voltages can only be judged by comparison with a device which fulfils the normal specifications. However, it will by now be obvious that, apart from catastrophic failures, a large proportion of detrimental effects are progressive in nature, so that information such as whether the leakage currents are rising or falling can provide valuable aids to the choice between the possible explanations of a spot check result.

The value of continuous monitoring of changes in breakdown voltage which often precede large changes in leakage current has already been noted. The voltage changes often lie within the specified range for good

**Table 1**  
Diagnostic Table

Primary indications	Additional indications	Interpretations and suggestions for further action
<b>Two-terminal characteristics</b>		
<i>Emitter-base junction</i>		
High $I_{EBO}$ (and low-level gain reduced)	(a) $V_{(BR)EBO}$ normal, ohmic current	External leakage path, or strong channel, base contact to emitter.
	(b) $V_{(BR)EBO}$ low, $I_{CBO}$ normal	Channel on base side of junction (especially n-p-n planar).
	(c) as (b), but little temperature dependence	Emitter inversion, giving tunnelling (especially p-n-p planar).
	(d) with instabilities of current and $V_{(BR)EBO}$	Crack across emitter junction.
Soft breakdown	(a) with high $I_{EBO}$ at lower levels	Device overheated, giving large diffusion current.
	(b) with excessive noise	Hot-spots under defective bond. Examine cross-section.
	(c) with entirely abnormal emitter behaviour (e.g. strong dependence of $I_{EBO}$ on bias)	Emitter abnormalities such as precipitate particles producing microplasmas.  Examine cross-section after looking for light emission below breakdown.
Resistive forward characteristic		High-resistance emitter or base contact.
Low slope to logarithmic low-level forward characteristic		Channel on base side of junction (especially n-p-n planar) or tunnelling due to emitter inversion (especially p-n-p planar).
<i>Collector-base junction</i>		
High $I_{CBO}$ , ohmic	(a) temporarily reduced below 0°C or above 100°C. May be unstable and/or noisy	Surface moisture. Puncture can; vacuum bake, and observe permanent disappearance of leakage.
	(b) not removed by baking	External leakage path or strong channel, base contact to collector.
High $I_{CBO}$ , in silicon devices, with normal voltage dependence	(a) $I_{EBO}$ also high when measured immediately after $I_{CBO}$	Large diffusion current, device may be overheating. Examine low-voltage forward characteristic for high logarithmic slope.
	(b) $I_{EBO}$ unaltered	Saturating channel, collector to base contact; may be removable by baking.
$I_{CBO}$ rises, above a threshold voltage, to a new saturated level		Isolated channel. Observe photocurrent as light spot is scanned across junction: response is obtained from channelled areas. Look for corresponding jump in junction capacitance above the threshold voltage. If surface impurity migration is responsible, channel may be removed by baking.
High $I_{CBO}$ , possibly drifting with time and applied voltage, and/or noisy	(a) $h_{FE}$ , $I_{EBO}$ , and floating emitter potential normal	Crack in collector-base junction, breakdown characteristic may be abnormal and noisy.
	(b) $h_{FE}$ low, $I_{EBO}$ and floating emitter potential high	Crack through both junctions.
Low $V_{(BR)CBO}$	(a) $V_{(BR)CBO} = V_{(BR)CEO} + V_{(BR)EBO}$	Punch-through, collector to emitter (Fig. 10). Check that $V_{(BR)CES} = V_{(BR)CEO}$ (i.e. that relationship is not fortuitous), and look for light emitted from avalanching emitter junction. Examine cross-section for abnormally thin base (though it may be a normal-thickness, high resistivity base).

**TRANSISTOR ABNORMALITIES AND  $I$ - $V$  CHARACTERISTICS**

Primary indications	Additional indications	Interpretations and suggestions for further action
	(b) unrelated to $V_{(BR)CEO}$ and $V_{(BR)EBO}$ , in epitaxial devices  (c) possibly 'walking-out'  (d) combined with low $h_{FE}$ and high $I_{CBO}$ , possibly walking-out  (e) sharp break in $I_{CBO}$ curve at $V_{(BR)EBO}$ , followed by saturated or ohmic leakage, up to true $V_{(BR)CBO}$	Punch-through to epitaxial substrate, due to thin, high resistivity, collector layer. Look for non-linearity of $V_{CE(Sat)}$ at low levels, confirming high resistivity, and change of slope in capacitance-voltage characteristic near $V_{(BR)CBO}$ . Examine cross-section. Accumulation layer on collector surface (especially in n-p-n planar). Collector channel (especially p-n-p planar). If emitter contact is expanded over collector, it may be severed and used as a gate electrode to cancel part of the channel, reducing $I_{CBO}$ . <sup>19</sup> Base channel or other current path collector to emitter (Fig. 10). Check that $I_{CBS} > I_{CBO} > I_D$ (the base current in the 'shorted' $I_{CBS}$ condition). Comparison with emitter-base characteristic measures shunt path resistance.
High $V_{(BR)CBO}$		Depletion layer on collector surface (especially in p-n-p planar).
Soft $V_{(BR)CBO}$ , with abnormally high voltage dependence of $I_{CBO}$ at lower levels		Local microplasma breakdown due to defects in the collector junction region. Observe light emission.
Loop on $V_{(BR)CBO}$ characteristic	(a) high leakage currents, possibly unstable  (b) excessive junction capacitance	Internal moisture. Check that there is no change in a dry gas ambient, and then observe loss of effect on puncturing can and baking. May be constructional fault, or effect of polarized impurities.
Forward characteristic resistive		High collector or base series resistance.
Low slope to logarithmic low-level forward characteristic <i>Collector-emitter characteristic</i>		Channel over high resistivity side of junction.
High $I_{CEO}$ , ohmic Sharp break in $I_{CBO}$ curve at $V_{(BR)EBO}$ , followed by a resistive region. $h_{FE}$ normal	(a)  (b) (c)	Strong base channel (especially in planar n-p-n).  External leakage path. Internal path between collector and emitter due to damage.
High $I_{CEO}$ , ohmic	$I_{CBO}$ also high, with $I_{CEO} = h_{FE} I_{CBO}$	High collector-base leakage (q.v.).
High $I_{CEO}$ , saturating	(a) $I_{CBO}$ and $I_{EBO}$ also high and saturating (b) $I_{CBO}$ also high and saturating. $I_{EBO}$ normal (c) $I_{CBO}$ and $I_{EBO}$ normal, $h_{FE}$ very high at low levels	Base channel (especially in planar n-p-n).  Saturating channel, collector to base contact.  Collector-emitter channel, not touching base contact, acting as a f.e.t. (especially in planar n-p-n). <sup>12</sup>
Low $V_{(BR)CEO}$	(a) Current limited beyond breakdown, $V_{(BR)CBO} = V_{(BR)CEO} + V_{(BR)EBO}$ and $V_{(BR)CES} = V_{(BR)CEO}$	Punch-through, collector to emitter. Examine cross-section for thin high resistivity base region.
Large snapback beyond breakdown to a characteristic between $V_{CE} = \text{const}$ and $I_C V_{CE} = \text{const}$		Second breakdown, due to thermal effects often involving high base resistivity and base width. Check thermal resistance versus input power for instability. Apply forward bias to base junction, with constant collector current, and observe increase in $V_{CE}$ .

Primary indications	Additional indications	Interpretations and suggestions for further action
$V_{(BR)CEO}$ high, with snapback to a normal sustaining voltage	(a) $I_{EBO}$ high, $h_{FE}$ low (b) low $f_T$ , $h_{FB}$ , and $h_{FE}$ . $I_{EBO}$ normal	Base-emitter leakage (q.v.). Wide base region limiting the contribution of emitter injection to the avalanche at the collector junction. Examine cross-section.
Linear forward characteristic		High series resistance in emitter or collector.
<b>Two-terminal characteristics with third electrode connected</b>		
<i>Collector-emitter, with base-emitter resistance</i>		
Little diagnostic value		
<i>Collector-emitter with base shorted to emitter</i>		
$I_{CES}$ high	(a) much higher than $I_{CBO}$ . $h_{FE}$ almost normal, but with parallel leakage (b) much higher than $I_{CBO}$ . $h_{FE}$ low (c) $I_{CBO}$ also high and almost equal (d) $I_{CBO}$ also high. Both recover in hot dry ambient	Base channel, or other path from collector to emitter. Comparison with $I_{CBO}$ measures shunt path resistance. Crack across both junctions. Check for high $I_{EBO}$ and floating emitter potential. Collector channel. Header leakage (external).
$V_{(BR)CES}$ showing snapback (possibly with $V_{(BR)CES}$ less than $V_{(BR)CBO}$ )		Significant series resistance to emitter or base (Fig. 11).
$V_{(BR)CES}$ low, equal to $V_{(BR)CEO}$		Punch-through, collector to emitter.
<b>Three-terminal characteristics</b>		
<i>Common base operation</i>		
$h_{FB}$ low at all input levels	$f_T$ and $h_{FE}$ also low	Thick or low resistivity base. Examine cross-section.
<i>Common emitter operation</i>		
$h_{FE}$ non-linear with base input	(a) low at low levels, and decreasing at high levels (b) very low at low levels, normal at higher levels. $I_{EBO}$ high, $I_{CBO}$ normal (c) very high at low levels, reducing to normal at high levels	Narrow and/or lightly-doped base. Examine cross-section. Base-emitter leakage (q.v.). Collector-emitter channel, not touching base contact, acting as a f.e.t. (especially in planar n-p-n). <sup>12</sup> Check that slope of a plot of $\ln I_C$ vs. $V_{BE} < q/kT$ .
$h_{FE}$ low for all input levels	(a) $h_{FB}$ and $f_T$ also low. Possibly 'looped' characteristics (b) $V_{(BR)CBO}$ low, $I_{CBO}$ and $I_{CEO}$ high	Thick or low resistivity base. Examine cross-section. Collector channel (especially in planar p-n-p). See above test for expanded contact devices. <sup>19</sup>
$h_{FE}$ high at all input levels	$I_{EBO}$ rather high, $V_{(BR)EBO}$ possibly low	Base inversion extending emitter area in devices of low uniform base doping (especially n-p-n).
$V_{CE(Sat)}$ high for all input levels	(a) $V_{BE(Sat)}$ normal. High thermal resistance (b) $V_{(BR)EBO}$ soft, $h_{FE}$ low, $V_{BE(Sat)}$ high	High collector resistance, or poor collector bond in header-mounted devices. Poor emitter bond. Examine cross-section.
$V_{CE(Sat)}$ low at low collector currents, increasing more rapidly at higher levels	$V_{(BR)CBO}$ possibly high	High resistivity collector region in epitaxial device. <sup>20</sup> (Fig. 12).
$V_{BE(Sat)}$ high for all input levels	$V_{(BR)EBO}$ soft, $h_{FE}$ low, $V_{CE(Sat)}$ normal	Poor base bond.
'Ballooning' and collapse of characteristics on curve tracer	Device runs hot	Thermal runaway. Increase of forward base drive reduces collector voltage for a given collector current (cf. opposite effect with second breakdown).

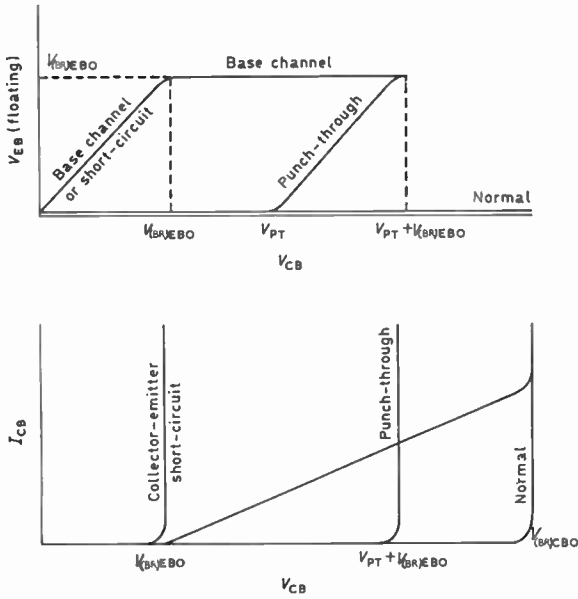
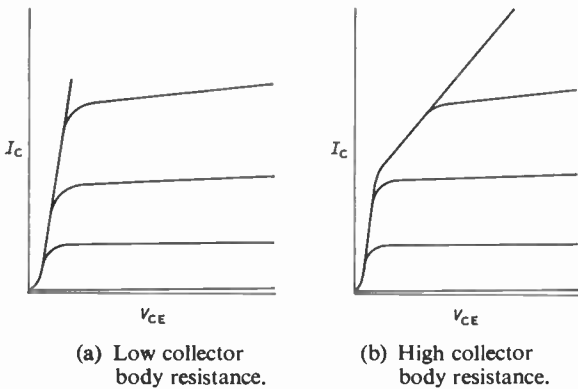


Fig. 10. Effects of emitter junction on collector-base characteristic.

devices, so that to detect them on a spot check might be impossible. However, the data recorded on life tests may reveal the trends, so that this is an area where the much-maligned long-term test may actually give useful information.

The details of leakage current changes with surface state are quite complex, but a very valuable simulation of some of the effects has been reported by Reddi,<sup>11</sup> who used a gate electrode over the emitter-base oxide to swing planar devices of various doping profiles from base inversion to emitter inversion. These emitter junction leakage current results are summarized in Fig. 13, in which the onset of tunnelling at high base doping levels will be obvious. The results shown are for n-p-n transistors; p-n-p devices give results which are basically similar, with the reservation that the common dopant (boron) used for p<sup>+</sup> emitters does not



(a) Low collector body resistance. (b) High collector body resistance.

November 1969

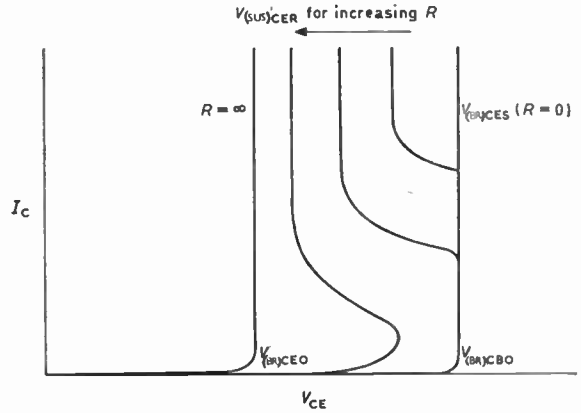


Fig. 11. Relationship of  $I_{CBO}$ ,  $I_{CBS}$ ,  $I_{CER}$  and  $I_{CEO}$  characteristics.

reach as high a surface concentration as the phosphorus used for n<sup>+</sup> emitters, so that the normal n-type surface tendency has an earlier incidence in the p-n-p results.

Figure 13(a) is for a base surface concentration of  $10^{18} \text{ cm}^{-3}$ . In this and subsequent curves, there is tunnelling current at the emitter inversion end of the scale, and minimum current at the ideal 'flat band' condition (when neither side of the junction is depleted or accumulated). As the base becomes depleted, there

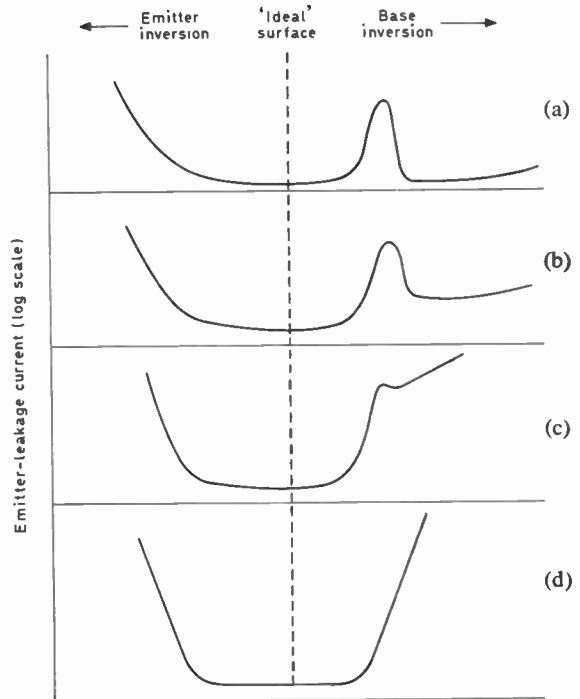


Fig. 13. Effect of changes of surface potential on emitter junction leakage currents.

- (a)  $C_{BS} = 10^{18} \text{ cm}^{-3}$
- (b)  $C_{BS} = 3 \times 10^{18} \text{ cm}^{-3}$
- (c)  $C_{BS} = 5 \times 10^{18} \text{ cm}^{-3}$
- (d)  $C_{BS} = 7 \times 10^{18} \text{ cm}^{-3}$

is a peak where the surface recombination takes effect, while beyond this, the field-induced junction moves the depletion layer inwards from the surface, and the bulk recombination rate operates to give a current similar to that under flat-band conditions. Figure 13(b) corresponds to a base surface concentration  $C_{BS}$  of  $3 \times 10^{18} \text{ cm}^{-3}$ . Here the bulk recombination rate is increased below the surface, so that when the field-induced junction moves in, the leakage current is higher than at flat-band. In Fig. 13(c), with  $C_{BS} \approx 5 \times 10^{18}$ , there is appreciable tunnelling beyond the surface recombination peak, while at  $C_{BS} \approx 7 \times 10^{18}$ , in Fig. 13(d), the peak is lost in the large tunnelling current to give a nearly symmetrical curve.

Since gain is inversely proportional to base current, we can take the inverse of these curves to represent gain changes, and if there is a progressive change in surface charge density, we can regard the horizontal axes as time axes. On this basis, according to the starting-point, we can simulate many of the upward, downward, or fluctuating changes of gain observed in the early life of many transistors.

Smith and Vaccaro<sup>7</sup> have discussed the rate laws governing the change of properties of p-n junctions in terms of the various known surface, volume, and contact degradation mechanisms. The application of this approach to transistors presents more difficulty, because of junction interactions. In any case, the problems of monitoring the very early stages of degradation and singling out likely specimens for detailed kinetic study of long-term mechanisms are not to be underestimated.

### 8. Conclusions

The Table shows that some features of transistor behaviour, as seen on a curve tracer display, can lead to quite firm conclusions as to the physical faults which exist. These faults are largely those concerning the bulk junction structure, and those surface and external features which are ohmic in character. When it comes to channels and other non-linear effects, ambiguity sets in rapidly, and although the electrical behaviour may be fully characterized, the physical origins can often be discovered only after extensive examination with a variety of techniques. Consideration of changes of gain, breakdown voltages, and leakage currents during life, can, if these have been recorded, help to remove the ambiguities. It is always important to obtain the maximum of electrical information about a suspect transistor in its encapsulated state, since any subsequent treatment by the failure analyst, even if not actually destructive, may produce irreversible changes which mask the original fault forever. Success in the overall field of failure analysis depends critically on this initial step of intelligent electrical testing.

### 9. Acknowledgment

This paper is published by permission of the Controller, H.M. Stationery Office. Crown Copyright Reserved.

### 10. References

1. 'Physics of Failure in Electronics,' Vol. 4, Rome Air Development Centre, 1966, and Proc. Sixth Annual Reliability Physics Symposium, Los Angeles, 1967, I.E.E.E., 1968.
2. Burford, W. B. and Verner, H. G., 'Semiconductor Junctions and Devices' (McGraw-Hill, New York, 1965).
3. Grove, A. S., 'Physics and Technology of Semiconductor Devices' (John Wiley, New York, 1967).
4. Lawrence, J. E., 'The cooperative diffusion effect', *J. Appl. Phys.*, 37, p. 4106, October 1966.
5. Grove, A. S., *loc. cit.*, pp. 298-305.
6. Fitzgerald, D. J. and Grove, A. S., 'Physics of Failure in Electronics,' Vol. 4, p. 315. Rome Air Development Centre, 1966.
7. Smith, J. S. and Vaccaro, J., 'Physical basis for evaluating the reliability of p-n junction devices' *Trans. I.E.E.E. on Reliability*, R-17, p. 20, March 1968.
8. Coppen, P., 'Causes, effects and a cure for channelling in silicon planar transistors', *Semiconductor Products and Solid State Technology*, p. 20, July 1965.
9. Holmes, P. J. (Ed.), 'The Electrochemistry of Semiconductors', p. 335. (Academic Press, London and New York, 1962).
10. Mathews, J. R., Griffin, W. A. and Olson, K. H., 'Inversion of oxidised silicon surfaces by alkali metals', *J. Electrochem. Soc.*, 112, p. 899, September 1965.
11. Reddi, V. G. K., 'Influence of surface conditions on silicon planar transistor current gain', *Solid State Electronics*, 10, p. 305, April 1967.
12. Rosenbaum, S. D. and Loro, A., 'Explanation of ultra-high current gain in silicon transistors', *Solid State Electronics*, 6, p. 545, September-October 1963.
13. Baird, S. S., 'The Chemistry and Physics of Semiconductor Reliability', Chapter in Proc. Conference on the Reliability of Semiconductor Devices and Integrated Circuits, U.S. Department of Defense, New York, 1964.
14. Steigler, R. W., 'Electric Detection of Surface Effects in Transistors', Texas Instrument Inc. Information Sheet.
15. Card, W. H., in 'Physics of Failure in Electronics' (Ed. M. E. Goldberg and J. Vaccaro) p. 231 (Cleaver-Hume, London, 1963)
16. Schafft, H. A., 'Second breakdown—a comprehensive review', *Proc. I.E.E.E.*, 55, p. 1272, August 1967.
17. Hakim, E. B., 'An advancement in transistor second breakdown performance using molybdenum metalization', *Trans. I.E.E.E., on Reliability*, R-17, p. 45, March 1968.
18. Young, M. R. P. and Elkins, O. M., 'Failure mechanisms in silicon transistors deduced from step stress tests', *Microelectronics and Reliability*, 5, p. 271, November 1966.
19. Workman, W., 'Failure modes of integrated circuits and their relationship to reliability', *Microelectronics and Reliability*, 7, p. 257, August 1968.
20. Hahn, L. A., 'The saturation characteristics of high-voltage transistors', *Proc. I.E.E.E.*, 55, p. 1384, August 1967.

Manuscript first received by the Institution on 25th February 1969 and in final form on 17th June 1969. Paper No. 1285(CC57.)

© The Institution of Electronic and Radio Engineers, 1969

# A 1MV Electron Microscope

The first of five one-million volt electron microscopes now nearing completion at the Harlow factory of AEI Scientific Apparatus Limited (part of the GEC-Elliott Automation Group), has already been operating successfully at its rated voltage during tests over the past few weeks. The Atomic Energy Research Establishment is shortly due to take delivery of this advanced instrument, the first commercial million-volt electron microscope to be built in Europe.

It will be used to investigate thicker sections of metals and materials than hitherto possible using an electron beam accelerated by 10 times the voltage used in a conventional high resolution electron microscope. Biologists will also use these electron microscopes to study the structure of cells; it is also possible that the great penetrating power of these new instruments may permit observation of living material in special protective surroundings in the microscope.\*

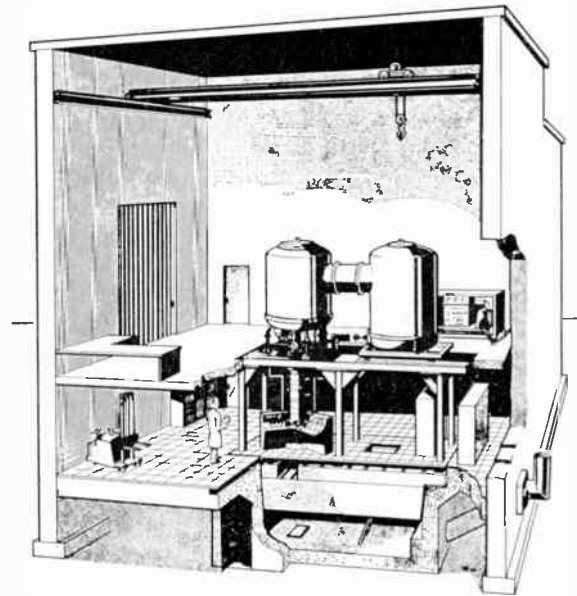
This project—funded by the company with the support from the Ministry of Technology—was announced just over two years ago. Similar EM7 million volt microscopes have been ordered from AEI for the National Physical Laboratory (financed by MinTech.), Imperial College, London, and Oxford University. A fifth instrument, to be installed at the British Steel Corporation's Rotherham Laboratory, has been ordered by BISRA. The Science Research Council are providing half the cost of this machine, and are funding the purchase of the instruments for Imperial College and Oxford University.

Overseas interest in the instruments is increasing and potential users from North America and Europe are currently evaluating them.

This EM7 one-million volt microscope design has been evolved in very close collaboration with the prospective users so that it incorporates an exceptional range of operating conditions and gives the facilities for future extensions without modifying the design.

The 1MV generator and electron beam accelerator are each housed in a pressure vessel, the components being insulated from the tank walls by sulphur

\* A discussion of high-voltage electron microscopes and their applications by Dr. V. E. Cosslett, on whose 750 kV instrument the new 1MV microscope is based, has recently been published in *Quarterly Reviews of Biophysics* (2, No. 2, pp. 95-133, 1969).



Artist's impression of typical installation of AEI million-volt electron microscope Type EM7.

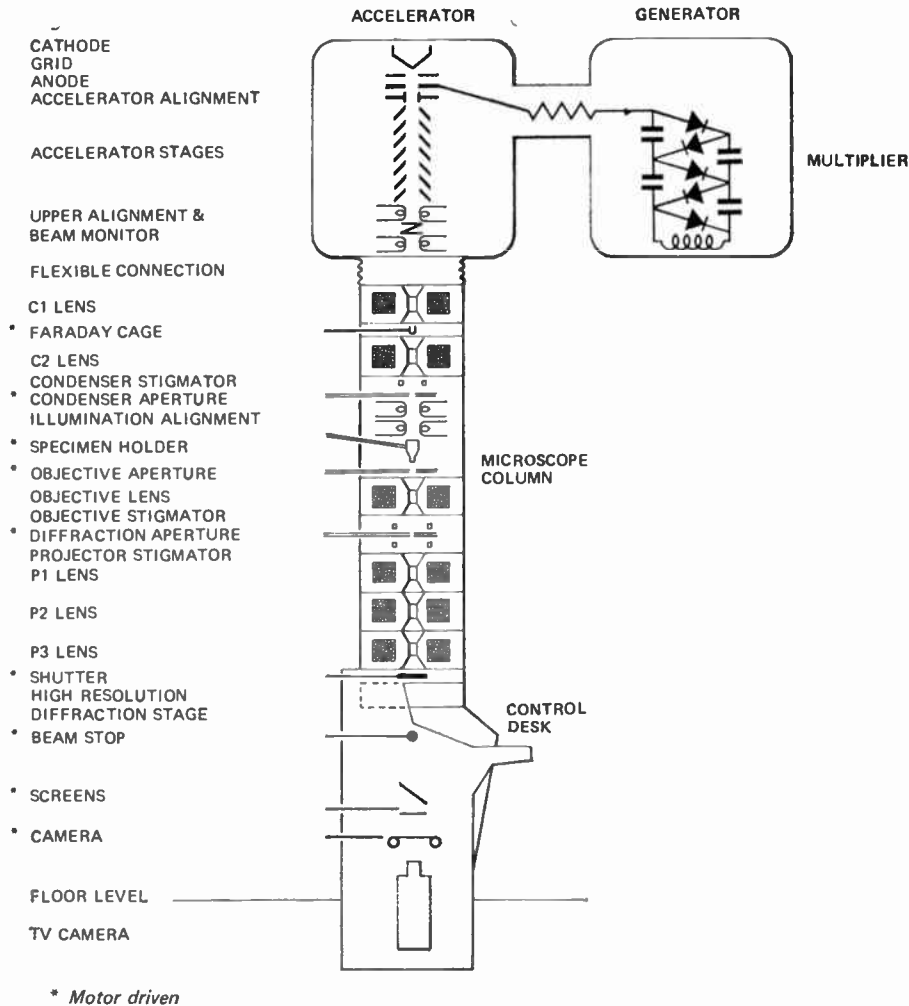
hexafluoride gas at a pressure of three atmospheres. This design provides a highly stable source of high tension and is extremely flexible in operating over the very wide range of 100 kV to 1000 kV, providing an exceedingly wide choice of experimental conditions in this microscope. Increased operating up to 1.2 MV will be possible.

The entire microscope is massive and weighs 22 356 kg (about 22 tons). Huge electromagnetic lenses, weighing about a quarter of a ton each, provide the very strong magnetic fields needed for focusing the high energy electron beam. They also provide the high degree of X-ray shielding necessary for the instrument to be operated in complete safety.

The specimen region is of crucial importance for the experimenter as this is where the material to be viewed is placed. A very large chamber has been provided with large access ports so that special experimental equipment can easily be accommodated. On the other hand the standard specimen handling facilities provide for rapid exchange of specimens and for operations such as tilting, heating, cooling and straining of the specimen to be carried out from the operator's position.

The specimen to be viewed is moved by a single 'joystick', a control which allows for movement in any direction with a wide range of speeds and motion. This is the first time that this kind of control system has been incorporated in an electron microscope.

The instrument provides magnifications from the low level of 63 times to the very high level of 1 600 000



Schematic diagram of the AEI one-million volt electron microscope Type EM7.

times. A wide range of camera lengths from 40 cm to 900 cm is available for studying the crystal structure of specimens under examination. Resolution with the EM7 microscope is currently at the conservative figure of 10 angstroms (1 nm); at present work is concentrated on ensuring the highest reliability of all operating systems but the project team will refine the control systems over the next few months to obtain the optimum resolution.

The image is projected on to one of two fluorescent screens, one screen for bright image working and the other for high resolution. This image is viewed through a very thick lead glass window to ensure that the operator is safe from any X-rays generated when the electron beam strikes the fluorescent screen. Below the viewing screen is a completely automated camera.

Because of the high penetrating power of the electron beam the camera plates have to be held out of the microscope column until required.

The lower part of the viewing chamber is supported on a plinth which is bolted to the concrete foundation block two feet below ground level, where a large space below the ground enables special equipment such as television camera, image intensifier, and energy analysers to be easily installed.

To reduce the size of the power supplies required to drive the electromagnetic lens, a 400 Hz generator is included with the equipment. The high tension equipment has been designed and supplied by Emile Haefely & Company of Basle, Switzerland, who specialize in the manufacture of high tension units for electron microscopes.

# Digital Computer Implementation of Bang-bang Process Control

By

P. ATKINSON,

B.Sc.(Eng.), A.C.G.I., C.Eng.,  
M.I.E.E., M.I.E.R.E.†

AND

R. L. DAVEY,

B.Sc.†

**Summary:** Optimum performance of a control system in terms of its time domain response can be achieved by the use of a bang-bang controller. The binary nature of the control signal together with the inherent complexity of a controller designed to achieve optimum bang-bang control of high-order systems, immediately suggests the use of an on-line digital computer. Previous methods of attempting bang-bang control using an on-line digital computer have encountered two major difficulties, namely excessively long computation time and excessive ripple at the output due to sampling. In such methods the amount of computation increases enormously as the order of the process to be controlled increases. This paper describes a new method which bypasses both of these major difficulties. The problem of long computation time is solved by trading computation time for computer storage. The information required for determination of switching times is determined once and for all at leisure in an off-line calculation. The information is then permanently retained in the store of the on-line computer. The problem of output ripple is solved by means of a dual-mode system. For large state errors the bang-bang algorithm is employed whilst for suitably small-state errors the computer changes the mode of control to a pseudo-linear mode in which the process receives an input signal which is still binary in form but which is pulse-duration modulated in such a way that the average value of the signal is that which it would receive from a tightly compensated linear controller.

The paper includes details of tests of the new method applied to a third-order type-0 process. These are a series of step-response tests on firstly a purely digital simulation and secondly a real-time hybrid simulation in which a digital computer is used on-line to bang-bang control a process simulated on an analogue computer. The results of these tests are compared with those in which the same process is controlled by means of a practical three-term controller. The comparison indicates the superiority of the new system.

## List of Principal Symbols

$v$	controller output	
$+V, -V$	full positive and full negative levels of controller output	
$e, \dot{e}$	process error and first derivative of error	
$H(s)$	open-loop transfer function of process	
$x$	process output	
$Dx$	first derivative of process output	
$D^2x$	second derivative of process output	
$x_g(j, k)$ $x_{g1}(j, k)$ $x_{g2}(j, k)$	arrays containing stored points on the switching surface	
$x_s, x_{s1}, x_{s2}$		values of $x$ for given values of $Dx$ and $D^2x$ found by interpolation on the switching surface
$Q$		input step demand

† Department of Applied Physical Sciences, The University of Reading, Reading, RG6 2AL.

## 1. Introduction

The control of process plants has been achieved conventionally by the use of analogue pneumatic and, at present to a lesser extent, analogue electronic controllers. These are incorporated into a feedback arrangement as shown in Fig. 1.

In general the best results have been achieved using three-term (proportional plus integral plus derivative) controllers. Most computer-controlled systems at present in operation employ algorithms which effectively produce the same control action. The parameters of this type of controller may be adjusted to obtain 'best' response on the basis of linear theory.<sup>1</sup> However, as the parameters of this or any type of linear controller are adjusted to obtain a faster and faster plant response, saturation of the controller output inevitably occurs. But for this effect a linear controller could be arranged to change the process from one state to another in zero time.

The best performance as regards plant speed of response is obtained using a time optimal control

system. It can be shown using Pontryagin's method<sup>2</sup> that the controller output in a time optimal system is at its positive or its negative saturation level at all instants in time. To obtain this form of control action, usually referred to as *bang-bang control*, the controller output  $v$  must switch between its full positive level ( $+V$ ) and its full negative level ( $-V$ ) at the correct instants of time. The fact that this type of controller has a binary output (i.e. has only two possible levels) makes the application of a digital computer as controller particularly suitable.

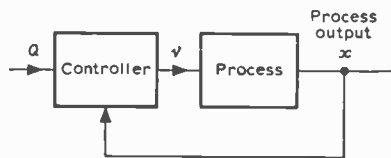


Fig. 1. Feedback arrangement for a typical process controller.

Although the concept of controlling a plant using only a simple two-state input signal is very attractive, its implementation for all but the simplest low-order processes is exceedingly difficult. In order to illustrate the problem let us consider the bang-bang control of a second-order process.

The phase plane diagram for such a process is a plot of the process error  $e$  and error derivative  $\dot{e}$ . With the controller output constrained to only two values the process error state ( $e, \dot{e}$ ) can only move along two sets of paths or trajectories in the phase plane. This is illustrated for the case of a process consisting of two pure integrations in Fig. 2.

For this there are two sets of parabolic trajectories, one for positive and one for negative control signals. If it is required to reduce an initial error from P (Fig. 2) to the phase plane origin O, then first a full positive control signal  $+V$  must be applied. The process state then moves along a parabolic trajectory of the  $+V$  set. At point M the control signal is switched to its full negative level ( $-V$ ) which causes the process to move along a trajectory of the  $-V$  set terminating at the phase plane origin. The trajectory MO and its corresponding trajectory NO together form a line often called the switching line. For time optimal control, the control signal must change its polarity whenever the state of the process crosses this line on the phase plane.

The determination of the switching trajectory for the second-order process is not difficult but the solution of the time optimal control problem for third or higher-order processes is much more complicated.

Again using Pontryagin's method it can be shown that the number of switchings from full positive to full negative control signal to change the state of a

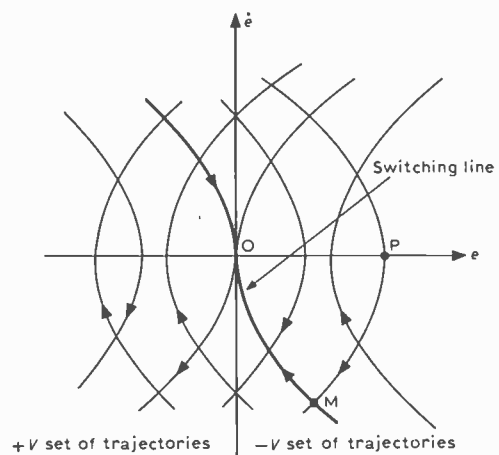


Fig. 2. Phase plane diagram for a second-order process.

process from any initial conditions to any final conditions depends on the order of the process. The second-order process requires two switching trajectories, a third-order would require three, a fourth-order four and so on. With the second-order process the switching trajectory is the locus of all states from which the state error can be reduced to zero by the application of full control signal for a single period. A third-order process requires three trajectories to bring the state error to zero from any initial conditions. The control signal must therefore change polarity when the state error crosses a switching surface rather than a line. In the course of an optimal control strategy the state error will cross this surface twice and the control signal must change its polarity at each crossing. This argument can be extended to an  $n$ th order process for which there is a set of  $(n-1)$  switching trajectories making an  $n$ -dimensional hyper-surface passing through  $n$ -dimensional phase space. In order to control a process from any general initial conditions to any final conditions the initial control signal is set according to the sign of the error. The process state is then observed and the control signal switched when the switching surface is reached. This is illustrated in Fig. 3 for a third-order process. The sign of the control signal at any time is dependent on the position of the process state error relative to the position of the switching surface. Referring to Fig. 3 the trajectory IJ is generated by a positive control signal. The trajectory JK, which should be on the surface, is generated by a negative signal. The final switching occurs when the trajectory reaches the point K on the switching surface. Point K makes a change in the direction of the surface relative to the trajectory JK. The control signal is switched so that the trajectory KO is followed to the final state at the origin.

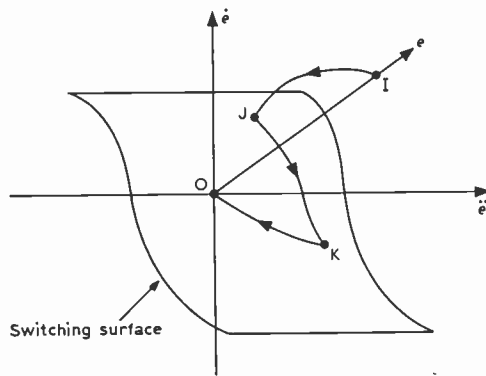


Fig. 3. Third-order process trajectory.

Although the method of obtaining bang-bang control by observing the state of the process relative to a switching surface is straightforward, the problems of determining and representing the switching surface remain. For second-order and some third-order systems an analytical solution may be obtained. This involves the elimination of the variable time from a set of equations for the trajectories. The switching surface is then represented by a non-linear equation in the state variables. For example, the switching surface for a third-order process containing three pure integrations has the form given by eqn. (1):

$$0 = x + \frac{(D^2x)^3}{3V^2} - \frac{DxD^2x}{yV} + \frac{y}{V^{1/2}} \left\{ \frac{(D^2x)^2}{2V} - yDx \right\}^{3/2} \dots\dots(1)$$

where

$$y = -\text{sign} \left( Dx + \frac{D^2x|D^2x|}{2V} \right)$$

The solution for processes containing exponential lags rather than pure integrations is very much more difficult to obtain. A schematic circuit based on an analytical solution for the control of such a process is given by Smith.<sup>3</sup> If control by this method were attempted using analogue means, complicated non-linear function generators would be required. If the control were attempted using a digital computer, evaluation of the non-linear terms would be time-consuming.

Another approach to solving the bang-bang control problem is to use a digital computer programmed to solve the equations iteratively. Analysis using Pontryagin's method<sup>2</sup> leads to a two-point boundary problem which may be solved iteratively. This results in the evaluation of points on the switch surface. Although this type of method has frequently been suggested as a solution to the bang-bang control problem, its implementation on-line appears to be impractical.

Another alternative approach to the bang-bang control problem involves the use of fast models.<sup>4</sup>

These fast models give repeated rapid predictions of the behaviour of the process showing the effect of switching the control signal at any particular instant. Higher-order processes require faster models within models. The speed of modelling seems to be a limitation of this method.

The reason why the introduction of time optimal bang-bang controllers has not been more widespread is that the increased complexity and computational time of the controller over its counterpart has not been justified by a corresponding improvement in performance. It appears to the authors that in an ideal method of controlling a time-invariant process, the bulk of the computation required should be carried out at the design stage and not during the on-line control. For a bang-bang controller this points to the precomputation and storage of the switching surface.

The object of this paper is to describe a new and convenient solution to the time optimal control problem which has been found suitable for implementation on a small digital computer working in real time. In this method points on the switching hypersurface are stored directly in the computer memory. A simple form of interpolation is used to estimate intermediate points on the surface so that a complete representation of the surface is obtained. Control action is achieved by observation of the state of the process relative to the position of the switching hypersurface in state space.

The work has been illustrated using a third-order, type-0 process having three exponential lags with a transfer function  $H(s)$  given by:

$$H(s) = \frac{1}{(1+s)(1+2s)(1+3s)} \dots\dots(2)$$

The choice of the type-0 process is especially significant because it is a practical problem raising some new difficulties which are not encountered when bang-bang control is applied to processes containing pure integrations.

For ease of explanation the method of controlling this process to the zero output state is first described. This is then extended to allow control to any final output.

The success of the technique may be judged by the fact that real time bang-bang control was established with a 4k, 12-bit word, PDP-8 computer using the relatively inefficient FORTRAN as the programming language.

## 2. Generation of Points on the Optimum Switching Surface

Many methods of finding points on the optimum switching surface have been put forward in the

literature. They are often presented as solutions to the bang-bang control problem itself and can include the control techniques mentioned in the introduction. The authors adopted a very direct approach. This involved tracing reverse-time phase trajectories from the state space origin. The first method that was attempted, using the computer to generate these trajectories, employed an approximate simulation of the process. This was however found to be unsatisfactory because when working in reverse time, simulation errors increase rapidly. In order to avoid this difficulty the reverse-time trajectories were calculated using the analytical expressions (see Appendix 1) for the process step response and its first and second time derivatives.

Starting from the phase space origin and using a small negative time increment, a computer program was arranged to step back along the final trajectory leading to the origin. At each time increment on this trajectory the control signal was reversed and a second trajectory was generated. The computer program thus gave a set of points lying on the switching surface. The form of the trajectories within this surface is shown in Fig. 4 plotted on the  $Dx$ ,  $D^2x$  plane.

In order to reduce the computation required during on-line control, it was decided to store the points on the switching surface as the set of values of  $x$  which lay on a square grid in the  $Dx$ ,  $D^2x$  plane. This implies that it was necessary to find a set of reverse-time trajectories each ending on a grid-crossing point. The difficulty in finding these points may be related to the computation required in other solutions to the time optimal control problem.

The first method that was attempted was to step out along all possible trajectories using a small time increment. Whenever the trajectory passed within a defined proximity of a grid-crossing point, the state space coordinates were recorded. Unfortunately, this

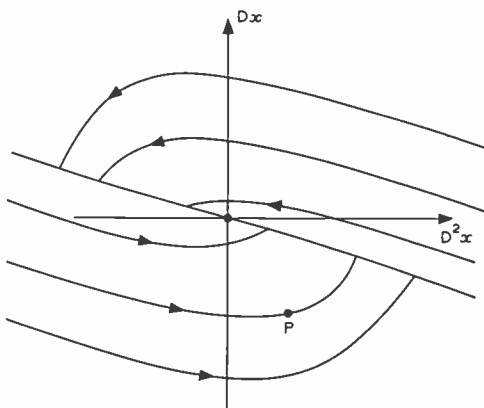


Fig. 4. Trajectories in optimum switching plane.

direct method required a very long computational time to obtain reasonable accuracy (an estimated 30 hours for a PDP-8 computer working on this specific problem). It was therefore decided to use a more sophisticated approach. This employed an iterative method which, starting from approximate values of final and second reverse trajectory times, adjusted the end point P (Fig. 4) to lie on a grid-crossing point. The optimization method first applied small time steps in the final and second trajectory times  $T_a$  and  $T_b$  to determine gradients in these directions. A two-dimensional linear extrapolation was then applied to adjust the times  $T_a$  and  $T_b$  to bring the state point nearer the grid-crossing point. The method was repeated using the new values of  $T_a$  and  $T_b$  until a suitable accuracy was obtained. Each grid-crossing point was treated in a similar manner. Details of the optimization technique are given in Appendix 2.

For the purposes of the third-order example (eqn. (2)) a square grid of 81 points in the  $Dx$ ,  $D^2x$  plane was chosen to represent the switching surface. The extent of this square grid was chosen on the basis of a plant simulation which gave the maximum likely excursions of the state variables.

### 3. Method of Control

It was explained in the introduction how bang-bang control of a process is implemented by observing the position of the process state in relation to the switching surface in state space. In the particular third-order system described here, this was most conveniently achieved by comparing the  $x$  value of the state of the process with the corresponding value of  $x$  on the surface for the same values of  $Dx$ ,  $D^2x$ . The difference measured in the  $x$  direction of the process state from the switching surface is thus continually monitored on-line. The sign of this difference determines the sign of the control signal to be applied to the process.

A point of the switching surface can be represented by three coordinates  $x$ ,  $Dx$  and  $D^2x$ . The switching surface here is defined at a set of values of  $Dx$ ,  $D^2x$  which lie on a grid in the  $Dx$ ,  $D^2x$  plane. This set of values is most conveniently stored in the computer as an array denoted by  $x_g(j, k)$ , (i.e. for specific values of  $j$  relating to values of  $Dx$  and  $k$  to  $D^2x$ ,  $x_g(j, k)$  represents a value of  $x$ ). This is illustrated in Fig. 5(a). To use the method of interpolation, knowledge of the state of the process in the  $Dx$  and  $D^2x$  plane can be used to locate the grid position of the state, indicated by its proximity to the grid point  $j, k$ .

The most simple possible form of interpolation was used to find the value of  $x$  (which will be called  $x_s$ ) on the switching surface corresponding to the current

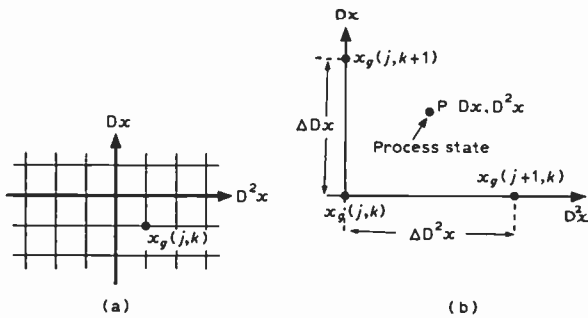


Fig. 5. Switching surface representation for storage in computer.

values of  $Dx$  and  $D^2x$  of the process at the point  $P$  (Fig. 5(b)). As indicated in Fig. 5(b) the interpolation was carried out using grid lines with positions  $Dx = a$  and  $D^2x = b$ , just less than the current state of the process. The interpolated value  $x_s$  on the surface for  $Dx, D^2x$  (Fig. 5(b)) is taken as  $x_g(j, k)$  plus the values interpolated between  $x_g(j+1, k)$  and  $x_g(j, k+1)$ . This interpolated value is given by eqn. (3):

$$x_s = x_g(j, k) + \{x(j+1, k) - x_g(j, k)\} \left\{ \frac{D^2x - b}{\Delta D^2x} \right\} + \{x_g(j, k+1) - x_g(j, k)\} \left\{ \frac{Dx - a}{\Delta Dx} \right\} \dots(3)$$

The surface generated using this method of interpolation is quite rightly open to objections, the main one being that the surface has discontinuities at the joins of all the segments. The authors however feel that the speed of computation in this method outweighs the disadvantages. The calculation has already to be carried out at each sampling instant and is the most time-consuming operation in the controller. There are many better methods of interpolation possible but all require a longer computational time.

4. Control of a Type-0 Process

The method of control which has been described uses one switch surface containing trajectories leading to the state space origin. The method is thus suitable for controlling a process from any initial conditions to a static output at zero. This is obviously not always required. Processes with transfer functions containing a pure integration present no difficulty as their dynamics are independent of the output. In a type-0 process however the effective full control signal in either direction appears to change with process output. For example, if the process (eqn. (2)) has a steady-state output of, say,  $+A$ , then the application of a control signal  $+A$  has no effect whilst the application of a control signal  $-A$  has however twice the effect it would have had if the output had been zero.

In order that the control system should cater for a

complete range of step input demands a different switch surface would be required for each step input. In effect an extra dimension has been added to the control problem. A practical solution to this problem was adopted. This involved introducing a limited number of extra switch surfaces leading to various final outputs. Linear interpolation was again carried out between these surfaces so that all possible outputs could be reached.

The method was tested using only one such extra surface, this one containing trajectories leading to a static output of  $x = 0.5$ . This surface and the one leading to the phase plane origin were defined by the same grid in the  $Dx, D^2x$  plane. During control of the process the values of  $x, (x_{s1}$  and  $x_{s2})$  lying on the surfaces were found for the values  $Dx, D^2x$  of the process state. If it were required to bring the process state to a static output of  $Q$  then the value of  $x, (x_s)$  on the surface leading to  $Q$  was determined using a simple linear interpolation given by eqn. (4).

$$x_s = x_{s1} + (x_{s2} - x_{s1}) \times Q/0.5 \dots(4)$$

5. Effects of Sampling

The use of the digital computer implies a sampled data system. This immediately presents a difficulty where optimum bang-bang control is desired. This difficulty is that the instant of control signal switching may not coincide with a sampling instant. The effect of this is most obvious when a bang-bang controlled process is under steady-state conditions. Here an almost random limit cycle of varying amplitude is produced, the magnitude of which depends on the complicated relation between sampling period and trajectory times. The authors have published<sup>5,6</sup> a solution to this problem which retains a bang-bang output from the controller. In essence this scheme contains a 'dual-mode controller'. For large state errors the bang-bang controller is operative; when the state error reaches a pre-defined minimum level a mode selector changes the control action to pseudo-linear. In this mode the binary output signal running at the sampling frequency is still retained but it is pulse-duration modulated in such a way that it has an average value equal to the output from a conventional linear compensated controller. The structure of the pseudo-linear controller will be dependent on the structure of the process being controlled; in many instances a satisfactory arrangement will be a three-term controller.

The dual-mode method has been successfully incorporated into the present scheme. The structure of the pseudo-linear controller required to control the particular process used as an example for the purposes of this paper is described in Section 6.3.

### 6. Simulation

The merit of the new technique for the implementation of bang-bang control was assessed by two independent methods. The first used an entirely digital simulation of both controller and process. The second, and more realistic, method used a hybrid arrangement with an on-line digital computer controlling an analogue simulation of the process in real-time.

#### 6.1 Digital Simulation

The digital simulation was carried out on a PDP-8 computer programmed using FORTRAN. The program contained three major sections:

- (i) The bang-bang controller algorithm.
- (ii) A pulse-duration modulation algorithm used for control when the process is under steady-state conditions.
- (iii) A purely digital simulation of the process under control.

The digital simulation of the third-order process containing three lags used the simplest possible form of numerical integration (Euler's method). Sufficient accuracy, however, was obtained by using a basic integration time step of 0.001 s, the three process time-constants being 1, 2 and 3 s respectively. The value of the process output  $x$  was sampled by the controller every 0.05 s by taking the value of the process output every 50 simulation steps. These sampled values of the process output  $x$  were used to evaluate the first and second derivatives ( $Dx$  and  $D^2x$ ) of the output, the evaluations being achieved by using the difference between two successive samples to calculate the first derivative  $Dx$ , and using the difference between two successive values of  $Dx$  to determine the second derivative  $D^2x$ . This method gives good accuracy providing that the sampling rate is high. If however the sampling rate is raised, then the difference between two successive sampled values of  $x$  becomes less and less. This difference ultimately has the same order of magnitude as the word length of the computer; this gives rise to inaccuracy and noise on the samples. The problem is further aggravated when calculation of  $D^2x$  is attempted using the difference between successive values of  $Dx$ . Tests were carried out on an exact simulation of the process which allowed accurate values of  $Dx$  and  $D^2x$  to be compared with those calculated by the method described using differing sampling rates. The sampling rate of 0.05 s was chosen as a compromise, this value giving the fastest possible sampling rate consistent with obtaining reasonably accurate values of  $Dx$  and  $D^2x$ .

#### 6.2. The Pseudo-linear Controller

The pseudo-linear controller had to take control satisfactorily from the bang-bang controller which, at

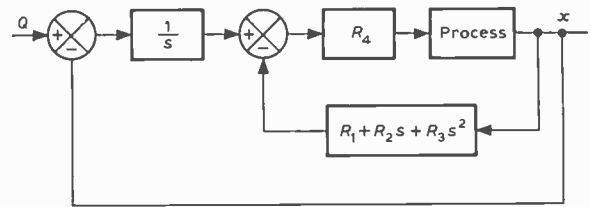


Fig. 6. A pseudo-linear controller.

mode change, left the process in an almost arbitrary state. The problem was thus not the usual one of obtaining a satisfactory response to a step command; it was the unusual problem of obtaining a satisfactory response from any possible initial conditions.

A suitable arrangement for the pseudo-linear controller was found to be that shown in Fig. 6.

Because the process investigated was type-0 it was necessary to introduce a pure integration term ( $1/s$ ) in the forward path of the controller. It was found that parallel compensation was sufficient to obtain stable control of the process from the set of initial conditions at mode change. In principle, values of  $R_1$ ,  $R_2$ ,  $R_3$  and  $R_4$  (Fig. 6) could be determined by various routine methods; pole cancellation is an example. It should however be borne in mind that pole cancellation will only ensure that the control system has good loop stability. It will not eliminate modes excited by the initial conditions. In fact more suitable values for the parameters were found by trial and error, the actual values used for most of the simulation work were:

$$R_1 = 30 \text{ s}, R_2 = 15 \text{ s}^2, R_3 = 5 \text{ s}^3, R_4 = 15 \text{ s}^{-1}.$$

#### 6.3 Hybrid Simulation

Two hybrid systems were set up. The first simulated the bang-bang controller on its own. The arrangement used is shown in Fig. 7.

Real-time control was obtained by using an interrupt clock to interrupt the digital computer at the sampling rate. Values of the process output  $x$  and output rate  $Dx$  were sampled from the analogue simulation and fed to the digital computer via an analogue to digital converter. Values of the second derivative of the process output were calculated by taking the difference between successive samples of the process output rate. In order to combat the noise problem associated with this type of calculation the analogue signal representing  $Dx$  was suitably filtered.

The second system which was set up simulated the complete dual-mode bang-bang controller. In order to allow control signal switching to occur at 'real' times other than at the basic sampling instants the interrupt clock rate was increased by a factor of fifty. A programmed routine was used to service these interrupt signals during the normal course of program

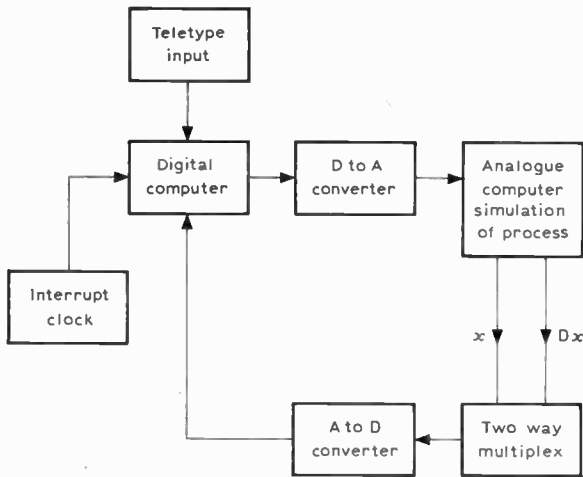


Fig. 7. Hybrid system simulating bang-bang controller.

operation. The analogue process simulation was sampled every fifty interrupts. When the process was operating in the pulse-duration modulation mode the controller output would switch at some time within the sampling period correct to one fiftieth of that period.

6.4. Simulation Results

The best tests which can be applied to this type of controller are step input demands. The results of step response tests carried out on the various simulations are shown in Figs. 8-11. The responses are shown superimposed for a range of positive step input demands. The main characteristic of these responses is that all follow the same response until switching occurs.

Figures 8 and 9 show the responses of the bang-bang controller alone computed with the purely digital (Fig. 8) and the hybrid (Fig. 9) simulations. These responses follow an almost exact optimal course until near the final output value. Both simulations

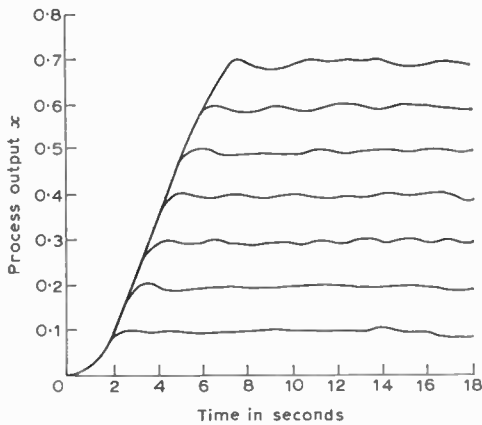


Fig. 8. Digital simulation of pure bang-bang system.

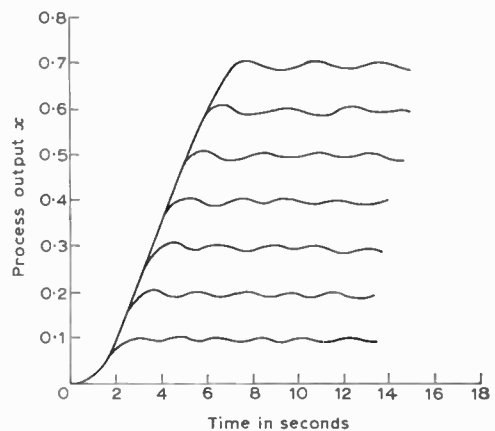


Fig. 9. Hybrid simulation of pure bang-bang system.

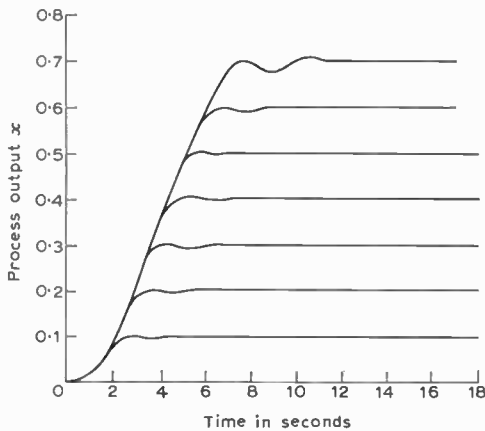


Fig. 10. Digital simulation of dual-mode system.

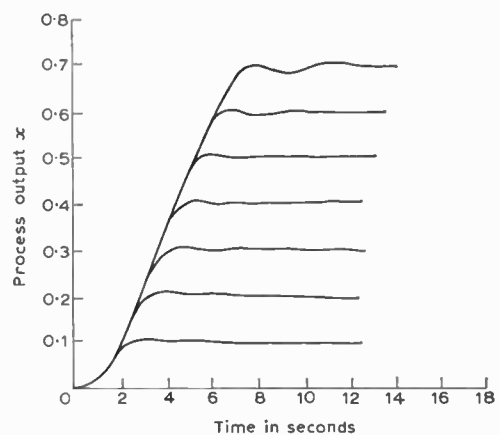


Fig. 11. Hybrid simulation of dual-mode system.

gave a steady-state ripple having the same order of magnitude. The small differences may be accounted for since different methods of obtaining the process output derivatives were used.

A marked improvement in the steady-state performance is shown when the step response was taken for the digital (Fig. 10) and the hybrid (Fig. 11) dual-mode control system simulations. A transient oscillation occurred when the controller changed mode from bang-bang to pulse-duration modulation. After this transient however the steady-state ripple was reduced to a very small value. Again the digital and hybrid simulations gave almost identical results.

Finally, in order to demonstrate the sort of improvement which can be obtained by using bang-bang control rather than traditional methods, a simulation was set up in which the same process was controlled by means of a three-term controller. The step-response of the system was then tested with various size inputs and the results of these tests are shown in Fig. 12.

This controller was simulated digitally and its output (i.e. the input to the process) was limited to the same values as the full positive and full negative outputs from the bang-bang controller. By this means a very realistic comparison can be made because saturation must occur in any practical controller. The parameters of the three-term controller were set up in the manner described by the authors in another paper.<sup>1</sup> This gave the following overall open-loop transfer function for the controller and process:

$$\frac{X}{Q}(s) = \frac{1 \cdot 1(1 + 1 \cdot 6s)(1 + 4 \cdot 8s)}{s(1 + s)(1 + 2s)(1 + 3s)}$$

The response to small step input demands is reasonably satisfactory although much slower than that which can be achieved using bang-bang control; however with progressively larger steps the overshoot and settling time become quite unsatisfactory.

### 7. Conclusion

The fundamental principles of bang-bang control have been outlined. A new digital computer-orientated method of implementation of bang-bang control has been described. Two problems associated with the digital implementation of bang-bang control have been isolated and solved. Firstly, the problem of switching the control signal at the correct instants has been solved using a matrix of stored points which represent the switching surface. Secondly, the problem of poor steady-state performance which inevitably arises with sampled data bang-bang control has been solved by a new method which retains the binary (bang-bang) nature of the controller output.

The method of digital bang-bang control which has been presented may be generalized to systems of

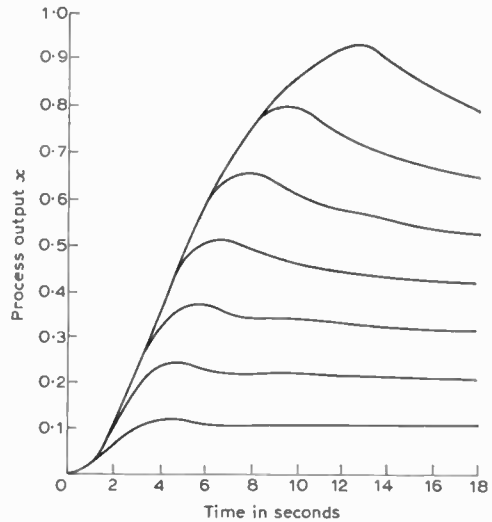


Fig. 12. Simulation of process control by three-term controller.

order higher than the third. Other methods of bang-bang control require long computational time due to either calculation of non-linear functions or the repeated running of nested process models. The method which has been described trades this problem for that of a larger computer storage requirement. Implementation of the method will require firstly identification of the process to be controlled, secondly, generation of the various switching surfaces. This work can be done using a powerful general-purpose computer which would provide data for use by a much simpler process control computer.

### 8. Acknowledgment

R. L. Davey wishes to acknowledge the Science Research Council for a three-year postgraduate research studentship which enabled him to participate in the research leading to the publication of this paper.

### 9. References

1. Atkinson, P. and Davey, R. L., 'A theoretical approach to the tuning of pneumatic three term controllers', *Control*, **12**, p. 238, March 1968.
2. Tou, J. T., 'Modern Control Theory' (McGraw-Hill, New York, 1964).
3. Smith, O. J. M., 'Feedback Control Systems' (McGraw-Hill, New York, 1958).
4. Adey, A. J., Billingsley, J. and Coales, J. F., 'Predictive control of higher order systems', *Proceedings of the Third IFAC Congress*, London 1966.
5. Atkinson, P., Davey, R. L. and Fellgett, P. B., 'Bang-bang controller using pulse-duration modulation to provide a central linear region', *Electronics Letters*, **4**, No. 6, p. 105, 22nd March 1968.
6. Atkinson, P., Davey, R. L. and Fellgett, P. B., British Patent Application No. 43091/67.

10. Appendix 1:

Determination of an Analytical Expression for Plant Step Response

The transfer function of the process given in eqn. (2) may be rewritten in general terms as

$$H(s) = \frac{X}{Q}(s) = \frac{1}{(1 + T_1 s)(1 + T_2 s)(1 + T_3 s)}$$

where  $T_1, T_2$  and  $T_3$  are time-constants.

Thus,

$$\frac{X}{Q}(s) = \frac{K}{(s+a)(s+b)(s+c)}$$

where

$$K = \frac{1}{T_1 T_2 T_3}$$

and  $a = \frac{1}{T_1}, b = \frac{1}{T_2}$  and  $c = \frac{1}{T_3}$

If the input  $Q$  is a step of magnitude  $V$  then

$$X(s) = \frac{KV}{s(s+a)(s+b)(s+c)} + \frac{D^2x_o + (a+b+c)Dx_o + (ab+ac+bc)x_o}{(s+a)(s+b)(s+c)} + \frac{sDx_o + x_o(a+b+c)}{(s+a)(s+b)(s+c)} + \frac{s^2x_o}{(s+a)(s+b)(s+c)}$$

where  $x_o, Dx_o$  and  $D^2x_o$  are the initial conditions of output, output rate and the second derivative of output respectively. Taking the inverse Laplace transform and simplifying gives the time response as:

$$x(t) = \frac{KV}{abc} + \frac{\exp(-at)}{(a-b)(c-a)} \left\{ \frac{V}{a} - D^2x_o - (b+c)Dx_o - bcx_o \right\} + \frac{\exp(-bt)}{(a-b)(b-c)} \left\{ \frac{V}{b} - D^2x_o - (c+a)Dx_o - cax_o \right\} + \frac{\exp(-ct)}{(c-a)(b-c)} \left\{ \frac{V}{c} - D^2x_o - (a+b)Dx_o - abx_o \right\}$$

11. Appendix 2:

Iterative Determination of the Position of the Switching Surface at the Grid Crossing Point

Suppose a point P is reached by moving backwards along the final trajectory with control signal  $V$  for a negative time period  $T_f$  and then moving backwards along the second trajectory with control signal  $-V$  for a negative time period  $T_m$ .

Referring to Fig. 13, point P has co-ordinates  $Dx_a$  and  $D^2x_a$  in the  $Dx, D^2x$  plane. It is required to find

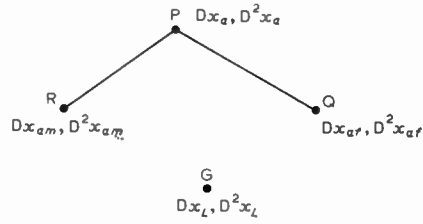


Fig. 13.

the values of the final and second negative trajectory times which will make the beginning of the second trajectory lie on a grid crossing point G ( $Dx_L, D^2x_L$ ). In order to do this a small time change  $\Delta T$  is made in first  $T_f$  and then  $T_m$  (with the original  $T_f$ ) bringing the start of the second trajectory to Q, ( $Dx_{af}, D^2x_{af}$ ) and R, ( $Dx_{am}, D^2x_{am}$ ). This is illustrated in Fig. 13. Providing that point P is reasonably near G, a linear extrapolation may be made to find the changes in  $T_f$  and  $T_m$  required to bring P closer to G.

Let

$$\begin{aligned} d &= D^2x_{af} - D^2x_a \\ e &= Dx_{af} - Dx_a \\ f &= D^2x_{am} - D^2x_a \\ g &= Dx_{am} - Dx_a, \end{aligned}$$

these being the changes due to the two time steps in the  $Dx$  and  $D^2x$  directions. Then

$$\begin{bmatrix} Dx_L - Dx_a \\ D^2x_L - D^2x_a \end{bmatrix} = \frac{1}{\Delta T} \begin{bmatrix} d & e \\ f & g \end{bmatrix} \begin{bmatrix} T_{fs} \\ T_{ms} \end{bmatrix}$$

from which

$$\begin{bmatrix} T_{fs} \\ T_{ms} \end{bmatrix} = \frac{\Delta T}{dg - ef} \begin{bmatrix} g & -f \\ -e & d \end{bmatrix} \begin{bmatrix} Dx_L - Dx_a \\ D^2x_L - D^2x_a \end{bmatrix}$$

where  $T_{fs}$  and  $T_{ms}$  are the changes required in  $T_f$  and  $T_m$  to bring the  $Dx_a$  and  $D^2x_a$  nearer to a grid crossing point. Hence

$$T_{fs} = \left\{ \frac{g(Dx_L - Dx_a) - f(D^2x_L - D^2x_a)}{(dg - ef)} \right\} \Delta T$$

and

$$T_{ms} = \left\{ \frac{d(D^2x_L - D^2x_a) - e(Dx_L - Dx_a)}{(dg - ef)} \right\} \Delta T$$

The new values of  $T_f$  and  $T_m$  are therefore  $T_f + T_{fs}$  and  $T_m + T_{ms}$ . Using these new values the above process may be repeated to improve accuracy still further.

Manuscript first received by the Institution on 11th June 1969 and in final form on 19th August 1969. (Paper No. 1288/IC16.)

## Contributors to this Issue



**Dr. Peter J. Holmes** took his B.A. in physics at Queens' College, Cambridge, in 1952. He was appointed research physicist at AEI Research Laboratory, Aldermaston, where he was concerned chiefly with materials aspects of semiconductors. During this period he worked for a doctorate of the University of Reading, his thesis being on 'Crystal Defects and Etching of Semiconductors'.

In 1963 he moved to the radio department of the Royal Aircraft Establishment where his work has since covered various aspects of microelectronics technology. He is now a principal scientific officer and in charge of the microelectronics group, specializing in physics of failure of semiconductor devices and in hybrid microcircuits. In addition to being the author of papers in technical journals he edited and contributed to 'The Electrochemistry of Semiconductors', published in 1962.



**S. Laurence Cachia** is engineer-in-charge of the electronic development laboratory of Federated Industries Limited of Sydney, N.S.W. He received his technical education in Malta and in London and from 1958 to 1961 was a development and design engineer with E.M.I. Electronics, latterly in the research laboratories of the airborne radar division. For the next two

years he was senior engineer at the Malta Television Station and in 1963 he went to Australia; he held engineering appointments with A.W.A. and Philips before obtaining his present position. He is the author of several papers and holds 14 patents on circuits and devices.



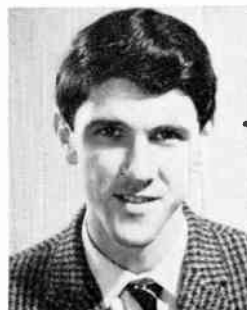
**L. A. Moxon** was educated at the City and Guilds Engineering College, London, and obtained an honours degree in electrical engineering from London University in 1929. After 2 years post-graduate research under a D.S.I.R. grant he joined the staff of Murphy Radio Ltd. where he was responsible for the development of broadcast receivers.

In 1941 he joined H.M. Signal School, Portsmouth, and was responsible during the war years for radar receiver development and research. From 1946 until his retirement in August 1969, he was a member of the Royal Naval Scientific Service.



**E. M. McKay** (M. 1961) joined the education section of the Building Research Station three years ago as a senior scientific officer. His early experience was in the field of telecommunications with the Post Office. This was followed by eight years teaching of physics, electronics and mathematics, the last two at Bristol University where he supervised student projects on a

p.c.m. telephony system. He is a graduate of London University having studied at The Polytechnic, Regent Street, and subsequently obtained his Master's degree for work done at Bristol in the field of vacuum measurement.



**R. L. Davey** was educated at Forest Grammar School, Winnersh, and Reading University, graduating in cybernetics with first-class honours in 1966. He is at present working for his Ph.D. in the Department of Applied Physical Sciences at Reading University, where he is engaged on research into the implementation of 'bang-bang' control using an on-line digital computer.

A biographical note on Mr. P. Atkinson was published in the July 1969 issue of *The Radio and Electronic Engineer*.

# Control of Gamma in C.R.T. Displays using Amplifiers with Exponential Negative Feedback

By

S. L. CACHIA,  
B.Sc., C.Eng., M.I.E.E.,  
M.I.E.R.E.†

**Summary:** It is shown that networks can be produced to correct accurately the effects of the non-linear transfer characteristics of a cathode-ray tube. The gamma correction required is related to the undesirable non-linearity in mathematical terms and the basic gamma equation evolved. A simple exponential equation can be converted into a gamma equation by the introduction of a linear function and the appropriate constants. A network with the required gamma characteristic is equivalent to an amplifying stage incorporating exponential negative feedback.

Circuits employing semiconductors are presented and discussed and the operational equations and performances are found to compare favourably with the theoretical gamma equation, and to support the theory. Networks employing negative feedback intended for operation at video frequencies call for special design to counteract the effects of gain and phase shift variation at those frequencies and a gamma stage suitable for television applications is presented. Stabilization of the operating point of the gamma stages with respect to temperature and power supply variations is described. Testing a gamma stage involves measurement of phase shift, frequency response and faithfulness of gamma as well as checks for the presence of waveform distortion.

Although the treatment deals in particular with the linearization of c.r.t. displays, the techniques are applicable to accurate logarithmic amplifiers, photographic-film contrast correction and in colour television camera tube applications.

## 1. Introduction

The correct rendering of signals of different intensities on a c.r.t. screen is important in order to distinguish signals which stand out very little from their background.

The contrast that can be achieved on a c.r.t. display is a function of several factors. The thickness of the screen tends to blur the edges of the signals, reducing contrast as do also focus limitations of the electron beam. Screens also have a certain amount of graininess and tend to saturate on strong signals which contribute to this effect. Other factors which to a lesser degree reduce contrast are scattered electrons within the tube and light reflections from its glass walls. The non-linear properties of the screen and all the other factors involved are, however, more than offset by the non-linear response of the gun with the overall result that the display is too contrasty and a gamma-lowering stage has to be incorporated in the video amplifier to compensate for the inherent non-linear characteristic of the tube.

The gain of the video amplifier should ideally be such that the electron beam is just fully modulated. If the amplifying stages provide too much gain, while detail in dark areas may be more defined, the signals from bright objects will have to be severely limited to

avoid 'blooming' of the c.r.t. with consequent loss of detail in the highlights. The converse is also true; that is, if the gain is low enough to enhance details in bright areas, it will be at the expense of the dark ones.

Different parts of the received picture should exhibit a relative luminosity corresponding to the reflective properties of the terrain in the case of radar or identical with that of the original scene in the case of television. Whereas in bright sunlight the contrast ratio is around 10 000 : 1, ratios above 50 : 1 prove to be entirely satisfactory for comfortable viewing.<sup>1</sup>

Advances in the manufacturing techniques of cathode-ray tubes, such as aluminizing to increase the forward light output by reducing the backward light scatter, graphite coating to eliminate light reflections from the walls as well as to remove scattered electrons, dark or tinted screens to reduce contrast dependence on ambient light, sharper electron beams, etc., have resulted in much improved realizable contrast ratios and, provided the non-linear gun transfer characteristic is neutralized, all shades of the original scene will be reproduced in their correct gradation and the gamma of the system would be said to equal 1.

## 2. Gamma

### 2.1. Principles of Gamma Correction

The characteristic that a gamma stage must have in order that it may properly drive a c.r.t. is determined

† Federated Industries Pty., Ltd., Sydney, N.S.W., Australia.

by the tube's modulation characteristic which is expressed by:<sup>2</sup>

$$i_s = K_0(V_g - V_b)^{\gamma_0} \equiv K_0 E_s^{\gamma_0}$$

where

$i_s$  = beam current

$K_0$  = grid drive factor

$E_s$  = signal voltage applied to c.r.t. grid

$V_b$  = voltage on grid to produce cut-off

$V_g$  = instantaneous voltage on control grid

$\gamma_0$  is defined mathematically as

$$\frac{d(\log i_s)}{d(\log E_s)}$$

The factors  $V_b$ ,  $K_0$  and  $\gamma_0$  are constant for a given tube geometry.

For c.r.t.s employing magnetic focusing, almost no current is intercepted by apertures in the gun and  $\gamma_0$  is approximately 3.5, differing somewhat from tube to tube, while for tubes employing electrostatic focusing, beam stops are introduced which take a considerable portion of the cathode current and in consequence the gamma is lower and is usually as low as 1.5.

We have

$$i_s \equiv K_0 E_s^{\gamma_0},$$

but since for complete linearity  $i_s \propto E_s$ , the gamma stage must modify the signal voltage in such a manner that

$$i_s \equiv K_0 E_s^{\gamma_0} = K V_{in} \quad \dots\dots(1)$$

where  $V_{in}$  = signal voltage applied to the stage.

$K$  = apparent grid drive factor of c.r.t. and gamma stage combined.

Hence from eqn. (1)

$$E_s = \sigma V_{in}^{1/\gamma_0}$$

where  $\sigma$  is a constant describing the linear amplification or attenuation of the stage.

Therefore if the gamma value of the stage is equal to  $1/\gamma_0$  the condition for complete linearity will obtain.

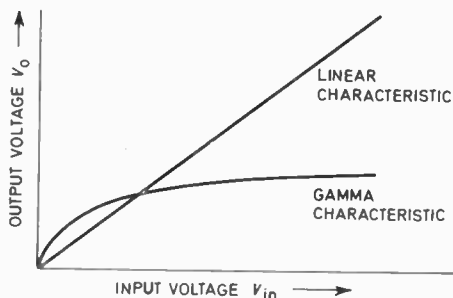


Fig. 1. Responses of ideal gamma stage and linear stage.

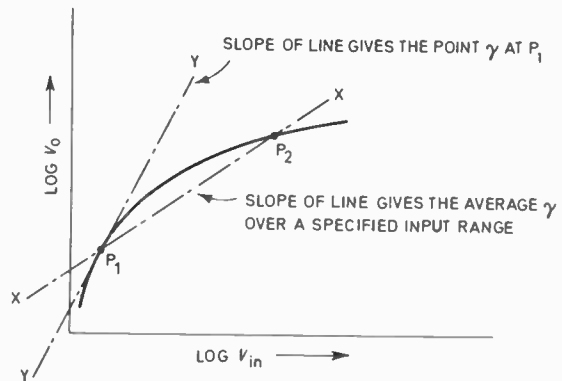


Fig. 2. Definition of gamma.

It should be noted that  $E_s$  is the output  $V_o$  of the stage, so that

$$V_o = \sigma V_{in}^{\gamma}$$

is the gamma equation,  $\gamma$  being equal to  $1/\gamma_0$ .

Figure 1 shows how the response of the ideal gamma stage differs from that of a linear stage. Note that for dark signals, i.e. signals whose amplitude is below unity, the stage must provide amplification that tends to infinity as the signal tends to zero, and attenuation that gets progressively greater as the signal increases above unity.

### 2.2. Definition of Gamma

'Gamma' ( $\gamma$ ) may be defined as the slope of the line obtained when the logarithm of the output is plotted against the logarithm of the input the output being related to the input by the equation

$$V_o = \sigma V_{in}^{\gamma}$$

$\log \sigma$  is given by the intercept on the  $\log V_o$  axis.

For an output not related to the input by the gamma equation the term 'average gamma' can be applied to define the mean value of gamma which obtains over a range of input voltages and is taken as being the slope of the line X—X in Fig. 2. 'Point gamma' on the other hand is referred to as being the gamma value at any particular input and is measured by the slope of the tangent at that point. This is also represented in Fig. 2 by the slope of the line Y—Y.

### 2.3. Exponential to Gamma Conversion

Since semiconducting devices exhibit an exponential form of conduction over a part of their conduction curves, this property will be examined to see if it can be adapted to give accurate gamma curves.

How near is an exponential curve to a power curve?

From the gamma equation,

$$\frac{d(\log V_o)}{d(\log V_{in})} = \gamma = \text{constant}$$

From the simple exponential equation  $V_o = e^{V_{in}}$ ,

$$\frac{d(\log V_o)}{d(\log V_{in})} = V_{in}$$

That is, the point gamma of this exponential equation varies widely over the characteristic and in fact is equal to the particular value of  $V_{in}$  at any instant. This is obviously not suitable, but a true power law can be approached, if, to the exponential function, is added a linear function.

For instance, suppose that

$$V_o = e^{V_{in}} + CV_{in}$$

where  $C$  is a constant then

$$\frac{d(\log V_o)}{d(\log V_{in})} = \frac{e^{V_{in}} + C}{(e^{V_{in}}/V_{in}) + C}$$

Interpreting this result, it is noted that if  $C$  is positive the point gamma  $d(\log V_o)/d(\log V_{in})$  changes more rapidly with  $V_{in}$  as  $C$  is made larger. However, if  $C$  is negative the point gamma can be made to change drastically over a small region of  $V_{in}$  and thereafter will reach an almost constant value of an order that can be usefully employed. Note that for  $V_{in} = 0$  the point gamma is indeterminate (see later).

More detailed analysis can be derived through graphical illustration than can be deduced directly, but first an effort will be made to work out the optimum value of  $C$ .

Ideally the gamma value should be constant and there is an optimum value of  $C$  which comes nearest to satisfy this requirement.

For the purpose of finding the best value of  $C$  it is legitimate to write

$$\frac{d(\log V_o)}{d(\log V_{in})} = \frac{e^{V_{in}} + C}{(e^{V_{in}}/V_{in}) + C} = \text{constant}$$

Hence

$$\frac{d\left(\frac{e^{V_{in}} + C}{e^{V_{in}}/V_{in} + C}\right)}{d V_{in}} = 0$$

giving

$$C = -\frac{e^{V_{in}}}{V_{in}^2 - V_{in} + 1}$$

It should be noted that for  $V_{in} = 1$ ,  $C = -e$ , but it is obvious that the value of  $C$  is dependent on the magnitude of  $V_{in}$  and its average value for a practical  $V_{in}$  range, say 0 to 4 V, must be found.

Average value of

$$C = C_{av} = -\frac{1}{4} \int_0^4 \frac{e^{V_{in}}}{V_{in}^2 - V_{in} + 1} d V_{in}$$

giving

$$C_{av} = -2.699$$

### 2.4. Graphical Analysis

A true gamma function plotted on logarithmic vertical and horizontal scales produces a straight line. Any other function plotted on such scales will produce curves whose divergence from a straight line depicts the degree of inconsistency in gamma.

From Fig. 3(a) it can be readily appreciated how the addition of the linear function  $CV_{in}$  affects the 'gamma' of the equation  $V_o = e^{V_{in}}$ .

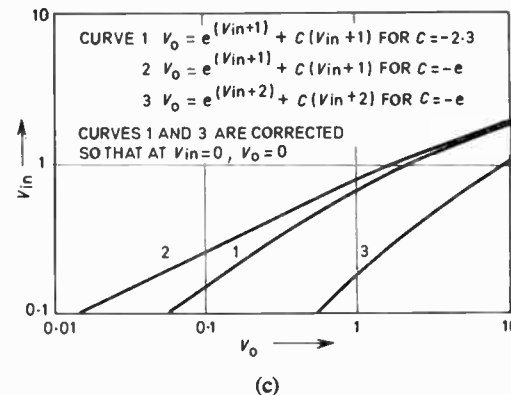
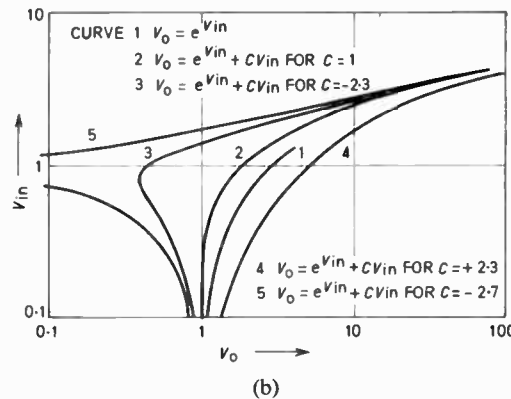
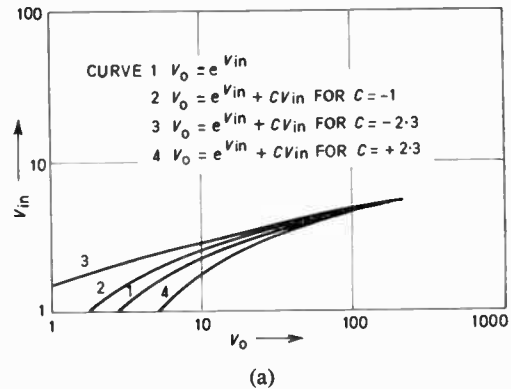


Fig. 3. Correction of gamma curves to obtain a straight line by adding linear functions.

Positive values of  $C$  have an adverse effect on the gamma (see curve 4) but negative values of  $C$  of the order already calculated result in curves approximating fairly closely to a straight line as can be seen from curve 3.

In order to comprehend the behaviour of the point gamma for small values of  $V_{in}$ —we have noted earlier its indeterminate nature for  $V_{in} = 0$ —reference should be made to Fig. 3(b) where it can be seen for curves 3 and 5 the gamma changes to a negative quantity for small values of  $V_{in}$ .

Fortunately here again matters can be improved by 'biasing'  $V_{in}$ , that is by adding a constant voltage to  $V_{in}$ , the resulting equation for  $V_o$  being

$$V_o = e^{(V_{in}+K)} + C(V_{in} + K)$$

where  $K$  is the bias to  $V_{in}$ , a constant.

It can be shown that  $K = 1$  is the right value for  $K$  when  $C$  is equal to  $-e$ .

That the gamma is indeed improved may easily be seen from curves 1 and 2 in Fig. 3(c).

Of secondary importance but one that can be put to practical use, is the fact that by altering the value of  $K$  the gamma or slope of the curves is altered. Compare curves 2 and 3 of Fig. 3(c). It should be noted that when the values of  $K$  and  $C$  are other than 1 and  $-e$  respectively a correction is applied to  $V_o$  in the form of a subtraction of a constant voltage so that at  $V_{in} = 0$ ,  $V_o = 0$ .

In the foregoing the operative exponential equation chosen for conversion into a gamma equation was taken simply as  $V_o = e^{V_{in}}$  so as to engender a clear exposition of the nature and method of correction entailed. Consequently it is now straightforward to apply the formulated principles to the general form of exponential equation given by

$$V_o = a e^{bV_{in}} + d$$

where  $a$ ,  $b$  and  $d$  are constants.

The resultant gamma equation is

$$V_o = a e^{b(V_{in}+K)} + C(V_{in} + K) \quad \dots\dots(2)$$

where  $K = 1/b$  and  $C = -e.ab$ .

$d$  is a constant added to  $V_o$  and does not affect the gamma.

2.5. Gamma Values Less than Unity

The gamma values given by eqn. (2) are greater than unity. However it is obvious that the reciprocal of these values will be given on interchanging  $V_o$  and  $V_{in}$  in the equation.

Therefore the relationship between  $V_{in}$  and  $V_o$  for gamma values less than unity can now be stated as

$$V_{in} = a e^{b(V_o+K)} + C(V_o + K)$$

and putting  $K = 1/b$  and  $C = -eab$ ,

$$V_{in} = e a (e^{bV_o} - bV_o - 1) \quad \dots\dots(3)$$

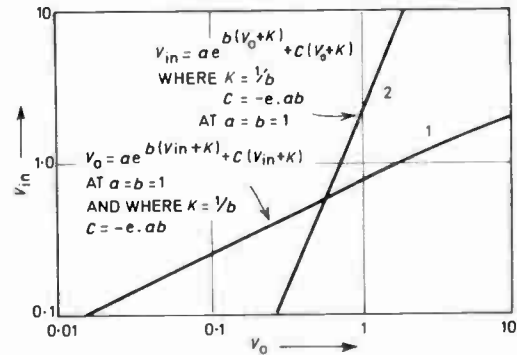


Fig. 4. Comparison of gamma equations.

For direct comparison the two gamma equations are plotted on Fig. 4.

Before proceeding with its practical application, eqn. (3) has to be modified in one more respect.

From eqn. (3), gain

$$\frac{d V_o}{d V_{in}} = \frac{1}{e a b e^{bV_o} - e a b}$$

now as  $V_{in} \rightarrow 0$ ,  $V_o \rightarrow 0$

and

$$\lim_{V_{in} \rightarrow 0} \frac{d V_o}{d V_{in}} = \infty$$

Since a gain of infinity is not realizable, the stage should have a gain consistent with practical feasibility and small errors. That the gain limitation is actually only an apparent one will transpire in noting that for  $V_o = \sigma V_{in}$  (say) the gain  $d V_o/d V_{in}$  at 10  $\mu V$  input is  $720\sigma$  and at 100  $\mu V$  input it is only  $61.6\sigma$ . If a practical gamma stage is limited to a gain of about  $500\sigma$  as  $V_{in} \rightarrow 0$ , the errors introduced at input voltages above a few microvolts will be entirely negligible. This will be all the more so because the chosen input voltages range is wide, 0-4 V.

In eqn. (3),

$$\sigma \simeq \frac{1}{b} \log_e \frac{e a + 1}{e a}$$

the gain required as  $V_{in} \rightarrow 0$  shall be taken to be  $500\sigma$  and hence the theoretical equation (eqn. (3)) amended to give the required gain as  $V_{in} \rightarrow 0$  can be written

$$V_{in} = e a \left[ e^{bV_o} - \left\{ b - \frac{1}{500 \log_e \left( \frac{e a + 1}{e a} \right)} \right\} V_o - 1 \right] \quad \dots\dots(4)$$

Earlier a practical input voltage range of between 0 and 4 V was chosen in order to calculate the average value of  $C$ . To adhere to these input voltages and the calculated value of  $C$  it is necessary to make  $b = 1$ .

For example if  $b = 4$ , the input voltage will have to be restricted to 0–1 V; or if  $b = 40$ ,  $V_{in}$  will have to be between 0 and 0.1 V if the same portion of the characteristic is to be used. To reiterate, taking the input voltage range between 0 and 4 V,  $b$  must be made equal to 1 or  $C$  will have to be re-evaluated.

**3. Application of the Derived Theoretical Equation**

Deliberating on eqn. (3) it becomes apparent that it has the same make-up as the relation between the input and output voltages of an amplifying stage incorporating negative feedback.

For instance, for an amplifying stage of amplification  $A$  and feedback voltage  $-\beta V_o$ ,

$$-V_o = (V_{in} - \beta V_o)A$$

where

$V_o$  = output voltage

$V_{in}$  = input voltage

$\beta$  = fraction of  $V_o$  fed back

and

$A$  = amplification without feedback

i.e.

$$V_{in} = \frac{1}{A} (A\beta V_o - V_o)$$

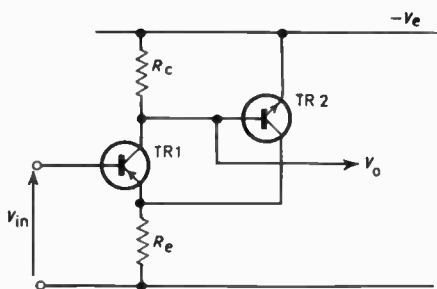


Fig. 5. (a) Basic circuit of linear amplifier with negative feedback loop.

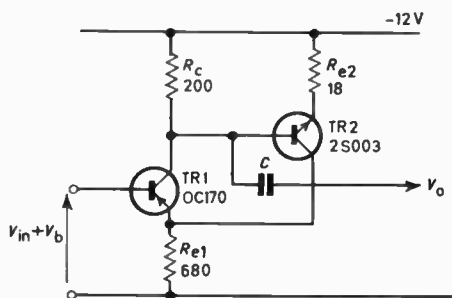


Fig. 5. (b) Practical realization of (a). These circuits are the subject of British Patent Application Nos. 8757/61 and 8758/61.

The one important difference is that for the gamma equation the feedback term is non-linear and is in fact exponential. The discrepancy in the constant terms of the two equations is not important since these can be suitably introduced at will.

We have now the basis on which to initiate a design exhibiting a gamma characteristic, namely, the fact that if a linear stage is operated upon by non-linear negative feedback it would exhibit a gamma characteristic.

If the idealized circuit equations of the circuit shown in Fig. 5(a) are examined it will be seen that the above deduction is borne out.

TR1 is a linearly-operated transistor whose collector is directly coupled to the non-linear element TR2. A negative feedback loop is then formed by connecting the collector of TR2 to the emitter of TR1.

$$I_{b2} = I_{sat} [e^{(q/KT)V_o} - 1]$$

where  $I_{sat}$  = saturation current; represented by  $a$  in eqn. (3)

$q$  = electronic charge

$K$  = Boltzmann's constant

$T$  = temperature in degrees Kelvin

Also

$$V_{in} = (I_{c1} + I_{c2})R_e$$

Therefore

$$V_{in} = I_{c1} R_e + \beta_2 I_{sat} R_e \{e^{(q/KT)V_o} - 1\}$$

and

$$I_{c1} = \frac{V_{in}}{R_e} - \beta_2 I_{sat} \{e^{(q/KT)V_o} - 1\}$$

Now

$$\begin{aligned} V_o &= -I_{c1} R_c \\ &= -\frac{V_{in} R_c}{R_e} + \beta_2 I_{sat} \{e^{(q/KT)V_o} - 1\} R_c \end{aligned}$$

Therefore

$$V_{in} = + \beta_2 I_{sat} \{e^{(q/KT)V_o} - 1\} R_c - \frac{V_o R_c}{R_e}$$

i.e.

$$V_{in} = + \beta_2 I_{sat} e^{(q/KT)V_o} - \frac{V_o R_c}{R_e} + R_e \beta_2 I_{sat}$$

which is seen to compare favourably with eqn. (3).

**4. Practical Gamma Circuit**

In evolving the actual circuit equations for the circuit of Fig. 5(b) along the lines of the preceding section, the extrinsic base and emitter resistances of TR1 and TR2 must be included. Then comparison of the individual terms in the circuit equation for  $V_{in}$  with those of eqn. (4) will yield the component values for

$R_{e1}$ ,  $R_{e2}$  and  $R_c$ . The choice of the component values as shown in Fig. 5(b) is partly the result of the approximate solution of these equations and partly based on experimental results.

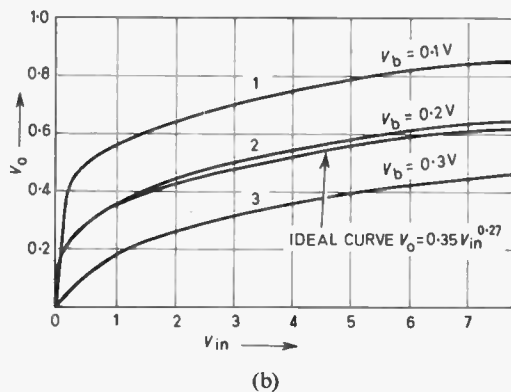
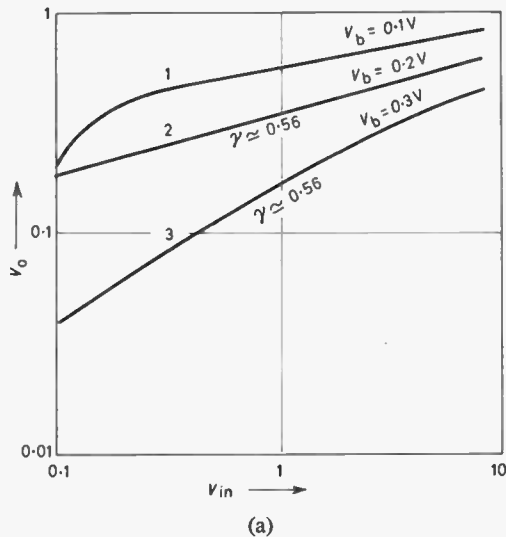


Fig. 6. Low frequency performance of the circuit of Fig. 5 (b).

The low-frequency performance of the circuit shown in Fig. 5(b) is illustrated in Figs. 6(a) and (b).

At  $V_b = 0$ , TR1 and TR2 are cut off for  $V_{in} = 0$  (where  $V_b$  is the bias voltage). To realize the expected results TR1 must be operating linearly, a condition which does not come about unless the base-emitter voltage exceeds a nominal value of about 0.2 V (with germanium transistors the amount of bias required is between 0.1 and 0.2 V, 0.6 to 1 V being the corresponding figures for silicon transistors). The unfaithful gamma of curve 1 can thus be attributed to the non-linear operation of TR1, the bias of 0.1 V not being quite sufficient to bring it into linear activity. A bias of 0.2 V resulted in curve 2.

In Fig. 6(b) comparison can be made between curve 2, which has an average gamma value of 0.27 and an ideal curve having the same value of gamma.

### 5. Other Gamma Circuits

#### 5.1. Circuit Two

The principle of non-linear negative feedback is again applied in the circuit of Fig. 7. The circuit showed great promise when first investigated at low frequencies and gave very low gamma values. However, due to severe phase shift introduced by the transistors, an undistorted output over a wide frequency range could not be obtained, even with the use of transistors having a gain-bandwidth product of 250 MHz.

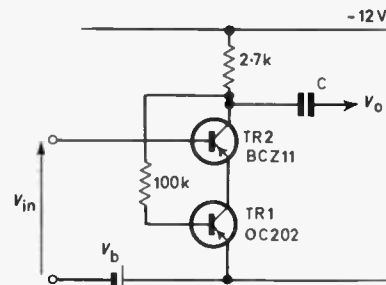


Fig. 7. Circuit 'two'.

TR1 is driven from a saturated state—corresponding to zero  $V_{in}$  and therefore zero collector-base voltage—to the threshold of normal linear operation by the excursion of  $V_{in}$ . TR2 is driven linearly from a point above cut-off towards saturation. Signal analysis of the circuit then must take into account the large variations of transistor parameters as the operating points and conditions vary over the range of input voltage and frequency.

A large number of physical processes takes place within the transistors and each of these exerts an influence on its circuit behaviour. Therefore a complete equivalent circuit valid throughout an extended range of frequency and input voltages involves a great many circuit elements. It has been shown that the use of progressive non-linear negative feedback produces a characteristic conforming to the derived theoretical gamma equation, and in this instance, the qualitative treatment that follows is only intended to promote a general understanding of the operation of the circuit.

In order to contribute to this understanding the 'large signal' equations which describe the voltage and current relationships in a transistor will be given. These may be written as follows:<sup>3</sup>

$$i_c = A_{11}[\exp(q\phi_c/KT) - 1] + A_{12}[\exp(q\phi_e/KT) - 1] \dots\dots(5)$$

$$i_c = A_{21}[\exp(q\phi_e/KT) - 1] + A_{22}[\exp(q\phi_c/KT) - 1] \dots\dots(6)$$

Here  $\phi_c$  and  $\phi_e$  represent the voltage across the collector-base and emitter-base junctions respectively. The coefficients  $A_{ij}$  may be related to the inherent transistor parameters as follows,

$$A_{11} = -I_{e0}/(1 - \alpha_{fb}\alpha_{rb})$$

$$A_{12} = \alpha_{rb}I_{e0}/(1 - \alpha_{fb}\alpha_{rb})$$

$$A_{21} = \alpha_{rb}I_{e0}/(1 - \alpha_{fb}\alpha_{rb})$$

$$A_{22} = -I_{c0}/(1 - \alpha_{fb}\alpha_{rb})$$

where  $I_{e0}$  is the emitter current for zero collector current;  $I_{c0}$  is the collector current for zero emitter current;  $\alpha_{fb}$  is the normal current amplification factor;  $\alpha_{rb}$  is the reverse transistor amplification factor.

The similarity of the voltage versus current relationships of a junction diode to the bracketed terms in eqns. (5) and (6) should be noted and any analysis restricted to transistors having negligible space-charge layer widening effects, and where no consequential voltage drops, unless relative to the junctions, take place within the transistors.

Equations (5) and (6) are applicable to all transistor configurations but are essentially more suitable for the common-base configuration. Noting that  $i_e + i_b + i_c = 0$  and substituting for  $i_e$  from eqn. (5) results in

$$i_c = [\alpha_{fb}i_b/(1 - \alpha_{fb})] - I_{c0}[\exp(q\phi_c/KT) - 1]/(1 - \alpha_{fb}) \dots\dots(7)$$

which may be applied directly to the common-emitter configuration.

Consideration of eqns. (6) and (7) shows that TR1, when under heavy saturation at near-zero input voltages and both the emitter and collector junctions are virtually biased in the forward direction, acts as a very low impedance providing for a high  $V_o : V_{in}$  ratio. As  $V_{in}$  increases,  $\phi_c$  becomes negative and the corresponding exponential argument is comparatively large and negative, also the voltages at the collector of TR2 fall lowering  $i_b$  and  $\phi_e$ . The value of the equations become relatively smaller indicating that the impedance offered by TR1 to TR2 is comparatively higher providing for a higher degree of feedback and therefore a lower  $V_o : V_{in}$  ratio. The degree of feedback increases progressively with  $V_{in}$  obeying an exponential law.

The gamma can be varied by introducing a voltage in series with  $V_{in}$ .

Figures 8(a) and (b) show the performance under d.c. conditions.

Curve 1 of Fig. 8(a) was produced for  $V_b = 0$  and in consequence TR2 was beyond cut-off for low values of  $V_{in}$ . By means of biasing, the stage was brought into normal operation and a gamma of approximately 0.14 obtained at  $V_b = 0.7$  V; see curve 2. The gamma obtaining for  $V_b = 0.8$  was approximately 0.45; see curve 3.

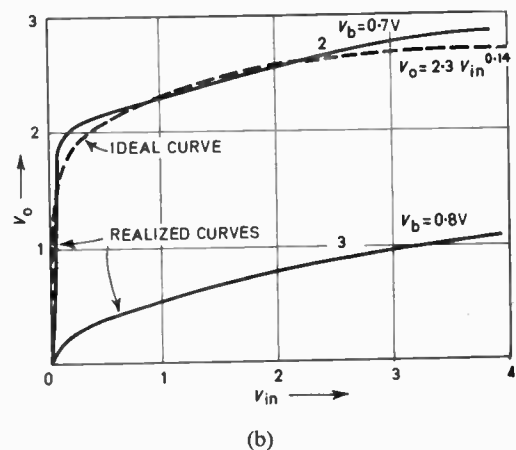
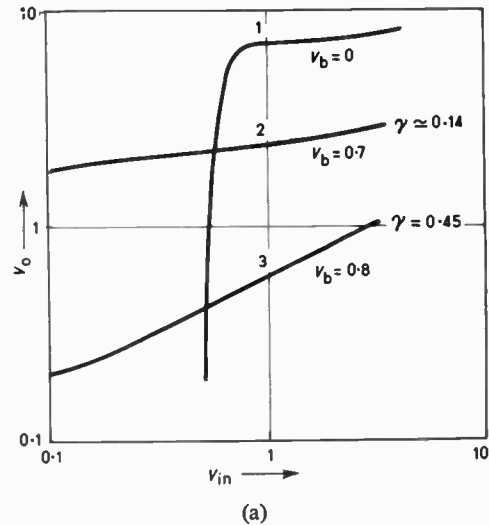


Fig. 8. Performance characteristics of circuit 'two' under d.c. conditions.

With reference to Fig. 8(b) the coordinates of the ideal curve for certain values of  $V_{in}$ —drawn for comparison against curve 2—differ somewhat from the corresponding coordinates of curve 2. This implies (as indeed can be seen from curve 2 of Fig. 8(a)) that the gamma value of the characteristic is not constant over the entire range of input voltage. By restricting this input range between say, 0 and 2 V, the realized curve can be made to approximate more closely to the ideal curve.

5.2. Circuit Three

The circuit shown in Fig. 9 provides yet another method whereby an applied signal is modified in compliance with a gamma law.

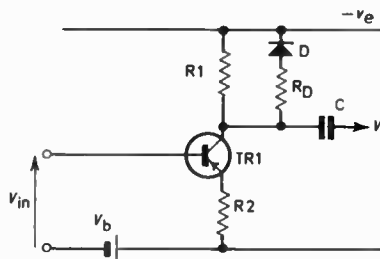


Fig. 9. Circuit 'three'.

The current through TR1 is linearly related to the input signal. A linear current flowing through a diode causes a logarithmic voltage to be developed across it. However, it should be noted that in Fig. 9 the current through the diode is not linear, due to the transistor current being partly diverted to flow through R1, a current which in turn is a function of the voltage across the diode and its internal resistance represented by RD. In consequence the voltage at the collector of TR1 is not logarithmic but is modified to approach a gamma characteristic.

The performance of such a circuit is illustrated in Figs. 10(a) and (b).

5.3. Circuit Four

In the circuit shown in Fig. 11 D1 and D2 are connected in series to increase the available voltage Vo. R2 helps to keep the power dissipation in the transistor within limits and at the same time, since its value is high compared with the combined effective resistance of D1 and D2 in parallel with R3, it develops a nearly linear voltage waveform at the collector of TR1. The ratio of R5 to R6 is chosen so that at the maximum excursion of Vin the amplitude of the voltage of 'B' which varies almost linearly with Vin, is equal to the amplitude of that of 'A' which obeys a gamma law.

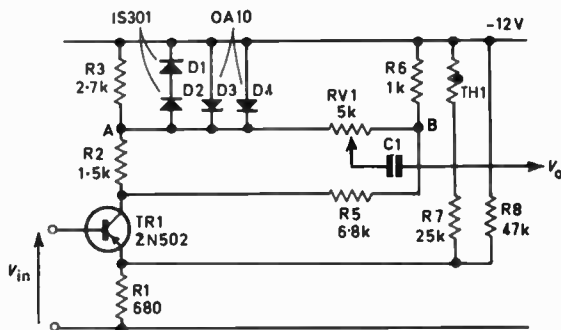


Fig. 11. Circuit 'four'.

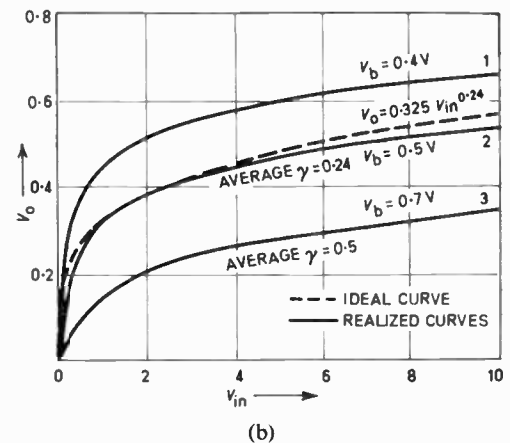
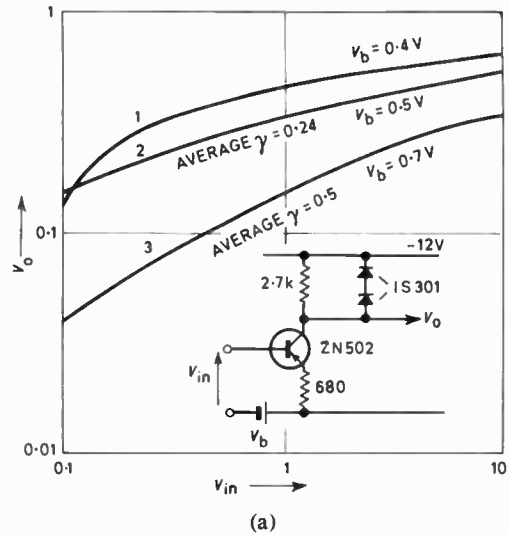


Fig. 10. Performance of circuit 'three'.

Thus, the network formed by R2, R5, R6 and RV1 provides for a constant amplitude output while the gamma is varied by means of RV1. (This method of varying the gamma does not yield high constancy of gamma.)

Other features of the circuit are the temperature sensitive network formed by R7, R8 and the thermistor Th1, which compensates for the changes in transistor collector current with temperature variations and the elements D3 and D4. These elements compensate the output voltage against its dependence on the temperature-conscious parameter Isat pertaining to the diodes D1 and D2. Reversed diodes are well suited for this purpose. The reverse resistance of D3 and D4 decreases with temperature and hence more current is bypassed from D1 and D2. This in its effect acts as if Isat or the standing biasing current has decreased. That is by lowering the resistance of D3 and D4 the resistance of the load as a whole has been increased.

6. Wide-Band Stages

The general requirements of video amplifiers have been well established. The amplitude response characteristic must be reasonably uniform over the frequency range of interest and at the same time there must be a constant time-delay over the entire frequency range. A constant time-delay demands that the phase-shift relation to frequency must be linear.

In the case of gamma stages employing negative feedback, requirements are more exacting in that there is the additional requisite that within the feedback loop the phase-shift should ideally be zero. Failure to observe this condition means that there will not be proper generation of harmonics due to the non-linear properties of the stage, resulting in waveform distortion.

The nature of the parameters and parametric spreads of the active elements in these stages must be thoroughly studied. At low frequencies the transistors themselves present no special difficulties, the parameters are real and constant, but at high frequencies transistor properties present major problems of gain and phase-shift variations which must be compensated for by proper circuit design.

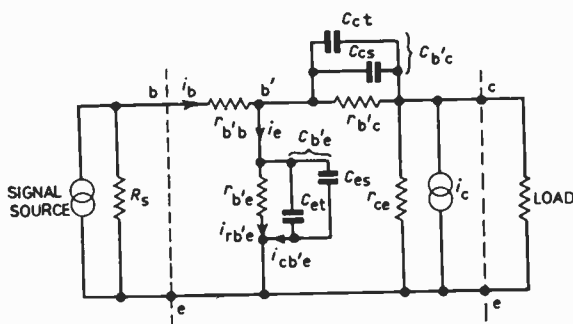


Fig. 12. Hybrid-pi grounded-emitter equivalent circuit of transistor.

The hybrid-pi grounded emitter representation of a transistor is given in Fig. 12. This circuit can be used in design with reasonable accuracy up to about half the frequency at which the modulus of the short-circuit current gain becomes unity. (Strictly, this is exclusive of rate-grown transistors where  $r_{b'b}$  is of a distributed nature and requires to be represented at any higher frequency by a complex impedance. In general, however, it is assumed that  $r_{b'b}$  is resistive.)

The best design philosophy for wide-band gamma stages is to compensate within the feedback loop against frequency dependence and then add such other compensation networks as are required, the nature of which will depend on the output impedance of the signal source and the input impedance of the following stage. This procedure can be applied for instance to

the circuit of Fig. 5 with the aid of the equivalent circuit in Fig. 13 combining both series and shunt peaking elements.

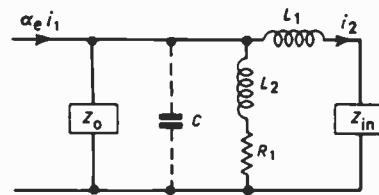


Fig. 13. Equivalent circuit of series and shunt peaking elements for feedback loop of Fig. 5.

$Z_0$  represents the internal impedance of TR1 and is given by

$$Z_0 \approx \left( \frac{1 - \alpha_{b0}}{j\omega C_{b'e}} \right) \left[ \frac{1 + j\omega/(1 - \alpha_b)\omega_{ab}}{1 + j\omega/\omega_{ab}} \right] \dots\dots(8)$$

$Z_{in}$  represents the input impedance of TR2 and is expressed by

$$Z_{in} \approx r_{b'b} + \left( \frac{r_{b'e} + R_{e2}\alpha_{b0}}{1 - \alpha_{b0}} \right) \times \left( \frac{1}{1 + j\omega/(1 - \alpha_{b0})\omega_{ab}} \right) + R_{e2} \dots\dots(9)$$

$C$  represents the stray capacitance and can be rendered negligible by careful layout.

In Fig. 13 the amplification or the ratio of  $i_2$  to  $i_1$  should be constant throughout the frequency range of interest and is given by

$$A_i = \frac{i_2}{i_1} = \frac{\alpha_e/(Z_{in} + j\omega L_1)}{1/Z_0 + 1/(R_1 + j\omega L_2) + 1/(Z_{in} + j\omega L_1)} \dots\dots(10)$$

Because of the absence of any coupling capacitor, the amplification at low frequency is the same as that at medium frequency which can be designated by  $f_m$ . The high-frequency limit can be designated by  $f_h$ .

On substituting eqn. (9) for  $\alpha_e$ , eqn. (10) becomes at  $f_h$ ,

$$A_{i(f_h)} = \frac{\alpha_{b0}/\{(1 - \alpha_{b0}) + jf_h/f_{ab}\} \{Z_{in} + j\omega L_1\}}{1/Z_0 + 1/(R_1 + j\omega L_2) + 1/(Z_{in} + j\omega L_1)} \dots\dots(11)$$

Although since  $Z_{in}$  decreases with frequency a degree of high-frequency compensation could have been obtained by using a small value of  $R_1$ , the value of  $R_1$  has already been dictated by the exigencies of a faithful gamma characteristic.

At a frequency  $f_m$ ,  $Z_{in}$  is approximately equal to

$$r_{b'b} + r_{b'e}/(1 - \alpha_{b0}) + R_2/(1 - \alpha_{b0})$$

and

$$Z_0 \gg Z_{in}$$

The current amplification is then

$$A_{i(f_m)} \approx \frac{R_1 \{ \alpha_{bo} / (1 - \alpha_{bo}) \}}{r_{b'b} + r_{b'e} / (1 - \alpha_{bo}) + R_2 / (1 - \alpha_{bo}) + R_1} \dots\dots(12)$$

Assuming  $L_1$  is zero and  $L_2$  is not zero, a shunt peaking circuit is obtained and eqn. (12) is reduced to

$$A_{i(f_h)} \approx \frac{\alpha_{bo} / Z_{in} \{ (1 - \alpha_{bo}) + j f_h / f_{ab} \}}{1 / Z_0 + 1 / (R_1 + j \omega L_2) + 1 / Z_{in}} \dots\dots(13)$$

Equating the magnitude of  $A_i(f_h)$  in eqn. (13) to the magnitude of  $A_i(f_m)$  in eqn. (12), the relation between  $R_1$  and  $L_2$  can be calculated.

Assuming  $L_2$  is zero but  $L_1$  is not zero, a simple series peaking circuit is obtained. Equation (11) is now reduced to

$$A_{i(f_h)} \approx \frac{\alpha_{bo} / \{ (1 - \alpha_{bo}) + j f_h / f_{ab} \} \{ Z_{in} + j \omega L_1 \}}{1 / Z_0 + 1 / R_1 + 1 / (Z_{in} + j \omega L_1)} \dots\dots(14)$$

By equating the magnitude of eqn. (14) to the magnitude of eqn. (12) the relation between  $R_1$  and  $L_1$  can be calculated.

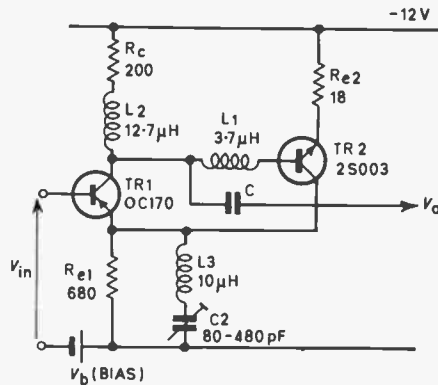


Fig. 14. Wide-band gamma control circuit.

Having carried out compensation for the effects of parameters  $h_{21}$  and  $h_{22}$  of TR1 and  $h_{11}$  of TR2 respectively, the same procedure can be reapplied to compensate for the same respective parameters of TR2 and TR1. However, due to the wide spreads of factors  $C_{b'e}$  and  $r_{b'e}$ , some form of variable compensating control is necessary and a series resonant circuit formed by  $L_3$  and a variable  $C_2$  across  $R_e$  was adopted.  $C_2$  is adjusted for minimum waveform distortion at  $f_h$ , with a sinusoidal voltage input.

Figure 14 shows a wide-band gamma circuit. The bias voltage  $V_b$  was adjusted to 0.22 for a gamma value of 0.3.

The frequency response is -0.2 dB to 6.5 MHz, -3 dB at 8.7 MHz at a signal input of 0.5 V.

The types of semiconductors used in the preceding experimental circuits are not the most suitable of the numerous commercially available types. The very low forward and reverse recovery times—of the order of 4 ns and indicative of low values of  $C_{b'e}$  and  $C_{b'c}$ —that are a feature of silicon junctions of mesa construction suggest that mesa transistors and diodes may be used to advantage. The recently introduced germanium, gallium antimonide and gallium arsenide 'back' diodes with their low capacitance and ultra-fast recovery times of less than 1 ns are ideal for use as the controlling element of the collector load of the circuit shown in Fig. 9.

7. Stabilization

It should be observed that one of the requisites for satisfactory gamma control is the stabilization of the operating point of the gamma stage with respect to temperature and power supply variations.

With the very effective techniques that can be employed in the stabilization of power supplies no problem need arise from this source. As regards temperature variation, whereas adequately stable operation of the circuit may be secured by the utilization of ordinary linear techniques for the majority of gamma control applications, in certain special cases where more stringent control is required non-linear compensation techniques may be used to advantage.

Although those circuits utilizing non-linear negative feedback are to a large extent self-compensating, any dissimilarities in the relevant transistor parameters and external circuit component values in each transistor branch may still entail compensation, depending on the nature of application.

The current-voltage relationship of a semiconductor junction, expressed in detail (after Hall), is given by

$$I = A e^{-q\phi/2KT} [e^{qV_{in}/2KT} - 1] = A e^{q(V_{in} - \phi)/2KT} - A e^{-q\phi/2KT} \dots\dots(15)$$

where

- $I$  = current through the junction
- $\phi$  = energy constant (so-called 'band gap')
- $T$  = absolute temperature of junction proper
- $V_{in}$  = voltage across the junction
- $A$  = area of the junction

The adverse effects of temperature on the gamma characteristic can be discerned by comparison of the temperature dependent factors in eqn. (15) above and their respective representative factors in the equation  $V_o = ae^{bV_{in}} + d$  used earlier on to evolve eqn. (2). Not only is the gamma value seen to be affected by temperature but the faithfulness of the gamma characteristics as well.

The use of reversed-biased diodes as corrective elements in temperature compensation practice is attractive, since their temperature-conscious properties are similar to those of the junctions that comprise the transistors in gamma circuits.

### 8. Testing of Gamma Stages

Where a stage can be isolated and examined under d.c. or low frequency a.c. conditions the plotting of input voltage versus output voltages on logarithmic scales would provide the best means for checking the faithfulness and value of gamma. The test signal should be as large as is likely to be met with under normal operation and, if no particular value of gamma is required, the biasing of the stage should be adjusted to give the lowest gamma in the required range of values.

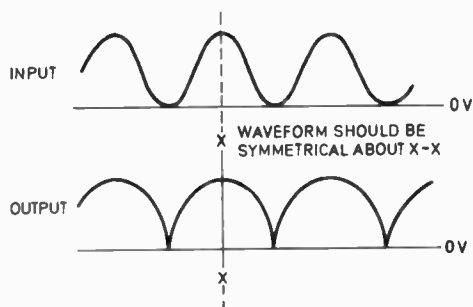


Fig. 15. Waveform distortion testing of gamma stages.

The application of sine waves at different frequencies to the input and the monitoring of the output on an oscilloscope facilitates checking of the frequency response and for the presence of waveform distortion (see Fig. 15), while the use of square wave indicates the presence and degree of phase-shift introduced by the stage.

### 9. General Applications

Gamma-control has of course other important

applications apart from linearizing the performance of a cathode-ray tube.

For instance, gamma-control may be employed in the form of accurate logarithmic networks in computers and measuring instruments.

Besides, in photographic films the resultant opacity after development of the exposed picture is not linearly related to the original subject brightness, although for positive film the complementary characteristic of the printing process affords a correction. In television the expense and time factors are of some considerable importance and if negative film with the necessary gamma correction is transmitted directly, these factors will be favourably reduced.

Furthermore, the majority of television camera tubes possess some non-linearity, while colour scenes, if transmitted via a linear system to be reproduced in black and white, tend to be dull due to lack of colour contrast, necessitating the implementation of gamma-control.

### 10. Acknowledgments

The author is indebted to Dr. Hugh McKibbin, former Head of Electrical Engineering Department at the Malta Polytechnic, for his encouragement and helpful suggestions.

### 11. References and Bibliography

1. Helt, S., 'Practical Television Engineering', p. 56 (Murray Hill Books, New York, 1950).
2. Moss, H., 'The electron gun of the cathode-ray tube', *J. Brit. Instn Radio Engrs*, 5, pp. 10-26, 1945.
3. Shockley, W., Sparks, M., and Teal, G. K., 'p-n transistors', *Phys. Rev.*, 83, pp. 151-62, 1st July 1951.

*Manuscript first received by the Institution on 3rd October 1968 and in final form on 10th February 1969. (Paper No. 1287/CC58.)*

© The Institution of Electronic and Radio Engineers, 1969

# LETTERS

## FLASHOVER PROTECTION

With reference to the paper 'Flashover in picture tubes and methods of protection',<sup>†</sup> I would like to draw attention to the following alternative method of protection as adopted by The M-O Valve Company. It is directed at the limitation of the discharge rather than protecting external components from its effects.

The current flowing from an external e.h.t. capacitor during a flashover may be limited by the introduction of an external resistance. In practice however, a significant part of the e.h.t. capacitance is provided by the internal and external wall coatings of the tube where the internal coating is connected directly to the final anode of the gun. Current from this capacitance cannot be limited by external means.

The internal coating of the bulb may be terminated above the gun, in the region of the cone to neck junction. The remainder of the internal coating, down the neck to the point where contact is made with the final anode of the gun structure, is then replaced by a resistive coating. The resistance of this coating must be of such a safe value as to reduce the current, during a flashover, to a safe value while at the same time not producing a significant potential drop due to the current trimmed from the beam by the final anode in the gun.

D. STYLES

The M-O Valve Company Limited,  
Brook Green Works,  
Hammersmith, London, W.6.

3rd September 1969

**Author's reply:** The line of approach suggested by Mr. Styles is a logical extension of the arguments put forward in my paper. There are however, considerable production difficulties. The resistor must handle peak voltages up to the e.h.t. value and a large amount of energy and it is essential that it performs this duty consistently throughout the life of a picture tube. The steps necessary to ensure these properties must be reflected in the cost of the finished product. While the actual increase is not known, the described method of flashover protection is cheap to apply. Perhaps the best evidence of the difficulties is the fact that so far no manufacturer has managed to put on the market a picture tube with an internal resistor.

A. CIUCIURA

Mullard Mitcham,  
Central Application Laboratory,  
New Road, Mitcham, Surrey.

20th October 1969.

<sup>†</sup> Ciuciura, A., *The Radio and Electronic Engineer*, 37, No. 3, pp. 149-68, March 1969.

## ANALYSIS OF IDEAL STEP-RECOVERY DIODE

With regard to the paper entitled 'A theoretical analysis of the ideal step-recovery diode in the series-mode of operation' in your May 1968 issue,<sup>‡</sup> we would like to point out a number of errors (listed separately below). Certain of these errors have led us to reach conclusions different from those which have been drawn by the authors.

Equation (33) should read

$$s^2 = \frac{[2(1 - \cos \psi) - \psi \sin \psi]^2}{(\psi - \sin \psi)^2 + (1 - \cos \psi)^2} \quad \dots\dots(A)$$

and eqn. (38) should read

$$P_n = \frac{E_1^2}{4\pi n^2} \cdot \frac{1}{R_s} \cdot \frac{s^2}{\psi} \quad \dots\dots(B)$$

where  $s^2$  is given by eqn. (A).

By numerical analysis using eqn. (A) we agree that the conduction angle for maximum step amplitude is  $\psi = 4.1$  rad. However, the maximum value of  $P_n$ , eqn. (B), is obtained for  $\psi = 3.7$  rad. The authors' solution,  $\psi = 3.9$  rad, cannot be obtained from eqn. (38) as published. Our value of  $\psi = 3.7$  does not make a significant difference to the numbers in eqns. (39) and (41).

The following errors are more significant, since they affect the conclusion given by eqn. (44).

Equation (42) should read

$$n^2 \eta = \frac{8\pi(\sin \theta - \sin \phi)^2}{\left(\psi^2 \frac{R_L}{R_s} + 4\pi^2 \frac{R_s}{R_L} + 4\pi\psi\right) \times \left(\psi - \frac{\sin 2\phi}{2} - \frac{\sin 2\theta}{2} + 2 \sin \theta \cos \phi\right)} \quad \dots\dots(C)$$

Equation (43) should then read

$$n^2 \eta = \frac{s^2}{\psi} \cdot \frac{D}{N} \quad \dots\dots(D)$$

where  $D = (\psi - \sin \psi)^2 + (1 - \cos \psi)^2$  and the third term of  $N$  should be multiplied by  $\psi$ .

A graph of  $n^2 \eta$  against  $\psi$  is shown in Fig. A.

We agree that the condition

$$\frac{s}{\psi} \leq \cos \theta \quad \dots\dots(E)$$

can be obtained from the equations stated.

<sup>‡</sup> van Loock, W. M. and Cardon, A., *The Radio and Electronic Engineer*, 35, No. 5, pp. 273-80, May 1968.

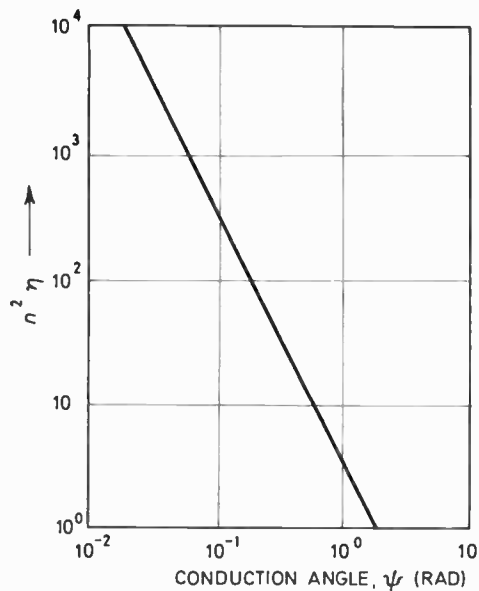


Figure A

Assuming that

$$\sin \theta \leq 0.89 \quad \dots\dots(F)$$

one can obtain  $\psi \geq 1.43$  rad giving, from Fig. A,

$$n^2\eta \leq 6.8 \quad \dots\dots(G)$$

compared to eqn. (44) which should read

$$n^2\eta \leq 15 \quad \dots\dots(H)$$

We cannot, however, derive (F) from (E). Although it was not stated in the paper,  $s$  was defined from eqns. (27) to (29) as

$$s = \sin \theta - \sin(\theta + \psi) \quad \dots\dots(I)$$

Substituting (I) and (26) into (E) and eliminating  $\theta$ , one obtains the condition

$$\psi^2 - 2(1 - \cos \psi) \geq 0 \quad \dots\dots(J)$$

This is true for all  $\psi$ , hence from eqn. (26) there is no limit on the value of  $\theta$ . As Fig. A shows that  $n^2\eta$  tends towards infinity as  $\psi \rightarrow 0$  some other constraint must be found. If this condition is a function of  $n$  then the efficiency is no longer proportional to  $1/n^2$ .

S. M. BOZIC  
R. J. STINCHCOMBE

Department of Electronic and  
Electrical Engineering,  
University of Birmingham,  
P.O. Box 363, Birmingham, 15.

1st November 1968.

**Authors' Reply:** We regret the existence of a number of errors in our paper and thank Dr. Bozic and Mr. Stinchcombe for drawing our attention to them. A list of corrections to errors, some of which have not led to incorrect conclusions, is given below.

Our conclusion that  $\sin \theta \leq 0.89$  seems to be in error and Dr. Bozic and Mr. Stinchcombe have proved that there is no limit on the values of  $\theta$  and that another constraint must be found. We agree with their remarks but we have not found an explanation yet: the problem is under investigation.

W. M. VAN LOOCK  
A. CARDON

Laboratorium voor  
Electromagnetisme en Acustica,  
Sint-Pietersnieuwstraat 41,  
Gent, Belgium.

27th December 1968.

### Corrections

In addition to the corrections referred to in the above correspondence, the following changes should be made to the paper 'A Theoretical Analysis of the Ideal Step-recovery Diode in the Series-mode of Operation'.†

page 274:

eqn. (6)  $\epsilon_n \sin(n\theta + \phi_n - \beta_n)$  instead of  $\epsilon_n \sin(n\theta + \beta_n)$  in the numerator.

page 276:

eqn. (29)  $T$  instead of  $U$  in the denominator.

page 277:

eqn. (30) The third term in the bracket should read  $\frac{1}{2} \sin 2\theta$ .

eqn. (31) should read

$$B_g = \frac{1}{2\pi R_s} (\sin \phi + 3 \sin \theta)(\sin \phi - \sin \theta)$$

with a corresponding change in the conclusions about the limits of  $B_g$ .

eqn. (32) 4's instead of 2's in the denominator.

eqn. (33)  $[2(1 - \cos \psi) - \psi \sin \psi]^2$  for the numerator.

eqn. (38)  $s^2/\psi$  for the factor containing  $\psi$ , with  $s^2$  given by eqn. (33).

The value for which  $P_n$  is maximum is obtained for  $\psi = 3.7$  instead of  $\psi = 3.9$ .

page 278:

eqn. (42) The second factor of the denominator should read

$$(\psi - \frac{1}{2} \sin 2\phi - \frac{1}{2} \sin 2\theta + 2 \sin \theta \cos \phi).$$

eqn. (43) The numerator should read

$[2(1 - \cos \psi) - \psi \sin \psi]^2$  and the third of  $N$  should be multiplied by  $\psi$ .

col. 2, 3rd para.:

$$\frac{s}{\psi} \leq \cos \theta \quad (\text{delete } \sin \theta \leq 0.89)$$

(There is no limit on the values of  $\theta$  or the normalized bias.)

† See second footnote on opposite page.

# **Conference on Digital Methods of Measurement**

**University of Kent at Canterbury  
23rd to 25th July 1969**

This summer was one of the finest in South Eastern England for many years and Canterbury in July was as attractive as this garden of England can ever be: but still the quality of the papers at the Conference held the interest of the audience so that more than one commented that the relevance of the subject matter to industry to-day was well above the average for technical conferences.

## **Physical Quantities**

The first day went some way to illustrate the extent to which digital methods had 'arrived' for it was concerned with the measurement of physical quantities using digital techniques. The first paper by J. E. Crawford, P. E. Osmon and J. A. Strong of London University dealt with spatial measurement using digitized vidicon cameras and so demonstrated that the span of digital instruments was much wider than voltmeters and counters. They were to come later. Nevertheless the paper by B. W. Barringer and A. J. Bonner described a method which relied on counting for length measurement by laser interferometer. Similarly, the paper by Dr. G. H. de Visme described the use of counters to measure angular speed and acceleration by converting the output of an incremental digitizer to a series of pulses. So familiar digital techniques lay behind many interesting applications.

The first afternoon session commenced with a paper by P. Diederich of the Decca Navigator Company entitled 'Extracting angular values in digital form from vectors expressed in rectangular co-ordinates'. Mr. Diederich showed how the equipment was based on an accurately run two-phase oscillator, the phase conditions of which are determined by the two rectangular co-ordinates. The results are obtained by counting the oscillator output and comparing the results with a calibrating standard based on fixed injected voltages only. The accuracy of the instrument was governed by the very high  $Q$  values achieved from the oscillator. The long-term drifts are compensated by the self-calibration techniques involved.

A totally different atmosphere was created by Prof. P. B. Felgett of the Department of Applied Physical Sciences at Reading University who spoke on the direct digital transduction of environmental properties. Beginning with the standpoint that many traditional areas of measurement, such as astronomy and meteorology, were in a significant area of change, he said that modern requirements of space and the use of national resources needed new information presented in a new way, and often over an area which had never been previously envisaged. Prof. Felgett expounded his philosophy of the need to

The Conference was organized by the Institution of Electronic and Radio Engineers with the association of the Electronics Division of the Institution of Electrical Engineers and the United Kingdom and Republic of Ireland Section of the Institute of Electrical and Electronics Engineers.

This article is based on reports compiled by the various Chairmen of Sessions of the Conference, namely Wing Cdr. D. R. McCall and Messrs. D. R. Ollington, A. G. Wray, R. I. Ostler, A. H. Appleyard and K. J. Dean; Mr. Dean, Chairman of the Organizing Committee, has co-ordinated the component parts. The full list of papers read at the Conference was published in the June 1969 issue of *The Radio and Electronic Engineer*; the papers presented are available as 'I.E.R.E. Conference Proceedings No. 15'.

---

digitize at the earliest stage of measurement and so deal with data in cheap computer form. The need to see how to digitize early in the measurement cycle coupled with the need for new and extended observation was changing the face of meteorological devices. He illustrated this with a new concept, typical of the trend, which involved an onization anemometer using field effect devices and radioactive isotopes.

G. Mayer, on behalf of his colleagues L. Simonfai and P. Potzy, presented the Hungarian paper on high accuracy digital linearization of frequency signals of sensors. The area of application of the device is for the linearization of the output of a mechanical resonator density meter. The linearization is achieved by the modulation of a series of clock pulses, which is part of a linear piece-part approximation to the required curve. There was some very significant discussion of the paper with reference to British equipment designed for similar industrial applications. Nevertheless, it was illuminating to see how electronics for industrial applications is being developed into commercial equipment in Hungary.

In the absence of the authors of another overseas paper K. J. Dean delivered an impromptu paper on the problems of teaching digital electronics. He challenged the audience of 270 (containing only 40 representatives of educational circles) to decide what were the trends in design needed now to inject into the student production line, whose quality would only be assessed in 3-4 years time. Circuit design was rapidly becoming obsolete. What was needed now was an 'interconnection engineer' dealing with hardware specially fabricated to specific needs and using functional building blocks such as adders, multipliers, shift registers and counters. General purpose concepts were outmoded in an age when an l.s.i. chip can contain a complete shift register or a long counter. Mr. Dean showed that multipliers and shift registers could be combinational rather than sequential circuits, thus yielding a worthwhile increase in operating speed.

After the heat and the pressure of question and discussion the day finished with an excellent cocktail party enjoyed in the coolness of the Cloister Court of Eliot College.

### Voltmeters and Other Digital Instruments

In the first paper of the second day of the Conference J. S. T. Charters of Heriot-Watt University read his paper on 'The design of logic and counting circuits capable of operating at 1 GHz pulse repetition rate. Mr. Charters described some of the problems of operating transistor counting circuits and said that the maximum counting speed of currently available units was about 350 MHz: the theoretical limitations with tunnel diode circuits was nearer 10 GHz. Tunnel diode circuits, he pointed out, had been used in nuclear applications for some time. Applications in commercial counters were few, partly due to difficulties experienced in the early 1960s, when the characteristics of the tunnel diodes manufactured at that time were very variable, and partly because most workers failed to appreciate the necessity to analyse the circuit fully and to design accordingly. Mr. Charters showed several equivalent circuits and demonstrated how, using a computer, he designed some basic bistables and shaping circuits. During questions after the paper he stated that reliability had been found to be very good during the seven to eight years he had used them at the Rutherford Laboratories.

Dr. R. F. Hall of the Mullard Research Laboratories described a new flat dot-matrix glow-discharge alpha-numeric tube he had developed. This used a 7-by-5 dot matrix formed by glows at the end of pins aligned in the direction of view. He said that the tube was cheaper than currently available neon number tubes but that the drive circuits were a little more expensive. In answer to a question Dr. Hall stated that development samples would be available by the end of the year.

The last paper before the coffee break was given by R. V. Wall of the Plessey Company who gave some background information to the design of an automatic weather station. This was illustrated by slides showing several installations around the country.

Following the break, J. R. Pearce gave the first of two papers on digital voltmeters. He described the techniques involved in isolating digital voltmeter input circuits. The paper was given in a very lucid style and illustrated by excellent diagrams (mostly in colour) using the overhead projector.

B. Mann, a post-graduate student at the College of Aeronautics, Cranfield, followed with a paper concerned with decision-making in digital voltmeter design. He described what was, in effect, a 'check-list' of decisions showing the dependency paths between decisions. Combined with this, he suggested a 'data-pack' consisting of a number of cards, each one carrying the decision to be made at the top, then underneath listing the input data and decisions required. Mr. Pearce followed with his second paper 'Digital carry applied to successive approximation voltmeters.'

At an early stage in the Conference the view was expressed, and frequently repeated, that the proliferation of conventional analogue and analogue/digital hybrid instruments should be discouraged. Measurement should be made by direct digital transducers capable of fundamental calibration. In many cases the digital output of such transducers would be presented to a small general-purpose computer for information processing. This view was also strongly presented by two of the speakers, K. F. Shrubbs and Dr. L. Molyneux in the informal discussion on the digital measurement of physical quantities which concluded the second day of the Conference. T. H. Thomas and D. J. Maxwell, also in sympathy with the philosophy, exposed the lack of hardware and ideas for direct digital transduction. R. V. Wall cast great doubts on the feasibility of developing true digital transducers. He expressed more concern for good analogue measurement followed by analogue to digital conversion. The discussion did not, of course, lead to complete agreement, but rather showed up the strong differences of opinion of the philosophy of measurement.

It is interesting to look back over the papers presented earlier in the afternoon to consider the views either implied or specifically expressed on this subject by the authors.

Of the seven papers, four were clearly concerned with self-contained laboratory instruments. The two contributions from D. Wheable showed the precision which can be achieved in the digital voltmeter field by careful analysis of the many factors affecting overall accuracy. By contrast, C. A. Sparkes and R. G. Clark demonstrated most effectively the high performance-to-cost ratio which they had achieved through novel and economic circuit design in their digital multimeter. The field strength measuring receiver described by D. G. Beadle, J. A. Fox and D. E. Susans was clearly an example of the application of digital techniques to what has been traditionally an analogue measurement problem. The benefits gained were ease of operation, unambiguous readout and repeatability.

The contribution from K. Heron and Dr. L. Molyneux demonstrated the use of sophisticated digital techniques in the measurement of the area under the somewhat ill-defined immuno-electrophoresis curves. Height was measured by conversion first to resistance, then to time and finally to a digital output which was processed by computing circuits.

J. D. Martin described circuits for pulse rate to digital code conversion. Either engineering into a laboratory instrument or coupling to a general purpose computer would be possible.

The remaining paper of the session, from H. E. Hanrahan, could be interpreted to be within the 'digital transducer coupled to general-purpose computer' philosophy. His proposals were far reaching and a pointer to the techniques to be employed in future instrumentation. Clearly designers of self-contained laboratory instruments can feel secure for the foreseeable future but they must face the challenge of bringing down the computer from its exalted position to become the practical servant of measurement.

The dinner traditional at I.E.R.E. Conferences was held in the spectacular dining hall of Eliot College whose huge south window frames a distant view of Canterbury Cathedral. The occasion was under the chairmanship of Mr. J. A. Sargrove, a Vice-President of the I.E.R.E., and other speakers were Professor H. Sutcliffe and Mr. K. J. Dean.

### Digital Communication Systems

The last day of the Conference was concerned with measurements on digital communication systems and the first two papers dealt with measurements on p.c.m. systems. The presentation was effectively a collaborative effort between G. H. Bennett of the Post Office Telecommunications Headquarters and A. N. Ramsden of Marconi Instruments.

The following four papers were concerned with evaluating and determining the error rate of data transmission. While the papers by M. B. Ashdown, A. G. Perna and P. Noakes related to conventional links, that by P. G. Farrall described equipment for assessing the performance and the results thereby obtained, on a short (450 m) optical laser link.

The final five papers of the Conference dealt with a variety of different techniques associated with digital communication systems, using the term 'communication' in the broader sense of implying 'information'. In their paper 'The correction of distortion in digital instrumentation systems' R. V. Leedham and J. A. Barker described the results of their investigations at the University of Bradford into the problems associated with the establishment of equalizer networks or inverse systems for correcting the non-linearity of transducer sensing heads. It is becoming common practice to use a digital computer to design such networks and the computer is a tool which naturally functions in the time domain. The authors showed how often examination of the problem in the frequency domain yields information in a form which can be more readily assimilated and can expose possible pitfalls in relation to the stability criteria of the compensation network proposed. If, for example, the transmission of the transducer falls to zero at any particular frequency, then information at that frequency can often be a timely warning that one may well be running into problems of noise.

R. Thomason of Cranfield admitted that in some senses he was at the conference under false pretences in that the current aircraft instrumented landing system to which he and Sqdn. Ldr. M. Mukutmoni make reference in their paper is primarily an analogue measurement of the modulation depth of a two-tone test signal of 90 Hz and 150 Hz. However, Mr. Thomason went on to show how most of the relevant information on this signal is contained in a small part of the complete cycle and that better discrimination and signal/noise ratio could be obtained by quantization using a delta modulation technique. First, single integration was considered and the improvement in information retrieval illustrated. He then pointed out how even better results still could be obtained if double

integration were used—that is, using every delta pulse to sense the change of slope rather than the amplitude of the two-tone modulated waveform.

To quote Dr. J. A. M. McDonnell of the University of Kent, 'Correlation may be required where observations are contaminated by noise and other extraneous stimuli; where the spectral content of the signal may be required, or when a system impulse function is to be obtained by low level random noise stimulation'. In association with his co-author, J. Forrester, he proceeded to show how much useful information can be derived from the simplest of units, a one-bit correlator operation on waveform polarity only. Supported by numerous graphs a convincing demonstration was given to its power as a tool for measuring the correlation function relating to various combinations of signal and noise. In one reference, for example, it was shown how the polarity coincidence technique had been carried into the field of radio astronomy in the search for the deuterium line—using an integration time of 21 weeks!

In the final paper of the conference entitled 'Standard l.f. noise sources using digital techniques and their application to the measurement of noise spectra' Professor H. Sutcliffe and Dr. K. F. Knott gave a glimpse of the work they have been doing at the University of Salford on l.f. and v.l.f. noise generation. They explained the limitations of the purely analogue noise generators so often employed at high frequencies and pointed out how greater precision and accuracy could be achieved from a digital approach to the problem. Basically the method they have chosen is to generate a chain of clock pulses at constant rate and then to select the polarity of each pulse in the chain on a completely random basis. The clock frequency and pulse amplitude can, of course, be precisely defined.

The authors then illustrated how the power spectral density of their type of generator was very much dependent upon the number of discrete lines involved, supporting their argument with a number of practical examples. They also examined the effects of introducing a pseudo-random element into their basic system by employing the well-known shift register technique and in so doing showed how this could reduce the time needed to make a specific measurement to a given degree of accuracy. However, they did conclude that this advantage conferred by the pseudo-random approach was, in their opinion, more than offset by the added complexity introduced into the experimental procedures.

Certainly, none of those who attended this conference could have left without being aware of the ever-widening sphere of influence of digital techniques. Indeed, at times one felt tempted to think that it would be quicker and perhaps even better to examine the digital approach to a problem—any problem—first of all, whether it be in measurement or other instrumentation or in communications. Such was the enthusiasm and persuasiveness of the speakers. Canterbury 1969 must surely, in the experience of all those who were privileged to be there, stand as a landmark in the digitization of electronics.

# Simulation of Steady State Fluid Flow in Pipes

By

E. M. McKAY,  
M.Sc., A.Inst.P., C.Eng.,  
M.I.E.R.E.†

**Summary:** After outlining some of the problems associated with the design of fluid flow networks a brief survey is made of the methods whereby such systems have been simulated. The use of analogue techniques for this purpose is discussed and an attempt has been made to compare the various methods proposed. As a result of this study certain improvements were considered to be worth seeking, and a new type of simulator is described based on the exponential family of pipe resistance laws. A novel feature is the independent control of simulated length and diameter.

## 1. Introduction

The design problems associated with fluid flow networks may take a variety of forms depending on the initial data. Thus we might have a system with pre-determined spatial layout, fixing the length of the elements, but their sizes (diameters or cross-sectional areas) are required. Alternatively an existing system may require extension or modification in some way and it is required to find the effect of this on the rest of the system. In general terms what is to be considered here is the engineering solution to the problem of optimizing the pipe system performance for a given set of conditions.

Fundamental to all such considerations is the relation between the pressure drop and the flow rate for each pipe element of the system. For a single straight length a variety of formulae exist. The choice from these will be based on the range of Reynolds' numbers involved and the accuracy required; there might also be, in the case of gaseous fluid flow, the question of compressibility. As examples of the difficulties we might cite: (1) the Reynolds' number may not be considered as an independent variable since it will, in part, be determined by the system parameters, (2) the 'accuracy' cannot be specified simply, for the system as a whole, using a single formula, (3) the effect of compressibility where applicable can only be determined when the fluid pressures in the various elements are known.

The question of accuracy deserves special mention since it has been fundamental to the argument concerning the 'best' method of solution. Generally speaking it has its roots in the adequacy or otherwise of the original data, e.g. the nature of the pipe surface and its constancy with time, the standardization of pipe sizes in discrete steps and the acceptance of a nominal value for each one. The design of such systems also invariably requires some estimate to be made regarding future requirements. As a result of such considerations there has been an obvious and understandable temptation to use approximations and employ the simpler formulae.

† Building Research Station, Garston, Watford, Hertfordshire.

## 2. Formulae for Pipe Flow

Of the formulae proposed that with the widest application is the Colebrook-White expression. This is a compromise between the smooth and rough pipe laws having two terms, one drawn from each law with an appropriate weighting coefficient obtained empirically. Other formulae are also in common use, their relative simplicity of form being considered to outweigh the disadvantages of reduced accuracy and range. Most of these are explicitly in, or may be converted into, the so-called exponential form. In these the pressure difference across a given length of pipe is proportional to the rate of flow through it, raised to some power, equal to or slightly less than two. A good account of these and the Colebrook-White expression may be found in Webber.<sup>1</sup>

## 3. Direct Analogues—General Considerations

Given the single class of problems to be solved, the alternative to a general-purpose digital<sup>2-5</sup> or analogue computer facility is the direct analogue simulator. The choice of the latter will rest basically on considerations of cost versus usefulness. To evaluate this at least two important questions must be asked: (1) Are the facilities offered by the general-purpose machine really equal to those of the purpose-made simulator? (2) Is there sufficient demand to justify such specialized equipment? These questions are of course related to some extent.

A variety of direct analogues have been devised to simulate fluid flow networks and in the main these have been electrical or electronic. A pneumatic analogue has been described by Linford<sup>6</sup> which is claimed to be 'much less expensive than the electronic equivalent', but no figures are given to support this claim. Indeed it immediately begs the question, what is meant by 'the electronic equivalent'? A complete answer to this must include consideration of the range of pipe resistances, pressures and rates of flow, facilities for measurement and range switching etc. Further whilst the real cost per function using electronic components has fallen steadily since the early days of the transistor, it is hard to imagine this occur-

ring to anything like the same extent with the specialized component described by Linford.

Comparison of the basic methods must also be made on the basis of the overall system, considering such features as programming (with the possibility of a program store) and adjustment of all elements by a single factor simulating an increase in total demand by some given percentage. Further there is the question of the form of read-out and its facility, if required, for recording and possibly further computation.

### 3.1. *Electrical and Electronic Analogues*

The first electrical simulator for fluid flow in pipe systems would seem to be that described by McIlroy.<sup>7</sup> This method has been fairly widely adopted in the U.S.A. and has as its basic element a tungsten filament in an evacuated enclosure giving the voltage current relation

$$v = ki^{1.85} \quad \dots(1)$$

This was chosen in order to simulate the Hazen-Williams formula, one of the exponential family of pipe flow laws much used in water supply. It is applicable with fair accuracy for Reynolds' numbers greater than 4000.

With such an approach the major handicap is one of inflexibility since each of the basic units has a fixed value of  $k$  corresponding to a given hydraulic resistance. Thus the first step in using such a simulator would be the selection of the correct unit corresponding to a given pipe.

The task is clearly straightforward when an analysis of the performance of a given system is required. However when it is a question of synthesizing a system in order to achieve a required performance (the more common situation in new system design), the advantages of a modular system with interchangeable units having a variable  $k$  are obvious.

An additional disadvantage results from the fact that the elements are not standard components readily available. Furthermore no information has been found regarding the ease with which such elements may be produced nor of the constancy of their characteristics with time. However the method does have the merit of simplicity in that single passive elements only are used requiring no separate power supplies. Finally it might be suggested that variation in  $k$  could be obtained simply by means of a scaled set of the basic elements. These may then be switched to form various combinations as will be described later (Section 4.2) in connexion with the biased diode function generator.

A number of other methods exist whereby the necessary non-linear relation may be obtained in order to simulate an exponential pipe flow formula. Thus

we may have function generators using resistor and biased diode combinations, voltage regulator (Zener) diode networks, avoiding the need of separate bias supplies, or voltage-dependent resistors in combination with linear resistors. The first two, which employ a linear segment approximation to the smooth curve, may be used with or without the aid of active devices; the last named must, for the kind of function required here, operate in the feedback path of an operational amplifier. This follows since the relationship obtainable with these devices takes the form  $v = ci^M$  where  $M$  is typically in the range 0.14–0.4.

The most sophisticated simulation for pipe flow is that due to Goberman.<sup>8</sup> This is based on the Colebrook-White expression and is specifically designed for complicated water supply networks where errors due to the use of the simpler exponential relations are said to be excessive (see Stuckey<sup>9</sup>). The resulting pipe unit is however of a complexity and cost which tends to rule out its general application to design offices and teaching establishments since many such units would be required for a worthwhile simulation study. Another method which might be mentioned here is that of McManns and Rushton.<sup>10</sup> Whilst this is not strictly a direct analogue it is nevertheless a special purpose set-up. Using pure resistance elements only it requires an iterative process, carried out manually, to achieve the desired results.

## 4. The Shunt Diode Function Generator for

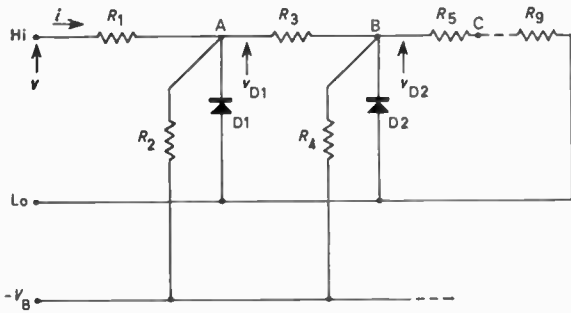
$$v = ki^n, \quad 1.75 \leq n \leq 2$$

### 4.1. *Basic Principles*

The biased diode function generator has found wide application generally in analogue computation and takes a variety of forms.<sup>11, 12</sup> The relevant types for the simulation of an exponential pipe flow relationship will now be discussed.

When used without the aid of an operational amplifier, as an integral part of the function generator proper, the network normally chosen is that of the shunt connexion. This is shown in Fig. 1, together with the kind of voltage-current characteristic obtained. The latter is seen to be a series of linear segments, approximating to the required relation. Five such segments are normally found sufficient for the present purpose, giving errors of less than 1% of full scale.

The principle of this circuit is simply that the effective resistance seen between terminals Hi and Lo is governed by the magnitudes of the resistors chosen and the state of the diodes. Thus as  $v$  increases from zero, points A, B, C . . . become more positive, switching off in turn the diodes D1, D2 . . . so giving a series of linear segments. The relationship between the segment slopes and the resistances  $R_1, R_3, R_5$ , is not simple in a practical case where the diode character-



(a). Shunt diode function generator.  
(b). (right)  $v-i$  characteristic.

Fig. 1

istics are non-linear and the forward voltage drop across each diode is taken into account. However, to a first approximation, the segment slopes are given by  $\tan^{-1}(R_1)$ ,  $\tan^{-1}(R_1 + R_3)$  etc. As an example of the errors involved, the slope of the second segment may be shown to be

$$\frac{dv}{di}\bigg|_2 = R_1 + \left(\frac{R_2}{R_2 + R_3}\right) R_3 + \left(\frac{R_2}{R_2 + R_3}\right) \frac{dv_{D2}}{di_1} \dots\dots(2)$$

Thus for the bias resistances (even subscripts) high compared with the slope resistances (odd subscripts) and further for  $v_D$  (in the on state) relatively constant, the approximation given is justified.

4.2. Methods Used to Obtain a Variable  $k$

Control of the  $k$  value is obtainable with or without the aid of an operational amplifier. In the latter case a simple approach would be to provide a number of these networks with binary scaled  $k$  values such that they may be switched in various series combinations giving

$$v = v_1 + v_2 + \dots = \sum v_i \dots\dots(3)$$

$$= k_1 i^n + k_2 i^n \dots = \sum k_i i^n \dots\dots(4)$$

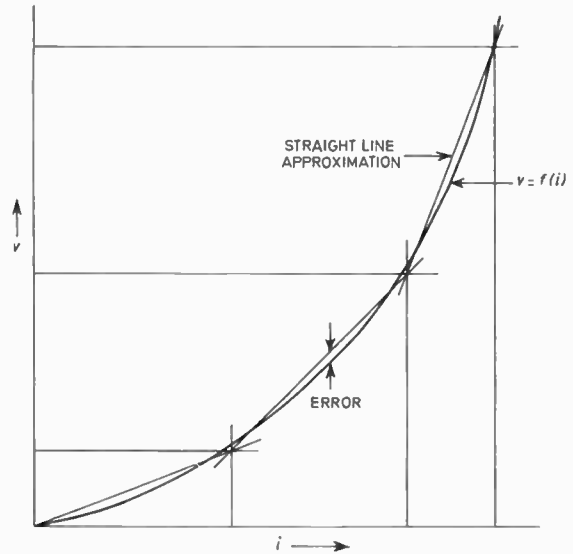
The parallel combination of such networks, suggested by one manufacturer to give further interpolation, is not however a practicable proposition except in the trivial case of networks having the same  $k$  values. This may be seen from the simple case of two networks only, having parameters  $k_1$  and  $k_2$ . Thus

$$v = k_1 i_1^n = k_2 i_2^n \dots\dots(5)$$

$$i = i_1 + i_2 = \left(\frac{v}{k_1}\right)^{\frac{1}{n}} + \left(\frac{v}{k_2}\right)^{\frac{1}{n}} \dots\dots(6)$$

giving

$$v = \left\{ \frac{1}{\left(\frac{1}{k_1}\right)^{\frac{1}{n}} + \left(\frac{1}{k_2}\right)^{\frac{1}{n}}} \right\}^n i^n \dots\dots(7)$$



Finally, even for the simple series connexion of these networks, nine would be required to give a range of 511 : 1 in discrete steps of unity. Remembering that the resistor values to be used will normally be other than preferred values the method whilst simple in principle will nevertheless not be cheap.

Using the same basic connexion Williams<sup>13</sup> found an alternative solution to the problem of a variable  $k$ . The circuit is illustrated in Fig. 2 and may easily be shown to develop the relation

$$v = \frac{k}{\{1 + (R_1/R_0)\}^n} i^n \dots\dots(8)$$

where  $v = ki^n$  is the relation obtained with the input to the operational amplifier (giving unity gain) disconnected. The range of values for this method is claimed to be of the order  $2 \times 10^4 : 1$  and is continuously variable by means of  $R_0$ , coarse and fine adjustment being provided.

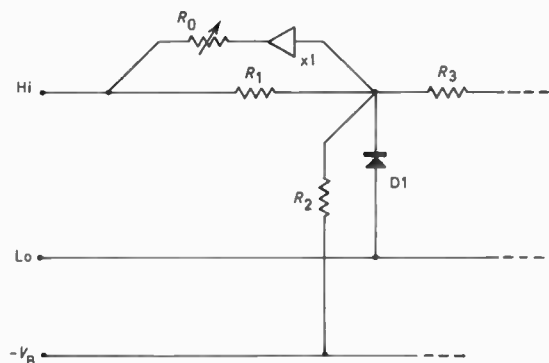


Fig. 2. Method for variable  $k$  (after Williams<sup>13</sup>).

### 5. Other Methods of Function Generation

#### 5.1. The Use of Voltage Regulator Diodes

As an alternative to the biased diode function generator one may use voltage regulator diode networks, thus obviating the need for a separate bias supply. A detailed account of the resistance value calculations may be found elsewhere.<sup>14</sup> The problem here, however, is the maximum terminal voltage of say 10V is assumed, is the relatively high value of the first break point. This may be partially overcome by also using asymmetric voltage-dependent resistors which provide substantially constant voltage characteristics at lower values than those obtainable with the regulator diodes (typically 3.3V minimum). Examples of these would be the two Mullard devices in the E295ZZ series giving constant voltages of 1 and 1.35V.

#### 5.2. The Use of Non-linear Resistors

A number of attempts have been made to apply voltage-dependent resistors (e.g. silicon carbide) to function generation but these have not been widely used for the purpose. However their application in this context may be assessed by reference to Kovach<sup>15</sup> and Brown and Walker.<sup>16</sup>

As has been previously pointed out it is necessary to use such devices in the feedback path of an operational amplifier by virtue of the magnitude of the exponent in the relation  $r = ci^M$ .

### 6. A New Simulator for Pipe Flow Problems

#### 6.1. Basic Principles

A basic objection to all the foregoing methods is that the  $k$  value whether variable or not is still treated as a single entity. However since it simulates the hydraulic resistance it is in fact a function of the length, diameter and surface nature of the pipe. Thus generally for the exponential form we would more usefully write

$$\delta p = \frac{Kl}{d^m} \cdot q^n \quad \dots\dots(9)$$

- where  $\delta p$  is the pressure difference across the pipe,
- $q$  is the rate of flow of fluid through it,
- $K$  is some constant determined by the nature of the pipe surface,
- $l$  and  $d$  are its length and diameter respectively,
- $m$  and  $n$  are empirical constants.

With the methods previously discussed there is therefore the need for computation, or reference to graphs or tables, in order to relate changes in length with those of diameter for a pipe of a given type. This clearly results in something less than full simulation.

In order to overcome this limitation ways have been sought by the author whereby the simulated length and diameter may be separately controllable.

Now in view of the inherent limitations of a direct analogue to a single class of problems, and since for practical systems many such units would be required, the cost of the basic unit was taken to be a major design criterion. Related to this was the question of simplicity since one of the applications envisaged would be in teaching establishments; these would include building science departments and schools of architecture where there is no great tradition of such experimental work.

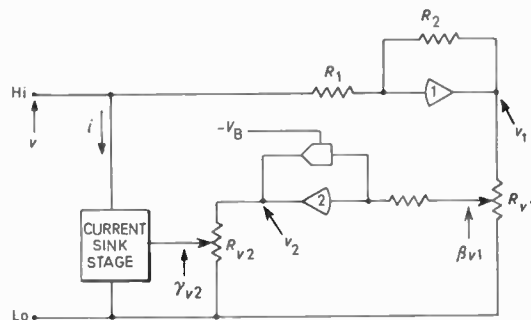


Fig. 3. A new simulator for pipe flow.

Figure 3 illustrates, in schematic form, the principle of the circuit chosen. The requirement, basically, is a two-terminal device with terminal voltage and current related in such a way as to give simulation of equation (9). Thus, taking all voltages shown with reference to the lower terminal, Lo (not ground) we have, firstly, the output of amplifier A1, given by

$$v_1 = -\frac{R_2}{R_1} v = \alpha v \text{ say} \quad \dots\dots(10)$$

This feeds the potential divider RV1 (which will be shown to provide control of the simulated length), giving  $\beta v_1$ , say, as the input to the function generator stage. The output from this,  $v_2$ , is arranged to take the form

$$|v_2| = k|\beta v_1|^n \quad \dots\dots(11)$$

where  $v_2$  is positive for  $v_1$  negative, i.e. the normal inverting arrangement. This output feeds a further potential divider stage, which will be seen to control the simulated pipe diameter, giving  $\gamma v_2$ , say, as the input to the current sink stage. Thus if the transconductance of this stage is  $g_m$  we have,

$$i = g_m \gamma v_2 \quad \dots\dots(12)$$

$$= g_m \gamma k (\alpha \beta v)^n \quad \dots\dots(13)$$

giving

$$v = \frac{1}{(kg_m)^n} \frac{1}{\alpha} \cdot \frac{1}{\beta} \cdot \frac{1}{\gamma^n} i^n \quad \dots\dots(14)$$

Thus comparison with equation (9) shows that we have the necessary simulation if,

$$\left. \begin{aligned} \delta p &= k_1 v \\ l &= k_2 \left(\frac{1}{\beta}\right), \text{ or alternatively } k_2 \left(\frac{1}{\alpha}\right) \\ d^m &= k_3 \gamma^n \\ q^n &= k_4 i^n \end{aligned} \right\} \dots\dots(15)$$

Taking  $\alpha$  as a fixed value, for convenience, we have from equations (9) and (15),

$$k_1 v = K k_2 \left(\frac{1}{\beta}\right) \cdot \frac{1}{k_3 \gamma^n} \cdot k_4 i^n \dots\dots(16)$$

Therefore

$$v = K \frac{k_2 k_4}{k_1 k_3} \cdot \frac{1}{\beta} \cdot \frac{1}{\gamma^n} \dots\dots(17)$$

which on comparison with equation (14) gives

$$K \frac{k_2 k_4}{k_1 k_3} = \frac{1}{(kg_m)^n} \cdot \frac{1}{\alpha} \dots\dots(18)$$

Now  $K$  is the constant determined by whichever of the exponential formulae is chosen for the original equation and the units adopted. Thus if we attribute fixed values to both  $\alpha$  and  $g_m$  it will be seen that the remaining parameters  $k, k_1 \dots k_4$  are interdependent.

Both  $\beta$  and  $\gamma$  take maximum values of unity. Thus since  $\beta = 1$  corresponds to the minimum simulated length of pipe this fixes  $k_2$ . For building services a useful range for  $l$  might be  $1 \leq l \leq 30$  metres. (It should be noted that if greater lengths than 30 metres arise two or more units may be connected in series.) For this range we then have  $k_2 = 1$ . Similarly  $k_3$  is fixed, since  $\gamma = 1$  corresponds to the maximum pipe diameter, thus  $k_3 = (d_{max})^m$ .

For the remaining three scale factors  $k_1, k_4$  and  $k$  it is simplest to fix the first two initially. This enables the scaling of the instruments used for measurement of voltage (pressure difference) and current (rate of flow) to be suitably chosen to accord with the units of the original problem. This then leaves the constant of the function generator stage to be determined in terms of the others.

One comment which might arise at this stage results from the different exponents for the diameter term in the original and simulated expressions. This may however be readily dealt with by suitably scaling the potential divider RV2. In fact a switched facility may be provided indicating standard pipe sizes only if this is required.

One significant advantage of the basic unit described is that the biased diode function generator may be provided on a plug-in facility. This then enables different values of  $k$  and  $n$  to be provided, enabling different exponential relations to be simulated with the same basic unit. For example, if fittings, T-junctions, elbows etc., be considered in terms of an equivalent length, they also may be simulated with the same basic unit (for building services the losses

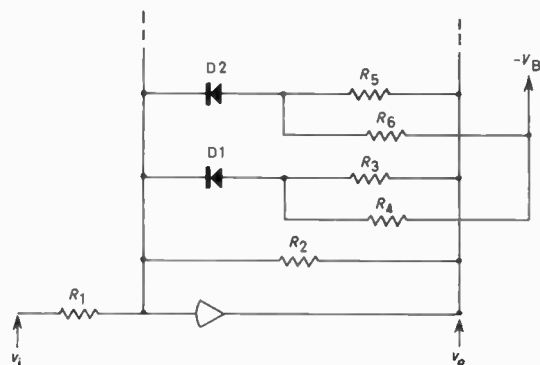
in fittings may well be of the same order as those of the pipes themselves).

Finally it should be pointed out that each unit requires its own floating power supply. This is required so that any unit may be connected in any position of the simulated network. Because of the separate supplies it is necessary, in order to keep down the total cost that the bias supply, for the diode function generator should be taken as one of those provided for the amplifiers, normally requiring both positive and negative rails. A simple stabilized supply effected by means of a regulator diode is sufficiently stable for the purpose as the currents drawn are in the tens of milliamperes range or less. The tolerance of such devices does however need consideration since the diode function generator characteristic is directly dependent on the bias voltage (see Appendix).

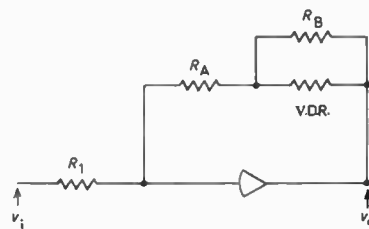
6.2. Circuit Elements

6.2.1. Function generation

Let us consider first the function generator stage. For this a series-connected biased diode function generator was chosen operating in the feedback path of an operational amplifier as shown in Fig. 4(a). Five segments, i.e. four diodes, were found to be adequate for the accuracy required. Calculation of the slope and bias resistors is considerably simpler for this mode than for the shunt connexion discussed earlier. The method for these calculations is given in the Appendix. When using this inverse type of func-



(a) Operational amplifier with diode function generator feedback path.



(b) Use of voltage-dependent resistor as alternative to diode function generator.

Fig. 4

tion generator it is also possible, as mentioned in Section 5.2, to use voltage-dependent resistors (see Fig. 4(b)). Design methods for the calculation of the series and parallel resistors may be found elsewhere.<sup>16,17</sup>

6.2.2. The current sink stage

For the current sink stage it has been found practicable to use a single transistor in the common emitter configuration. This offers an incremental resistance ( $1/h_{oe}$ ) which is sufficiently high for the accuracy attempted here, i.e. better than  $\pm 1\%$  of full scale.

The effect of bottoming on the current sink transistor may be overcome simply by taking its emitter to a potential slightly negative ( $-0.7V$  say) with respect to the low potential terminal (Lo). In the circuit used this was obtained from a potential divider comprising a resistor and diode connected in series between the negative rail and Lo. A suitably low value of the series resistor enables the voltage drop across the diode to be maintained sufficiently constant.

To obtain a linear transfer characteristic, i.e. constancy of  $g_m$ , the base must be current-driven. Thus a base resistor of a few kilohms is required to mask the low output resistance of the operational amplifier A2. This resistor could of course be a variable, offering alternative or additional control over the simulated pipe diameter. Its more restricted range however makes it less suitable than the potential divider RV2 as a single control.

The addition of a multi-stage amplifier to drive the current sink offers considerable advantages in that both greater linearity and the elimination of the offset could be achieved. This solution was not however adopted here on the grounds of cost. Finally the voltage and current ranges chosen, i.e. 0-10V and 0-150mA respectively, necessitated the use of a medium-power transistor (BD124), for the current sink. This has sufficiently high current gain to provide the maximum terminal current without overloading the output of A2.

6.2.3. Operational amplifiers

The choice of operational amplifiers is wide but it is possible to achieve satisfactory results using the lower cost units such as those of the C type from the Plessey SL700 series. These have limitations in that the output signal of one of them (SL701C) is restricted to about 0 to  $-5V$ , and the other (SL702C) to about 0 to  $+9V$ . This however does not prohibit their use here since the first may be employed for amplifier A1 giving a fixed attenuation,  $\alpha = \frac{1}{2}$ , and the SL702C may be used for A2. The usual care must be taken with such wideband units to control h.f. instability. Further there is the question of offset, both voltage and current.

The significance of the various factors giving rise to such problems has been adequately covered elsewhere.<sup>18</sup>

Slightly more expensive devices such as the Motorola MC1433G may be used with advantage since they have lower offset voltages and currents which may conveniently be reduced to zero by means of a voltage applied to a terminal specially brought out for the purpose. The other major advantage with such units is their ability to operate over the normal range for transistor operational amplifiers, i.e.  $\pm 10V$ , before limiting. Thus when used for A1, a simple inverting amplifier arrangement may be used giving  $\alpha = 1$  in the previous expression. When used for A2 the greater output enables a higher base resistance to be used for the current sink.

6.3. Alternative Forms of the Simulator

It has already been pointed out that certain limitations and difficulties exist with the use of the diode function generator. Resulting from these an alternative arrangement, having the same external characteristics and control features, is also being considered and will now be outlined. It will be more expensive than the simulator already given yet might be preferred in certain circumstances especially as it provides a simple method for controlling the exponent,  $n$ .

Basically the generation of the function  $y = x^n$  is achieved here using three operational amplifiers, the first performing a log function, the second fixing the exponent and the third performing an antilog function. This is shown in schematic form in Fig. 5. A transistor operating in the common base mode has been chosen for the generation of the logarithmic response. Also, in order to ensure a relatively constant value of  $\alpha_N$ , the normal common base current gain, this is of the diffused base type. With this arrangement a range of three decades (100mV-10V) is

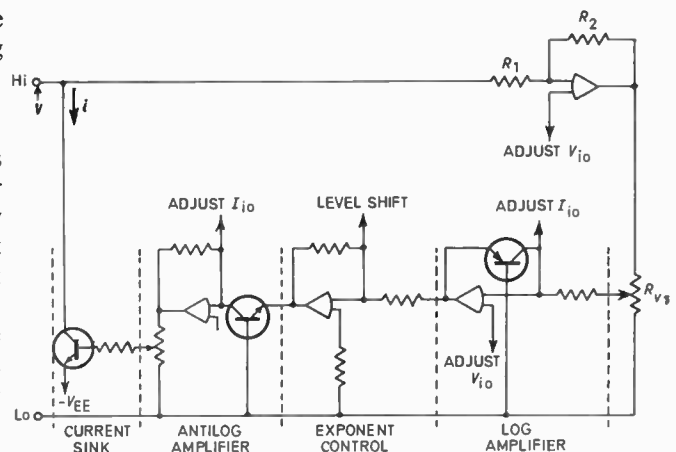


Fig. 5. Simulator using log-antilog function generation.

considered to be both adequate for the purpose and also relatively easy to obtain. The lower end of the range does however make it necessary to provide separate controls for both voltage and current offsets.

Another alternative also being considered is shown in Fig. 6. In this the current sink stage is seen to present an infinite impedance across the simulator terminals and providing ideal current sink characteristics. The principle may be outlined as follows:  $R_s$  is a resistor which is part or all of  $R_1$  in the shunt diode function generator (Fig. 1). This gives rise to a voltage  $\gamma R_s i_1$  say, which feeds the input of a differential input—differential output amplifier, of unity gain. The input to amplifier A3, also of unity gain, is therefore fed by a voltage  $v - (v - \gamma R_s i_1)$  giving for the current through  $R$  a value

$$i = \frac{\gamma R_s i_1}{R} = \frac{R_s}{R} \gamma \left( \frac{\beta v}{k} \right)^n \quad \dots\dots(19)$$

where  $\beta v = k i_1^n$  is the relation developed by the function generator proper. Thus rearrangement of equation (19) leads to

$$v = k \left( \frac{R}{R_s} \right)^n \frac{1}{\beta} \frac{1}{\gamma^n} i^n \quad \dots\dots(20)$$

which is of the same form as that of the previous proposals. Thus the same control features are again provided.

## 7. Conclusions

A number of analogues for pipe flow have been developed which have found application in pipe network design and analysis. With one exception these have been based on an exponential form of the pipe equation. They have all been relatively simple, due presumably, to the large number required for useful pipe network simulation and also to their special purpose nature.

The restricted capability of these simulators is seen as a possible reason for their limited use and for this reason a more complete simulator providing separate length and diameter control has been considered. The basic form of the new simulator has been described based on the use of a diode function generator and integrated circuit operational amplifiers. Alternatives to this are possible providing improved response at slightly greater cost.

## 8. Acknowledgments

This paper is published by permission of the Director of the Building Research Station.

## 9. References

1. Webber, N. B., 'Fluid Mechanics for Civil Engineers' (Spon, London, 1965).

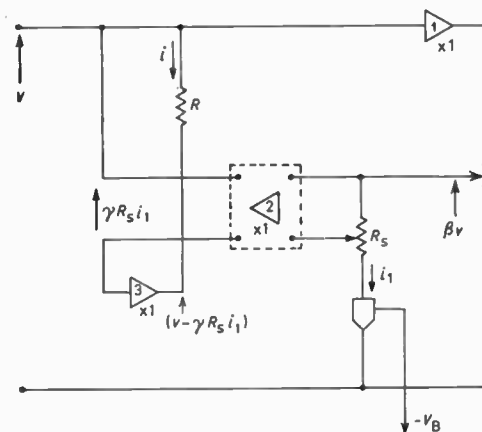


Fig. 6. Proposal for simulator with ideal current sink characteristics.

2. Hardy-Cross, 'Analysis of flow in networks of conduits or conductors', University of Illinois Engineering Experimental Station Bulletin No. 286, November 1936.
3. Adams, R. W., 'Distribution analysis by electronic computer', *J. Instn Water Engrs*, 15, p. 415, 1961.
4. Martin, D. W. and Peters, G., 'The application of Newton's method to network analysis by digital computer', *J. Instn Water Engrs*, 17, p. 71, 1964.
5. Dubin, Ch., 'Analysis of mesh networks by digital computer', Proc. Intl Water Supply Congress, Stockholm, 1964.
6. Linford, A., 'Electronic and air computers for water pipe network design', *New Scientist*, 35, p. 443, 31st August 1967.
7. McIlroy, M. S., 'Direct reading electrical analyser for pipeline networks', *J. Amer. Water Works Assoc.*, 42, p. 347, 1950.
8. Goberman, G., 'New simulator for the flow of fluids in pipes', *Electronics Letters*, 2, No. 3, p. 124, March 1966.
9. Stuckey, A. T., 'The evaluation of pipe constants from field measurements and their significance in the solution of distribution problems', *J. Instn Water Engrs*, 21, p. 337, 1967.
10. McManus, B. D. and Rushton, K. D., 'A pure resistance electrical analogue for the analysis of pipe networks', *Civ. Engng Pub. Works Rev.*, 59, p. 585, May 1964.
11. Gilbert, C. P., 'The Design and Use of Electronic Computers' (Chapman and Hall, London, 1964).
12. Korn, G. and Korn, T., 'Electronic Analogue and Hybrid Computers' (McGraw-Hill, New York, 1965).
13. Williams, R. W., 'A direct analogue equipment for the study of water distribution networks', *Industrial Electronics*, 2, p. 457, 1964.
14. Mullard Ltd., 'Voltage Regulator (Zener) Diodes'. May 1967.
15. Kovach, L. D. and Comley, W., 'A new solid state non-linear analog component', *I.R.E. Trans. on Electronic Computers*, EC-9, No. 4, p. 496, December 1960.
16. Brown, E. and Walker, P. M., 'The design of function generators using silicon carbide, non-linear resistors', *Electronic Engng*, 30, p. 361, March 1958.
17. Brown, G. and Bond, R. A. B., 'Design data for voltage dependent resistor function generators', *Electronic Engng*, 37, p. 584, September 1965.

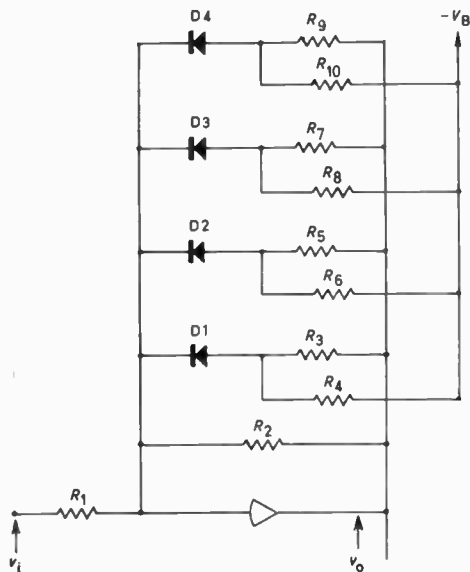


Fig. 7 (a) Inverse diode function generator circuit.

18. Stata, R., 'Operational Amplifiers', Pt. IV, 'Offset and drift in operational amplifiers,' Application Note, Analogue Devices Inc., Cambridge, Mass.

10. Appendix

Referring to Figs. 7(a) and (b) in which a five-segment approximation to  $v_0 = kv_i^{1/n}$  is to be obtained, we will assume initially ideal diodes with zero forward voltage drop and infinite reverse resistance. Further we will consider voltage magnitudes only, the polarity of the signal voltage being dealt with by an appropriate bias polarity and the direction of the diodes.

Now for  $v_i = 0$  all diodes are non-conducting. Then as  $v_i$  increases the output  $v_0$  is given by

$$v_0 = \frac{R_2}{R_1} v_i$$

This continues until the first break point  $v_{0a}$  given by

$$v_{0a} = \frac{R_3}{R_4} V_B$$

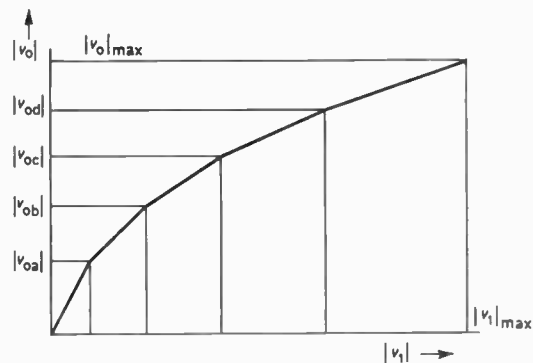
when diode D1 turns on. From this point on  $v_0$  increases with a decreased slope, given by

$$\text{slope of segment 2} = \frac{R_3 // R_2}{R_1} = S_2$$

where  $R_3 // R_2$  is the combined resistance of  $R_3$  and  $R_2$  in parallel. Thus  $R_3$  may be determined.

For the second, third and fourth break-points we have

$$v_{0b} = \frac{R_5}{R_6} V_B, \quad v_{0c} = \frac{R_7}{R_8} V_B, \quad v_{0d} = \frac{R_9}{R_{10}} V_B$$



(b). Inverse d.f.g. transfer characteristic.

For the remaining slope resistors we have, for segment 3

$$S_3 = \frac{R_5 // R_3 // R_2}{R_1}$$

Now  $R_3 // R_2 = S_2 R_1$

Therefore

$$S_3 = \frac{R_5 \cdot S_2 R_1}{(R_5 + S_2 R_1) R_1}$$

and

$$R_5 = \frac{S_3 S_2 R_1}{(S_2 - S_3)}$$

Similarly

$$R_7 = \left( \frac{S_4 S_3}{S_3 - S_4} \right) \cdot R_1, \quad R_9 = \left( \frac{S_5 S_4}{S_4 - S_5} \right) \cdot R_1$$

This shows clearly that the slope resistances are all linearly related to  $R_1$ . Thus if any value is found to be inconvenient a single scale factor only need be applied to all values to produce the required change.

The effect of a finite voltage across the diodes in the on-condition may be seen from the following. Consider as an example the conditions for the second break point, involving the change of state of D2. Let the forward voltage drop be  $V_d$ , then for conduction to start

$$(v'_0 + V_B) \cdot \frac{R_3}{R_3 + R_4} - v'_0 = V_d$$

where  $v'_0$  is the actual value of the amplifier output voltage which causes D2 to turn on.

This gives

$$\frac{R_3 V_B - R_4 v'_0}{R_3 + R_4} = V_d$$

Therefore

$$v'_0 = \frac{R_3}{R_4} V_B + \frac{R_3 + R_4}{R_4} V_d$$

This will be seen to reduce to the simpler expression, previously given, when  $V_d = 0$ .

Manuscript received by the Institution on 17th March 1969. (Paper No. 1288/1C16).

© The Institution of Electronic and Radio Engineers, 1969

# Methods of Increasing Global Communications Capacity by Adaptive Selection of Channels

By

L. A. MOXON,  
B.Sc., C.Eng., M.I.E.E.†

**Summary:** This paper is concerned with the selection of optimum channels for communication through media of which the quality is varying from any cause, including changing levels of interference. In particular it demonstrates the advantage of adaptive frequency selection when a block of channels is shared by relatively large numbers of random intermittent users, as is now the case with many portions of the h.f. band. Various methods of channelling including the broad-band spread-spectrum approach are discussed, and it is shown that adaptive selection of narrow band channels could be compatible with existing non-adaptive usage. The argument is further extended to include a discussion of adaptive use of the v.h.f. and u.h.f. bands for satellite communication on the basis of non-interference with existing services.

## 1. Introduction

There is currently taking place what has been described as an 'information explosion' and increasing demands are being made on the limited number of communication channels available. If this process continues unchecked, the supply will soon be exhausted, and it is therefore pertinent to ask whether the methods of frequency allocation evolved during the early years of radio and still employed are the ones best suited to the tasks which lie ahead. One alternative to formal allocation of frequencies is adaptive selection of channels by users on a non-interference basis.

Radio communication takes place through media which are, to a greater or less extent, unpredictable in so far as the quality of the propagation path, and the spectrum occupancy, are subject to random variations. To the extent that these variables are random, optimum use of the media cannot be specified precisely in advance and the use of a system of fixed frequency allocations must therefore lead inevitably to some degree of inefficiency. An extreme instance of this is provided by the present situation in the h.f. band where 'congestion' has long been a matter for much concern<sup>1, 2</sup> although, as pointed out recently by A. J. H. Oxford,<sup>3</sup> the effective channel occupancy is quite low. Conceivably, a similar situation could arise at higher frequencies if these were to be exploited for satellite communication by large numbers of mobile or other small terminals operating intermittently. In all cases of inefficient use of spectrum caused by random variables, it is appropriate to consider the use of adaptive techniques; depending on circumstances an adaptive system may have a high or

low cost-effectiveness rating but, in most instances, the basic merits or demerits of such an approach are likely to be over-shadowed by the problems of compatibility with existing systems which represent a considerable investment, and with which the adaptive system must live in harmony for an indefinite period.

The term 'adaptive system' has been applied to a wide range of possible devices, including systems which match the characteristics of a communication link to those of the propagating medium. In the present paper adaptive techniques are of direct concern only in the context of channel selection, but even with this restriction the term embraces a wide field extending from simple manually-operated procedures involving no instrumentation, such as operate in the amateur bands, to sophisticated systems which incorporate ionospheric sounding and automatically select suitable channels. To be suitable, a channel must be free of interference, interference must not be caused to other users, and propagation must be satisfactory for the type of communication envisaged. Moreover, channelling need not be restricted to conventional frequency division but may employ time division, code division (i.e. spread-spectrum) or combinations of these.

This paper seeks to present some basic ideas suitable for the evolution of adaptive systems of channel selection, discusses some of the practical aspects of the implementation and problems of compatibility with non-adaptive systems.

## 2. Basic Principles

### 2.1. Frequency Division

The following model provides a convenient starting point. Let A and B be two terminals between which it is desired to establish two-way communication. Instead of using allocated frequencies, a search is

† Lately with the Ministry of Defence, Admiralty Surface Weapons Establishment, Portsmouth, Hampshire.

made for a suitable channel on the basis of a pre-arranged time-frequency schedule, absence of interference to or from other users being included in the criterion of suitability. For simplicity it is assumed that simultaneous transmission by both terminals is not required, thus allowing a single frequency channel to be used for two-way communication. It is further assumed that all other terminals which might want to use the same frequency are technically identical and use similar operating procedures. A and B are allowed to use any channel they wish, subject to the following rules:

- (a) A or B must not attempt to initiate communication on a frequency which the initiator, by previous listening, knows to be occupied.
- (b) If the station addressed hears another station using the frequency, it does not reply.
- (c) Having established contact, and prior to the exchange of message traffic, both A and B recheck the frequency so that a third station C (having prior use of the frequency) can make its presence known, in which case A and B look for another frequency.
- (d) Communication links must be designed to tolerate the brief interruptions which may be caused by transmissions operating in accordance with conditions (a) and (c).
- (e) The propagating medium must be stable.

These rules appear sufficient for the prevention of harmful interference, condition (c) taking care of the situation that C, in range of A or B, may be engaged in copying a fourth station, D, not audible at A or B. The need for this provision may be avoided by stipulating that no transmission shall exceed some duration  $t$  without an acknowledgment or other transmission in the reverse direction, and that  $t$  shall represent a minimum listening period on any given frequency by A and B prior to attempting contact. With some further extension of the listening period it may be possible to dispense with condition (e), since extended listening will provide additional chances of hearing signals which may have been missed on the first attempt owing to fades of brief duration.

It is clearly essential that A and B should operate, as stipulated, in accordance with a pre-arranged frequency and time schedule so that communication takes place on the first suitable frequency; otherwise much time may be wasted in establishing contact and interference caused by the search process may become significant. It will be evident that the suggested procedure is not restricted to pairs of participants; communication may for example be established by any station with any other member of a group on a discrete-address basis by allocating orthogonal time-frequency schedules to all members.

So far the scope of the argument has been restricted to interference-avoidance and the stated conditions are clearly sufficient for this purpose. It has not been established that they are necessary conditions, and this aspect is further considered in Section 3. It will be noted, however, that the procedure for interference-avoidance also ensures that the propagation conditions are satisfactory and to embody the equivalent of ionospheric sounding into the frequency-selection process it is merely necessary to ensure coverage of a sufficient range of frequencies in the search schedule. This range may be comprised of a number of narrow bands spaced throughout a sufficient portion of the h.f. spectrum to allow for the uncertainties of existing long-term predictions of usable frequencies and any desired criteria, such as signal distortion caused by multi-path effects, may be embodied in the signal recognition process so that attempts to communicate on an unsatisfactory channel are prevented; alternatively the probing signals may be used to investigate the channel characteristics so that the modulation can be adjusted to exploit these to best advantage.

## 2.2. Broad-band Systems

As an alternative to channelling by the allocation of separate frequencies, a given band can be shared by time-division. In this case each user might radiate a succession of short equally-spaced pulses occupying the entire band and in principle the same number of users can be accommodated in a given frequency band as in the case of frequency channelling; in practice, however, difficulties may arise from the following causes:

- (a) The energy required per information bit tends to be constant as the bit-length is varied, hence with shorter time slots higher peak powers have to be provided.
- (b) Synchronization is required and becomes more difficult as time slots get shorter, particularly as propagation time delays tend to be different for each pair of communicators.
- (c) If multi-path effects are present, a signal which starts as a short pulse may be received as a longer pulse or a succession of pulses.

Assuming these problems to be soluble, it would be possible to work out an adaptive system closely analogous to the frequency-division proposals of the previous section. It may be of interest to note that whereas a system of allocated time slots would require a master clock common to all users, an adaptive system would require only uniform spacing of time slots.

Because of the difficulties listed above and incompatibility with existing usage, it seems unlikely

that time-slotting will solve any problems in the h.f. band; on the other hand when several signals are passed through a common repeater, as in satellite communication, time-division has the advantage of avoiding the generation of intermodulation products in the satellite.

There are in existence a number of wide-band systems which employ time-frequency matrices,<sup>4</sup> the allocation of different combinations of time and frequency slots providing each of a large number of users with a 'discrete address code' to which only his receiver will respond intelligibly. Unfortunately other simultaneous users generate noise due to chance overlapping of pulses, and the efficiency of spectrum utilization is poor. There seems to be no objection in principle to an adaptive version of these systems whereby users would search for unused codes in the same way as a frequency division system might search for unused frequencies.

Another approach<sup>3-5</sup> employs superimposed noise-like broad-band signals which may be separated at the receiver by a correlation process using stored replicas of the modulation envelope. Channelling is effected by using different modulation-waveforms or 'codes'; this process is sometimes known as code-division or spread-spectrum modulation. As with time-division, synchronization must be achieved to within a time-interval which is less than the reciprocal of the overall system bandwidth. With this system, assuming all signals to be of equal strength, the efficiency of spectrum utilization is comparable with that achievable with perfectly co-ordinated or fully self-adaptive time or frequency division, so that if an information bandwidth of say 1 kHz is spread over 1 MHz, a thousand users can be accommodated. However, when the limit of occupancy is reached any signal of less-than-average strength is lost.<sup>5</sup> In view of this, in conjunction with the large variations of received signal levels and the need for compatibility with older systems during any transitional period, this approach is considered unlikely to provide an acceptable answer to the problems of h.f. communication.

### 3. Adaptive Power Control

Consider now the situation that A and B can hear C and D and vice versa, but in each case the unwanted signals are weaker than the wanted. This should, in principle, permit all four stations to operate on the same frequency or in the same time slot, thereby conserving spectrum, but this is precluded under the above rules which accordingly need amendment to ensure that use of a channel is forbidden only if interference would actually be caused thereby.

In another typical situation, A and B are close together and perhaps centrally located between C and

D which are widely separated so that A, B interferes with C, D but not vice versa. In this case A and B by reducing power can create the situation envisaged in the previous paragraph. The efficiency of spectrum-utilization may therefore be increased (intuitively, one might think, by orders of magnitude), assuming adaptive power control in conjunction with a channel-acceptability criterion based on interference-potential rather than prior occupancy. Such a system presents no theoretical difficulty on the basis of previous assumptions, together with the insertion, at suitable intervals in each transmission, of some suitably-coded indication of the radiated power level and received signal level. If A and B wish to communicate on the frequency of C, D and the relevant path-losses are known, the feasibility of this, and the required power level for interference avoidance, can be computed. If the path-loss between A and B is not known, A may attempt communication using a power level low enough to avoid causing interference at C or D; A and B lose nothing by this except possibly a little time and, if successful, tend thereby to conserve vacant space in the spectrum for other users.

As an alternative to the transmission of power-level information, a procedure for frequency-division systems may be evolved on the basis of condition (c) of Section 2. A and B, having established (e.g. from prior knowledge) their own required power level, radiate brief probing pulses. Any station experiencing a significant level of interference notifies this by, for example, the radiation of similar pulses, receipt of which by A or B causes them to look for another frequency. Apart from its basic simplicity, this procedure is advantageous in so far as it takes into account propagation anomalies and antenna characteristics. It thus becomes possible to dispense with most of the conditions imposed in Section 2; of the remainder, (c) is embodied in the above procedure whereas (d), the ability to tolerate brief interruptions, requires the provision of some form of redundancy-coding and is a normal requirement for conventional circuits. For compatibility, however, other services using the same frequency band would need to have in common the ability to recognize the probing pulses and signal the occurrence of interference. To operate in an adaptive mode, services need the ability to change frequency rapidly in accordance with some carefully organized procedure, and the full potential of such systems will not be realized until all participating stations are equipped with adaptive power control.

In the case of code-division systems the control of radiated power is particularly important, since, as previously discussed (Section 2.2), radiation of excessive power leads to a reduction in the number of stations which may communicate simultaneously.

#### 4. Comparison of Adaptive and Non-adaptive Systems

For simple situations as discussed in Section 2, the advantage of adaptive versus non-adaptive frequency allocation is readily calculable, as shown in the Appendix. For the example illustrated in Fig. 1 and by Table 1, it is found that if a reliability of communication better than 95% is stipulated, adaptive selection allows up to sixteen times the number of

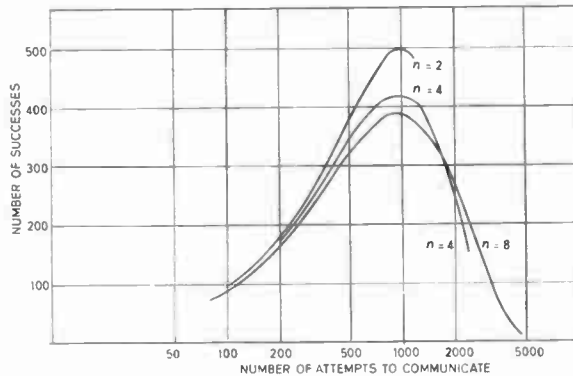


Fig. 1. Efficiency of spectrum utilization for non-adaptive systems, assuming 1000 channels and  $n$  subscribers per channel.

Table 1

Reliability of communication (%)	Number of successful simultaneous attempts to communicate per 1000 available channels	
	Fixed allocation	Adaptive selection
95	60	1000
90	90	1000
80	200	1000
70	280	1000
50	380	1000

part-time users. The actual probability of interference on an h.f. circuit is in general not calculable since it depends on many factors, some of them random; on the other hand it seems reasonable to suppose that the situation as it appears to any one observer, at a particular instant of time, can be represented by an equivalent point on the curves, and the example can therefore be taken as likely to convey a qualitative indication of the kind of improvement which might be expected as a result of adaptive frequency selection in portions of the h.f. band.

The figures in the second column of Table 1 are approximate, based on the assumption of at least four equally-probable part-time users per channel, the probability of attempts to communicate being adjusted to fit the stated reliability figures. These figures are not greatly dependent on the number of part-time users per channel, assuming there are two or more.

The figures do not tell quite the whole story. For example, with non-adaptive operation in which the sender repeats messages if no acknowledgment is received, each unsuccessful attempt will add to the interference so that fewer users are able to communicate. This might precipitate a chain reaction leading to total paralysis. With adaptive selection there are no lost messages but if the number of users wishing to communicate is, on average, greater than the total number of channels, there will be a lengthening queue. For example, with an average use period of 10 minutes and 105 would-be users per 100 channels, there will be a queue of 5 after 10 minutes, 10 after 20 minutes etc., and after 3 h 20 min there will be an average delay of 10 minutes in completing a circuit. If the same proportion of users attempt to communicate with fixed allocations it is found from Fig. 1 that about 60% of messages will be lost at the first attempt for 4 or more users per channel. Thereafter the number of attempts will presumably increase, and the success ratio will diminish.

#### 5. Compatibility between Adaptive and Non-adaptive Systems

Consider a band of frequencies divided into channels which have been fully allocated (perhaps several times over) in accordance with existing procedures. In general it will appear to the observers at A and B that there are gaps in the spectrum, as a result of discontinuous use of allocations or the absence of propagation. It is interesting to suppose that A and B in addition to their adaptive channel-selection equipment, possess frequency allocations on which they are experiencing interference; when communication fails on the allocated channel, A and B by prior agreement switch to synchronized frequency-scanning with A radiating interrogation pulses (e.g. 1 ms in duration) and B operating in a transponder mode with inhibition of response when the channel is occupied. A must, of course, not interrogate on a channel known to be occupied.

Interference may now be caused at a receiver within range of A or B if the signal which is being received is not audible at either A or B. This risk is obviously less than that entailed by non-adaptive operation in which operation may take place on allocated frequencies regardless of prior occupancy, and will be further reduced if A and B use no more power than they need.

Moreover, if the station which experiences interference has the capability of transmission on its own listening frequency, it can notify the situation to A or B who move frequency so that the interruption of service is only of brief duration. On balance therefore, all users of a frequency band should tend to benefit when some of them change over to adaptive channel selection.

Figure 2 demonstrates the feasibility of adaptive communication in a frequency band already congested to the point of breakdown, without adding to the congestion. As an example, suppose that a non-adaptive system is considered viable provided the reliability exceeds 80%; at this point, assuming 1000 channels shared by 4000 or more non-adaptive users, 250 would be trying to communicate, 200 would be

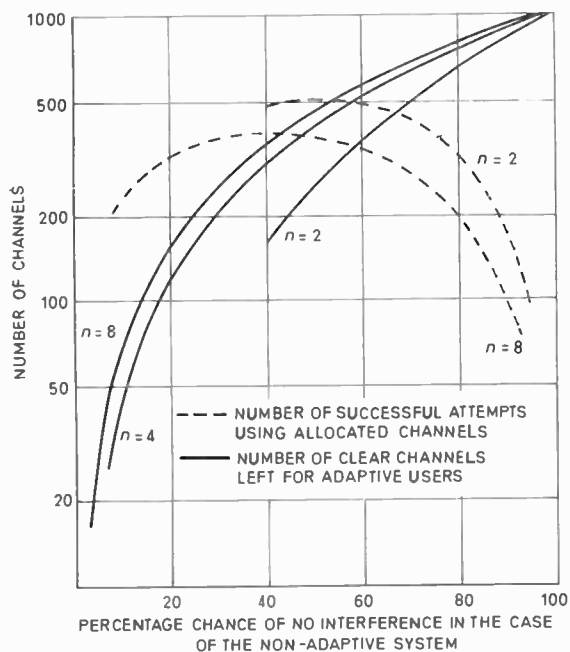


Fig. 2. Compatibility of adaptive and non-adaptive systems.

succeeding, and 780 channels would remain available for adaptive use. It is interesting also to consider a non-adaptive but 'intelligent' system such that users know how frequently they should attempt to communicate in order to pass the greatest number of successful messages. Figure 2 shows a rather flat optimum such that a maximum of about 390 messages can be passed at a given time; in this situation 610 unsuccessful attempts are being made but despite this 350 interference-free channels remain available for adaptive use. Hence, even in this situation, an adaptive capability could almost double the number of usable channels, the added channels being of much greater reliability than the allocated frequencies.

It will be appreciated that in practice situations will be less simple. Adaptive users will be aware almost immediately of co-channel interference and should usually be able to find a new channel quickly, but if the spectrum is almost fully occupied so that only one or two channels are free, these will not be easy to find; hence as the system approaches saturation the search time will tend to increase rather sharply. Non-adaptive users will be dependent on acknowledgments, or requests for repetition, and both requests and repetitions may involve several attempts before success is achieved; these requests and repetitions will add to the congestion.

## 6. Principles of Band Allocation

For the allocation of frequency bands for adaptive systems certain broad guide-lines can be established. Bands must obviously be narrow enough to be within the range of available techniques for making rapid changes of frequency, separate bands are required for widely differing types of service, and spacing between bands should be small enough to allow propagation differences to be exploited.

In the h.f. band, low-power circuits require to operate near the m.u.f. to minimize attenuation, and existing frequency bands are believed to be, in general, too widely spaced. There is a dearth of information on this point as oblique ionograms usually indicate only whether a path exists and not the path attenuation but, from the author's experience, the need is certainly not less than 4 bands per octave above about 10 MHz or so. For high-power services (e.g. point-to-point, or broadcasting) precise choice of frequency is less important in view of the wider gaps between the l.u.f. and the m.u.f. (lowest and maximum usable frequencies).

## 7. Application to Satellite Communication

### 7.1. General Considerations

In satellite communication the solution of multiple-access problems involves the considerations of a wide range of possible modulation and multiplexing techniques including time-division, frequency-division, spread-spectrum (or code-division) and various combinations thereof. It is possible that certain systems, having sufficiently-different characteristics could co-exist in the same spectrum with very little inter-system interference, but to keep the discussion within reasonable bounds it is proposed to assume channelling by conventional frequency-division; if foreseeable problems can be solved on this basis there is clearly no need to introduce greater complexity into the present argument.

To achieve the highest possible spectrum density of satellite communication, each satellite must be

arranged to respond only to those signals which it has the task of relaying and in the case of frequency-division the bandwidth of each channel must be restricted to the information-bandwidth. It is reasonable to suppose that not all satellites will be part of the same system, so that A wishing to communicate with B can use some satellites but not others; on the other hand the desire to avoid mutual interference will be common to all systems. Because of the assumption of a varying demand, and also because of channel-spacing requirements for minimizing intermodulation products in multiple-access satellites, the allocation of a fixed frequency block to each satellite will not be consistent with most-efficient utilization of the spectrum. Ideally therefore each satellite would be provided with the requisite number of suitably-spaced channels having their width determined by the information bandwidth, both the number and bandwidth of channels being adjustable to suit varying demands in accordance with instructions transmitted over a control channel. Adaptive frequency allocation would be comparatively simple in the case of the up-link since the criterion of suitability would be absence of interference on the corresponding down-link channels, care being taken of course to avoid causing interference by the up-link to channels used for line-of-sight communications in the vicinity of the ground terminals. On the other hand the satellite operator would have no direct indication of interference caused to ground services by the satellite down-link and an adaptive system should therefore be designed to work with a down-link spectral power density low enough to avoid causing interference.

Fixed services, with sufficient traffic to justify expensive ground terminals and using stationary satellites, are unlikely to have to resort to adaptive procedures in view of the large amount of discrimination provided by the narrow beamwidth; thus assuming a uniform  $1^\circ$  spacing between satellites using any given band of frequencies, a beamwidth less than  $1^\circ$ , and 500 MHz of total spectrum, it would be possible to operate about 36 000 television or  $5 \times 10^7$  voice channels using links distributed uniformly round the globe. In practice satellites would probably not be evenly spaced, on the other hand  $1^\circ$  is a somewhat generous estimate for the spacing required to achieve discrimination on the basis of aerial beamwidth. The use of non-synchronous equatorial satellites might be open to objection on the grounds that such vehicles would spend some time in the same line-of-sight as other satellites, and interference would occur. If inclined synchronous orbits were used (e.g. to provide polar coverage) their use could be inhibited when they were within say  $1^\circ$  of the equatorial plane, and their function taken over if necessary by a stationary satellite. It is therefore concluded that

within the foreseeable future interference between fixed-service satellite systems should be preventable without resort to adaptive processes.

### 7.2. V.H.F./U.H.F. System for Mobile Communications

If it were decided to establish a satellite system catering for the needs of small ground terminals including ships, and more especially aeronautical mobile terminals, a very different situation could arise because antenna beamwidths will be relatively wide, there may be large numbers of such terminals requiring to pass traffic at relatively infrequent intervals, and the number of simultaneous accesses to any one satellite will be restricted to some figure which might be small compared with the total number of terminals. Tracking problems and cost considerations may tend to favour use of the v.h.f. or u.h.f. bands, but these are already congested and existing users will obviously be reluctant to surrender their allocations. It is therefore of interest to consider the possibility of communication to and from small terminals through a v.h.f./u.h.f. satellite using adaptive selection of frequency to prevent interference to or from existing services.

It is suggested that the transmitter in a satellite might be commanded on to frequencies not already in use by other satellites, suitable frequencies being determined by either

- (a) adequate co-ordination (on a real-time basis) between satellite operating agencies, or
- (b) monitoring by ground terminals.

The v.h.f. and u.h.f. bands are typically used by mobile terminals employing more-or-less non-directional aerials and noisy receivers for line-of-sight communication, so that use of directional aerials and low-noise receivers for the satellite links should in principle enable the field strength from the satellite to be reduced to a level which will not cause interference to these services. Alternatively spread-spectrum techniques may be used to distribute the satellite signal over a band several times the information bandwidth without loss of signal/noise ratio. A speech signal transmitted at a spectral power density 6 dB below the noise level in a 100 kHz band might typically emerge from this process at a signal/noise ratio of about 11 dB in a 3 kHz post-detector bandwidth and should cause negligible interference to conventional a.m. or f.m. signals sharing the same r.f. spectrum.

Up-link frequencies could be selected by commanding the receiver in the satellite on to various channels in turn, whilst monitoring the down link for signs of interference. A single fixed-frequency narrow-band down-link channel would probably be sufficient for the purpose of notifying up and down link communication frequencies to all the mobile terminals. Any failure by

other users to respect this allocation would result only in interference to themselves and not to the satellite systems.

### 8. Conclusions

If the requirements for frequency allocations exceed the availability, self-adaptive procedures for channel selection and control of radiated power can lead to an increase of several times in the efficiency of spectrum utilization. Moreover, the gradual introduction of adaptive systems should considerably increase the number and quality of available channels with negligible degradation of the service enjoyed by prior users of the same frequency bands.

Adaptive techniques for frequency selection are likely to be of particular value for improving the situation in the h.f. band, where they can take on the dual role of interference prevention and oblique sounding of the ionosphere to determine the propagation quality of available channels. Implementation of such systems on a world-wide basis will raise difficult problems of administration and economics, but against this must be weighed the predicted consequences of present trends, should these be allowed to develop unchecked.<sup>1, 2, 6</sup>

The adaptive approach can also be applied to problems likely to arise in the field of satellite communication and, in particular, might help satellite communication systems operating in the v.h.f. and u.h.f. bands to co-exist with present services, which, not being subject to tight control, would be likely to cause interference from time to time with the satellite up-link.

Channelling by methods other than frequency selection is unlikely to be acceptable on any large scale for h.f. communication, but time-division and spread-spectrum techniques would probably be useful in the development of adaptive v.h.f./u.h.f. satellite systems.

### 9. Acknowledgments

The author is indebted to A. J. H. Oxford and R. T. A. Standford for useful discussions and, in particular the measurements of h.f. spectrum occupancy which provided much of the inspiration for the present paper. This paper is published by permission of the Ministry of Defence, Navy Department, but the opinions expressed are personal to the author.

### 10. References

1. Panel of Experts, Final Report, International Telecommunications Union, Geneva, 1963.
2. 'Too often "saved by the gong";' *Wireless World*, 73, No. 11, p. 517, November 1967.
3. Oxford, A. J. H., Contribution to Discussion on 'Long distance radio spectrum re-allocation', Conference on 'Radio Receiver Systems', University College of Swansea, September 11th-15th, 1967. (Reported in *Wireless World*, 73, No. 11, pp. 526-7, November 1967.)
4. Schwartz, J. W. *et al.*, 'Modulation techniques for multiple access to a hard limiting satellite repeater', *Proc. Inst. Elect. Electronics Engrs*, 54, No. 5, pp. 763-77, May 1966.
5. Costas, J. P., 'Poisson, Shannon and the radio amateur', *Proc. Inst. Radio Engrs.*, 47, No. 12, p. 2058, December 1959.
6. Hitchcock, R. J. and Morris, P. A. C., 'The h.f. band: is a new look required?', *Wireless World*, 67, No. 7, pp. 375-8, July 1961.

### 11. Appendix

Let each channel be allocated to  $n$  users, and let  $p$  be the probability that any one user is transmitting at a given time.

The probability that any specified channel is unoccupied is then

$$P_0 = (1-p)^n$$

The probability of one occupant is

$$P_1 = n(1-p)^{n-1}p$$

The probability  $P$  of more than one occupant is therefore given by  $1 - (P_0 + P_1)$ , i.e.

$$P = 1 - [(1-p)^n + n(1-p)^{n-1}p]$$

If there are  $m$  channels, the total number of attempts at communication is given by  $pnm$  and the number of successes by  $mP_1$ . This relation is plotted in Fig. 1. The number of channels usefully employed and the number of unused channels are plotted in Fig. 2 as a function of the success-ratio  $P_1/pn$ .

*Manuscript received by the Institution on 27th May 1969.  
(Paper No. 1289/Com.24.)*

# Radio Engineering in India

Papers published in the *I.E.E.-I.E.R.E. Proceedings-India*, Vol. 7, No. 3, July-September 1969.

## Automatic Conversion of Line Records to Digital Information

H. R. PISHAROTY and H. N. MAHABALA (*Indian Institute of Technology, Kanpur*)

It is often necessary to convert line records to digital form for use on a digital computer. A conversion attachment for a conventional X-Y recorder has been built for this purpose. The ordinate is scanned from bottom to top and the digital equivalent of the Y-deflection voltage at incidence of a dark line is made available for recording on an incremental tape recorder. The incidence of the dark line is detected by using a cadmium sulphide photocell and an illuminating arrangement. The system described can be used for single-valued functions but can be easily modified to handle multi-valued functions. In the Y-direction there are 128 levels of quantization. In the X-direction the quantization is 20 cm at present.

## A Self-Tuning Filter for Detection of a Class of Signals in Background Noise

P. C. MAJHEE and K. P. RAJAPPAN (*Indian Institute of Technology, Madras*)

This paper describes the design and construction of an electronic self-tuning filter for detection of signals in noisy background. It is assumed that neither the signal nor noise is known completely. The information needed for the adjustment of the filter parameters is obtained directly from measurements made on the noisy signal itself.

## Constructing Normal-Mode Helical Antennas

M. N. ROY (*Jadavpur University, Calcutta*)

Compared to the circularly polarized axial-mode helical antennas, little attention has been paid to normal-mode helical antennas because of small bandwidth and low efficiency. It has been suggested elsewhere that it is quite possible to use normal-mode helical antennas in the medium and short wave region, thereby reducing the height of the mast antenna by a factor of 5 to 10. This paper discusses the design and construction of vertically polarized normal-mode helical antenna structures.

## A Frequency Standard for a Microwave Spectrometer

B. M. BANERJEE, A. CHATTERJEE, MISS S. CHOWDHURY, P. K. GUPTA and K. S. PATEL (*Saha Institute of Nuclear Physics, Calcutta*)

Details of the frequency standard being used in Saha Institute since June 1966 are presented. The 100 kHz output of a G.R. 1100 AP 'primary' standard is multiplied to produce several hundred milliwatts at 50 MHz and 500 MHz. These are applied to a K-band harmonic generator and produce marker frequencies spaced by 50 MHz in the 18-16 GHz band. The microwave absorption line is compared to and interpolated with these markers by a communication receiver. The accuracy and stability of these markers is the same as that of the standard which is a few parts in a billion. To get decimally related output frequencies, the system uses a chain of quintuplers and doublers.

## STANDARD FREQUENCY TRANSMISSIONS—October 1969

(Communication from the National Physical Laboratory)

Oct. 1969	Deviation from nominal frequency in parts in 10 <sup>10</sup> (24-hour mean centred on 0300 UT)			Relative phase readings in microseconds N.P.L.—Station (Readings at 1500 UT)		Oct. 1969	Deviation from nominal frequency in parts in 10 <sup>10</sup> (24-hour mean centred on 0300 UT)			Relative phase readings in microseconds N.P.L.—Station (Readings at 1500 UT)	
	GBR 16 kHz	MSF 60 kHz	Droitwich 200 kHz	*GBR 16 kHz	†MSF 60 kHz		GBR 16 kHz	MSF 60 kHz	Droitwich 200 kHz	*GBR 16 kHz	†MSF 60 kHz
1	-300.0	-0.1	+0.1	573	487.9	17	-299.9	0	+0.1	585	495.2
2	-300.0	-0.1	+0.1	573	488.4	18	-300.0	-0.1	+0.1	585	496.2
3	-300.0	-0.1	+0.1	573	488.9	19	-300.0	0	+0.1	585	496.4
4	-299.9	0	+0.1	572	488.9	20	-300.0	-0.1	+0.1	585	497.4
5	-300.3	0	+0.1	575	489.2	21	-300.1	0	+0.1	586	497.6
6	-299.9	0	+0.1	574	489.4	22	-300.0	-0.1	+0.1	586	498.2
7	-300.1	-0.1	+0.1	575	490.0	23	-300.0	-0.1	+0.1	586	499.0
8	-299.9	-0.1	+0.1	574	490.6	24	-300.0	0	+0.1	586	499.2
9	-300.0	-0.1	+0.1	574	491.2	25	-300.0	-0.1	0	586	500.0
10	-300.0	-0.1	+0.1	574	491.8	26	-300.0	0	+0.1	586	500.0
11	-300.1	0	+0.1	575	492.2	27	-300.0	0	+0.1	586	500.3
12	-300.1	0	+0.1	576	493.0	28	-300.0	0	+0.1	586	500.5
13	-300.1	0	+0.1	577	493.3	29	-300.1	0	+0.1	587	500.9
14	-300.0	-0.1	0	577	494.0	30	-300.0	-0.1	+0.1	587	501.6
15	-300.0	-0.1	+0.1	577	494.6	31	-300.1	0	+0.1	588	501.7
16	-300.0	0	+0.1	577	495.0						

All measurements in terms of H.P. Caesium Standard No. 334, which agrees with the N.P.L. Caesium Standard to 1 part in 10<sup>11</sup>.

\* Relative to UTC Scale: (UTC<sub>NPL</sub> - Station) = + 500 at 1500 UT 31st December 1968.

† Relative to AT Scale: (AT<sub>NPL</sub> - Station) = + 468.6 at 1500 UT 31st December 1968.